Effect of Adiponectin Overexpression on the Metabolic Phenotype of the *Ceacam1-/-* Mouse

CHARBONNEAU ALLARD, Anne-Marie
Department of Biochemistry
McGill University, Montreal

August 2007

A thesis submitted to McGill University in partial fulfilment of the requirements of the degree of master in sciences

Your file Votre référence
ISBN: 978-0-494-48351-0
Our file Notre référence
ISBN: 978-0-494-48351-0

ABSTRACT

CEACAM1 is a membrane glycoprotein expressed in many cells and tissues, amongst them liver and intestine. *Ceacam1-/-* mice are hyperinsulinemic and display certain MetS (metabolic syndrome) parameters. Adiponectin (Ad) is an insulin-sensitizing adipokine involved in MetS. *Ceacam1-/-* mice have increased tumour burden in models of intestinal carcinogenesis.

OBJECTIVE: The goal of this project was to attempt to reverse the insulin resistance of *Ceacam1-/-* mice by overexpression of Ad, to quantify metabolic parameters in the different genotypes and to evaluate the suitability of the *CC1 : Ad* mouse model in studying the role of CEACAM1 insulin resistance in tumour progression.

PROCEDURE: The *Ad* transgene was transferred from the FVB to the C57Bl/6 mouse background. Mice with different *CC1 : Ad* genotypes were produced. 6 month-old mice were bled and dissected after a five hour fast. Total body, fat pad (interscapular, inguinal, gonadal) and liver weights, as well as glucose, insulin and Ad levels were measured.

RESULTS: The *Ad* transgene was correctly transferred from the FVB to the C57Bl/6 mouse background. Ad was similarly over-expressed and secreted. All parameters observed display comparable profiles between both strains, with slight differences in net levels induced by the susceptibility of the C57Bl/6 strain to insulin resistance. No difference between *Ceacam1* wt and ko mice was observed for all parameters. However, some differences appear in presence of Ad overexpression, with *CC1+/- : Ad* tg+ *and* *CC1-/- : Ad* tg+ females being heavier than *CC1+/+ : Ad* tg+ females. *CC1-/- : Ad* tg+ males also have lower insulin and higher Ad levels than *CC1+/+ : Ad* tg+ males.

DISCUSSION: The absence of differences between *Ceacam1* wt and ko mice in the parameters examined in this study did not allow evaluation of the rescue by Ad. The rescue will now be evaluated for insulin resistance by the hyperinsulinemic euglycemic clamp technique, on the development of fatty liver and on hepatic lipogenic enzyme expression. Other metabolic parameters will be investigated in *Ceacam1-/-* mice.

RÉSUMÉ

CEACAM1 est une glycoprotéine membranaire exprimée notamment dans le foie et les intestins. Les souris *Ceacam1-/-* sont hyperinsulinémiques et ont certaines caractéristiques associées au syndrome métabolique (SMet). L'adiponectine (Ad) augmente la sensibilité à l'insuline et est impliquée dans le SMet. Après induction de tumeurs, ces souris montrent une augmentation du nombre et de la taille des tumeurs intestinales.

OBJECTIF : Ce projet vise à tenter de renverser la résistance à l'insuline des souris *Ceacam1-/-* par sur-expression d'Ad, à quantifier les paramètres métaboliques pour différent génotypes *CC1 : Ad* et à évaluer l'utilité de ce modèle pour l'étude du rôle de la résistance à l'insuline dans la progression des tumeurs intestinales chez les souris *Ceacam1-/-*.

PROCÉDURE : Le transgène de l'*Ad* a été transféré de la souche murine FVB à celle de C57Bl/6. À 6 mois, les souris ont été saignées et disséquées après un jeûne de 5 heures. Le poids total, de certains tissues adipeux (interscapulaire, inguinal, gonadal) et du foie ainsi que les niveaux de glucose, d'insuline et d'Ad dans le sang ont été mesurés.

RÉSULTATS : Le transgène a été correctement transféré d'une souche à l'autre. L'Ad est sur-exprimée et secrétée de façon comparable dans les deux souches de souris. Tous les paramètres observés montrent des profiles similaires pour les deux souches. De légères différences au niveau des données brutes mettent en évidence la susceptibilité des souris C57Bl/6 à la résistance à l'insuline. Aucune différence entre les souris *Ceacam1* wt et ko n'a été observée. Toutefois, certaines différences sont apparues lors de la sur-expression d'Ad. Les femelles *CC1+/- : Ad* tg+ et *CC1-/- : Ad* tg+ ont un poids supérieur aux femelles *CC1+/+ : Ad* tg+. Les mâles *CC1 -/- : Ad* tg+ ont moins d'insuline et plus d'Ad que les mâles *CC1+/+ : Ad* tg+.

DISCUSSION : L'absence de différences entre les souris *Ceacam1* wt et ko au niveau des paramètres observés dans cette étude n'a pas permis l'évaluation du traitement par l'Ad. L'effet de l'Ad sera maintenant évalué sur la résistance à l'insuline, pour la présence de gras dans le foie et pour l'expression hépatique d'enzymes lipogéniques. D'autres paramètres seront aussi investigués dans les souris *Ceacam1-/-*.

ACKNOWLEDGMENTS

This thesis involved the input and help of several people. I wish to acknowledge my supervisor, Dr. Nicole Beauchemin, for having offered me a place in her laboratory and given me the opportunity to participate to this interesting project. A mention for her amazing flexibility in special circumstances, which allowed me to go on and finish this M.Sc. I would like to specially acknowledge Claire Turbide and Nelly Leung, two precious people whose constant help was indispensable. Thanks to both of them for their immense patience, their advice and their answers to my millions of questions. Thanks for their moral support. Thanks to Claire particularly for the mouse work, the thesis editing and the help with orders. Thanks to Nelly specifically for her patience in teaching me and for her work which led to and complements to this wonderful project.

Thanks to other members of the laboratory, Dr. Anne-Laure Nouvion for helpful discussion, Sarah LeBlanc for having carefully corrected my English in this thesis, Valérie Breton and Lyudmila Kerusenko for their precious help with mouse genotyping. I would like to mention Dmitry Rodionov for his amazing work in repairing the radioactive γ counter.

Thanks to my research comittee, Dr. Imed Gallouzi for his disponibility and scientific comments and Dr. Roland Savard for his precious knowledge on adipose tissue.

Thanks to our collaborators for their contribution to this amazing global metabolic project, notably Dr. André Marette, but also Dr. Émile Lévy and Dr. Roland Savard. Thanks to Dr. André Veillette, Dr. Dominique Davidson, Dr. Annie Bourdeau and Renée Atallah for their help on the T cell project.

Finally, but most importantly, I would like to thank my mother Rachel Charbonneau, for her unconditional love and support in my life at every level as well as for the model she is to me.

My master was funded by scholarships from the Fonds de Recherche en Santé du Québec (FRSQ) and from the Canadian Institutes of Health Research (CIHR). The project was funded by the Canadian Cancer Society through the National Cancer Institute of Canada (NCIC).

ABBREVIATIONS USED IN THE TEXT

aa	amino acids
ACC	acetyl CoA carboxylase
Ad	adiponectin
AdipoR	adiponectin receptor
AMPK	AMP-activated protein kinase
Apc	adenomatous polyposis coli
BAT	brown adipose tissue
BMI	body mass index
CC1	Ceacam1
CCHS	Canadian Community Health Survey : Nutrition
CEA	carcinoembryonic antigen
CEACAM	CEA-related cell adhesion molecule
CRP	C-reactive protein
CVD	cardiovascular diseases
ER	endoplasmic reticulum
FA	fatty acids
FABP	fatty acid binding protein
fAd	full-length adiponectin
FAS	fatty acid synthase
FFA	free fatty acids
G-6-P	glucose-6-phosphatase
gAd	globular adiponectin
GLUT-4	glucose transporters-4
HDL	high density lipoprotein
HFD	high fat diet
HMW	high molecular weight
L	long
LPL	lipoprotein lipase
LPS	lipopolysaccharide

IFNγ	interferon gamma
Ig	immunoglobulin
IGF	insulin like growth factor
IL	interleukine
iNOS	inducible nitric oxide synthase
IR	insulin receptor
IRS	insulin receptor substrate
ITIM	immunoreceptor tyrosine-based inhibitory motif
ITT	insulin tolerance test
JNK	c-Jun N-terminal kinase
ko	knockout
LAR	leukocyte related-antigen
LDL	low density lipoproteins
LMW	low molecular weight
LPL	lipoprotein lipase
MAPK	mitogen-activated protein kinase
MCP-1	monocyte chemoattractant protein 1
MetS	metabolic syndrome
MHV	mouse hepatitis virus
mTOR	mammalian target of rapamycin
NAFLD	nonalcoholic fatty liver disease
ND	not determined
NEFA	non-esterified fatty acids
NFκB	nuclear factor kappa B
NO	nitric oxide
OGTT	oral glucose tolerance test
PCR	polymerase chain reaction
PEPCK	phosphoenolpyruvate carboxykinase
PI3K	phosphoinositide 3-kinase
PKB	protein kinase B
PKC	protein kinase C

PPARγ	peroxisome proliferative activated receptor γ
PTP	phosphotyrosine phosphatases
RAGE	receptor for advanced glycation end-products
ROS	reactive oxygen species
S	short
SOCS	suppressor of cytokine signalling
SREBP	sterol regulatory element binding protein
T2DM	type 2 diabetes mellitus
TD	tendency
TG	triglycerides
tg+	transgenic
TZD	thiazolidinediones
TNF-α	tumor necrosis factor α
UPR	unfolded protein response
VEGF	vascular epidermal growth factor
WAT	white adipose tissue
wt	wildtype

TABLE OF CONTENTS

I. INTRODUCTION

A) Metabolic syndrome (MetS)

1. Clinical features

a) Definition

In 2004, the Canadian Community Health Survey: Nutrition (CCHS) indicated that 23% of Canadian adults were considered obese and 36% overweight. This demonstrates a huge increase in obesity in comparison to the 14% surveyed in 1979 by the Canada Health Survey (*1*). In addition, this trend is reflected in children and adolescents among which 8% were obese and 18% overweight, twice more than in 1979 (*2*). In its analysis, the CCHS concluded that the body mass index (BMI), a measure of obesity, was directly related to the risk of hypertension, diabetes and cardiovascular diseases (CVD) (*1*). Indeed, the prevalence of diabetes in the Canadian population is approximately 5.1% (*3*), 90% of this percentage being represented by type 2 diabetes mellitus (T2DM) patients (*4*). In 2001, 29% of deaths were due to heart diseases, 6.8% to cerebrovascular diseases and 22.9% to cancers in the United States (*5*). MetS is defined as the co-occurrence of metabolic abnormalities which, together, increase the risk for CVD, T2DM and global morbidity/mortality by 2-3 times (*6, 7*). Some features of MetS were first mentioned in 1923 (*8*), but MetS importance was revealed with Reaven's description of syndrome X in 1988 (*9*). Over the years, it was given a multitude of different names among which is the insulin-resistance syndrome (*10*).

Different organizations established different definitions of MetS, with either a T2DM or a CVD orientation (*11*). They mostly look at the same features, but some parameters and their limits are different. MetS is characterized usually by more than three parameters, with certain definitions putting more emphasis on one of the features. Impaired glucose/insulin regulation is diagnosed as diabetes, glucose intolerance, insulin resistance, hyperinsulinemia and/or fasting hyperglycemia ($\geq$ 5.6-6.9 mmol/L). Another feature of MetS consists of obesity, either abdominal, determined by the waist-to-hip ratio ($>$ 0.85-0.90) or by the waist circumference ($\geq$ 80-102 cm), or total obesity, measured by the BMI

(>30 kg/m^2). In more recent definitions, the first two parameters have different limits for men and for women as well as for members of different ethnic groups. Dyslipidemia is diagnosed by triglycerides (TG) levels higher or equal to 1.7-2 mmol/L and/or by levels of high density lipoprotein (HDL) lower than 0.9-1.3 mmol/L, with higher thresholds for men. Finally, the last consensus feature of MetS is a ratio of systolic/diastolic blood pressure superior or equal to 130-140/85-90 mmHg (*12*). Confirmatory factor analysis revealed that MetS is mostly explained by obesity and insulin resistance, followed by dyslipidemia and finally by high blood pressure (*13*). However, neither of these factors alone can explain MetS (*14*). Recently, the American Heart Association and the National Heart, Lung and Blood Institute added treatments for hyperglycemia, dyslipidemia and/or blood pressure as criteria for MetS (*15*). It is worth noting that the limits set for MetS diagnosis are below those established for individual pathology diagnosis (*16*). Thus, a patient with MetS could have no overt disease. The World Health Organization includes microalbumineria as a parameter, whereas the International Diabetes Federation suggests also looking at pro-atherogenic determinants such as increased small and dense low density lipoprotein (LDL), abnormal fibrinolytic and coagulation activities, inflammation mediators, oxidative molecules, endothelial dysfunction and altered postprandial lipid levels (*17, 18*). Some definitions are best suited for clinical diagnosis and epidemiological studies, whereas it is proposed that in clinical and mostly fundamental research, the most complete portrait should be envisioned. This can be achieved by a combination of all factors cited in all definitions (*12*). Many other markers of MetS have been discovered such as high plasma concentration of leptin (*19*), retinol-binding protein 4 (*20*), fatty-acid binding protein (*21*) and resistin (*22*) and low plasma concentration of adiponectin (*23*). Over the years, controversy was raised about the usefulness and advantages of a MetS diagnosis over diagnosis of individual abnormal parameters (*24*). Whether or not MetS exists, it is currently a convenient term to discuss several metabolic abnormalities arising together.

b) Prevalence

The actual prevalence of MetS world-wide is unknown due to the different methodologies and definitions used for diagnosis. However, from a summary of several studies, it can be

approximated at 15-25% (*12*). In Canada and the USA, the prevalence of MetS increases with age and with time, following the increase in obesity and aging of the population. Prevalence is not homogeneous in people originating from different countries and there is no consensus about prevalence in men vs women (*25, 26*). In the United States, an increase has also been reported in adolescents (*27*), but there is no official data in Canada. MetS is not restricted to the developed world as these trends were also recently reported in developing countries (*28*). The major therapy for MetS is a decrease in weight through appropriate diet and, most importantly, exercise (*29*).

c) Etiology

i) Genetics

The individual parameters of MetS all have a percentage of genetic etiology (*11*). However, scientists were interested in finding a "clustering" factor to explain MetS. One study concluded that the MetS cluster is more readily inherited than individual components (*30*). Childhood obesity and a familial history of MetS significantly increase the risk for MetS in adults (*31, 32*). In children, MetS is maintained as they age (*33*). A large amount of work has been studying the genetic basis of MetS, but no consensus has been reached on which genes or precise mutations/polymorphisms in these genes are implicated. That said, mutations in 14 genes show an association with 2 or more elements of MetS (*11*). A large number of different quantitative trait loci were also obtained by genome-wide linkage analysis. The most promising genes from these studies are the *Ad (adiponectin)* and the *presenilin-associated rhomboid-like* genes situated on the chromosome segment 3q27, which is often associated with T2DM and obesity, as well as the *leptin* gene (*34*). However, both genes and environmental factors act on every step along the cascade of events leading to MetS.

ii) Lipocentric

Teran-Garcia and Bouchard proposed a lipocentric origin of MetS (*11*), a hypothesis also endorsed by the International Diabetes Federation (*35*). Obesity, through abnormal tissue biology and excess fat, particularly abdominal fat and ectopic (organ) fat accumulation, would lead to insulin resistance and later to hyperinsulinemia and T2DM (*36, 37*). It is

generally accompanied by adipocyte hypertrophy, which is associated with increased TG synthesis, lipolysis, fatty acids (FA) transport and secretion, decreased lipid storage and glucose uptake. These effects are partly due to decreased insulin sensitivity in adipocytes (*11*). Increased mass generates more pro-inflammatory molecules, such as CRP (C-reactive protein), TNF-α (tumour necrosis factor-α) and IL-6 (interleukin-6), and less of the anti-inflammatory molecule Ad. There are also changes in concentrations of leptin, resistin, angiotensinogen, plasminogen activator inhibitor-1. Cytokines and angiotensin II increase blood pressure slightly through vasoconstriction (*38*).

The excess FFA in the blood are taken up mainly by the liver and muscles, but also by the pancreas, leading to impaired function and decreased insulin sensitivity of these organs through a phenomenon called "lipotoxicity". Insulin resistance and high levels of FFA (free fatty acids) in the pancreas lead acutely to increased insulin secretion and, in the long term, cause damages decreasing insulin release (*39-41*). This phenomenon explains the hyperinsulinemia found in MetS patients and the hypoinsulinemia characterizing T2DM. Insulin also normally inhibits its own secretion (*40, 42*). It is worth noting that postprandial hyperinsulinemia develops before fasting hyperinsulinemia (*43*). In muscles, ectopic fat creates abnormal FA oxidation leading to accumulation of diacylglycerol and fatty acid acylCoA and decreased glucose uptake after the release of insulin (*44*). This translates into hyperglycemia, which, with excess FFA, creates excess TG in the liver (*45*). It has been shown that the amount of TG in the liver is proportional to insulin resistance (*46*). A greater level of TG for the same amount of protein gives lower HDL cholesterol levels (*47*). Non-alcoholic fatty liver disease (NAFLD) is the stage preceding steatosis and is the first liver problem to occur in obesity/insulin resistance. Its early appearance makes it a suitable marker of present or future MetS (*48*).

Excess abdominal fat is composed of subcutaneous fat, visceral fat and retroperitoneal fat. It was first postulated in 1990 by Bjoïrntorp that visceral fat was more important in MetS due to its increased lipolysis, decreased sensitivity to insulin and proximity to the hepatic portal vein (*49*). Most researchers in the field adhere to this theory even though several studies have since attributed the effect on hepatic function to subcutaneous fat (*50, 51*).

There is still controversy about the respective role of visceral and subcutaneous fat. Figure 1 illustrates the interactions between MetS components.

iii) Insulino-glucocentric

The other position on MetS etiology is insulin resistance (*43, 52*). The insulin resistance view is supported by the fact that many lypodystrophies show several MetS features such as insulin resistance, dyslipidemia and ectopic fat distribution (*11*). Insulin resistance is found in all BMI categories. Presence of insulin resistance in slightly overweight people is called primary insulin resistance, whereas obesity creates secondary insulin resistance (*53*). The degree of insulin resistance in children is directly linked to the number of MetS characteristics (*54*). Increased FFA and insulin resistance amplify each other. In mice fed a high sugar and fat diet, insulin resistance develops before obesity (*55*).

The first enzyme that resists to insulin signals is the cAMP-dependent hormone sensitive lipase in adipocytes, which transforms TG into FFA and is usually inhibited by insulin. Thus, insulin resistance leads to increased circulating FFA, and ectopic fat in muscles, liver and pancreas as described above (*56*). In return, excess fat in these tissues creates insulin resistance. This is observed as decreased glucose uptake in muscles, increased glucose output from the liver due to decreased inhibition of gluconeogenesis and glycogenolysis, increased *de novo* lipogenesis in the liver, and increased insulin secretion from the pancreas. Most of insulin's effects on lipogenesis in the liver are mediated through SREBP1c and produce mono-unsaturated FA (*57*). This pathway is never resistant to insulin (*58*). Hyperglycemia also activates ChREBP (carbohydrate regulatory element-binding protein) to further increase lipogenesis (*58*). In patients suffering from NAFLD, *de novo* lipogenesis accounts for 25% of the fat found in the liver in comparison to 5% in normal livers (*59*). In the liver, NAFLD is also accompanied by prothrombic factors secretion (*43*). Increase in circulating FFA generates increased synthesis of very-low density lipoprotein and consequently increased levels of TG in the blood, which are good indices of insulin resistance (*60*). Higher levels of TG are also associated with higher levels of small dense LDL and lower levels of HDL cholesterol due to decreased cholesterol ester, and to increased HDL clearance (*61, 62*). Small and dense LDL are

more atherogenic because they cross the endothelial basement membrane, bind to glycosaminoglycans, are more readily oxidized, and bind more readily to scavenger receptors on monocytes in atherogenic plaques (*63*).

Insulin resistance contributes weakly to hypertension (*64*). Insulin usually dilates blood vessels, increases sodium reabsorption by kidneys signalling through the sympathetic nervous system. However, insulin resistance affects only blood vessels, leading to more vasoconstriction concurrent to increased blood volume (*65-67*). In addition, FFAs also cause vasoconstriction (*68*). Recently, it has been proposed that the renin-angiotensin system plays a role in insulin signalling. Angiotensin II receptor inhibitors, which are common anti-hypertensive drugs, have been shown to increase insulin sensitivity (*69*).

In addition to the features mentioned above, insulin resistance has been associated with an increase in asymmetric dimethylarginine, which inhibits nitric oxide synthase leading to endothelial dysfunction (*67*), an increase in uric acid due to decreased insulin inhibition of reabsorption (*70*) and an increase in homocysteine (*71*). Normally, in the fed state, leptin and insulin increase energy expenditure and thermogenesis and decrease food intake through the anorexigenic pathway in the hypothalamus. This allows for weight regulation over a long period (*72*). Leptin also decreases ectopic fat accumulation, but leptin resistance is a common feature in MetS (*73*).

iv) Inflammation

A new position that is gaining popularity is the role of inflammation in MetS's etiology. The adipose tissue secretes several adipokines such as TNF-α and Ad. TNF-α is the most important autocrine and paracrine molecule secreted by the adipose tissue and it increases lipolysis and secretion of FFA. It inhibits, through NF-κB (nuclear factor κ B), the expression of adipocyte genes implicated in glucose and FFA entry and storage (*74*). It also decreases the expression of *Ad, GLUT-4 (glucose transporter 4), IRS-1(insulin receptor substrate 1), PPAR-γ (peroxisome proliferative activated receptor γ)* and *perilipin* genes in adipocytes. It increases the expression of *vascular cell adhesion molecule 1, plasminogen activator inhibitor 1, IL-6, IL-1β, angiotensinogen, resistin and*

leptin genes (*75*). However, its inducing factor is unknown (*76*). The levels of TNF-α increase with weight (*77*). TNF-α increases maturation and activation of SREBP1c (*78*). IL-6 inhibits adipogenesis and Ad secretion and induces insulin resistance in the adipose tissue and the liver (*79*).

Adipose tissue also contains macrophages that secrete and respond to different cytokines (*80*). Under normal physiological conditions, macrophages found in adipose tissue do not participate in insulin resistance. In a situation of obesity-induced inflammation, MCP-1 (monocyte chemoattractant protein 1) secreted by adipocytes attracts activated macrophages, which secrete inflammatory mediators and increase insulin resistance (*81*). Inflammation triggers oxidative stress, which leads to hypertension, atherosclerosis, diabetes and obesity (*82*). More precisely, pro-inflammatory cytokines activate NF-κB in the endothelium, which increases nitric oxide (NO) production (*83*). NO produces reactive oxygen species, which decrease insulin secretion in the pancreas, induce insulin resistance and create oxidized-LDL that are engulfed by macrophages in the atherosclerotic plaques (*84, 85*). Oxidized-LDL further stimulate this pathway by activating NF-κB (*86*). CRP increases LDL uptake and cytokine secretion from macrophages as well as expression of adhesion molecules at the surface of the endothelium, leading to endothelial dysfunction and intimal-medial thickening (*87, 88*). IL-1β and interferon-γ inhibit insulin signalling and glucose uptake also via NF-κB (*89, 90*). Glucose, FFA and insulin also activate NF-κB and FFA increase reactive oxygen species directly through mitochondrial uncoupling and β-oxidation (*84*). In opposition, PPAR-γ, which is known to be involved in adipocyte differentiation and insulin sensitivity mediated by thiazolidinediones (TZD), inhibits NF-κB signalling (*91*).

v) Endoplasmic reticulum (ER) stress

A fourth and novel hypothesis is ER stress. The ER is a suitable location to modify cellular stress into inflammatory signals (*92*). ER stress is due to accumulation /overexpression of unfolded/mutant proteins, increased synthesis of secretory proteins, altered protein glycosylation, energy and nutrient variations, hypoxia, toxins, viruses, lipids, calcium depletion, and increased reduced state (*93, 94*). ER stress triggers the

unfolded protein response (UPR), which is a quality control mechanism. UPR is even more important in secretory cells (*94*). UPR increases protein folding through chaperones, increases protein degradation through the ERAD (ER-associated degradation pathway) and decreases protein synthesis (*94*). Chronic ER stress (also called ER stress response) uses up a lot of energy (*95*). It also releases calcium from the ER, which increases mitochondrial oxidative stress leading to inflammation through NF-κB (*96*). Activation of the CREBH transcription factor increases the amount of CRP and inflammation (*97*). Lipogenesis is increased in the liver due to the release of SREBP from the ER, allowing its translocation and activation in the Golgi (*98, 99*). ER stress is associated with increased VLDL and decreased HDL blood concentrations (*100*). It also increases G-6-Pase (glucose-6-phosphatase) levels and activity, leading to increased glucose production by the liver (*101*). ER stress is proportional to insulin resistance *in vitro* and *in vivo* (*102*). Administration of a huge quantity of chaperones restores insulin sensitivity (*103*). ER stress triggers insulin resistance by activation of JNK (c-Jun N-terminal kinase), which phosphorylates IRS-1 on serine residues, and by decreased insulin mediated tyrosine phosphorylation of IRS-1 and Akt (*104*). ER stress is found in the liver and adipose tissue, but not in the muscles, of obese mice. The exact causes of ER stress in obesity are still unknown (*105*). ER stress is also implicated in reduced insulin secretion from the pancreas through β-cells apoptosis (*106*).

2. Insulin

a) Insulin signalling

Insulin binding to its receptor triggers a large intracellular cascade implicating many factors (Figure 2). Only part of the total amount of cell surface insulin receptors (IR) is required for maximal response (*107*). There are two isoforms of the IR, which differ by the presence of exon 11 in IR-B. IR-A has a higher affinity for insulin, goes through increased internalization, and shows increased activation through the PI3K (phosphoinositide 3- kinase) pathway (*108, 109*). Alternative splicing is regulated differently in different tissues. Several studies were not conclusive about the role of different levels of IR-A vs IR-B in tissues (*110*). IR-A also has a higher affinity for IGF-I (insulin-like growth factor) and II than IR-B. IR-A is found in low amount in adult tissue,

but is more mitogenic (*111*). IR/IGF-1R hybrids are located all over the body (*112*). They act like IGF-1R, but have an additional affinity for insulin which is lower than IR (*113, 114*). Insulin regulates IR numbers as well as amount of IGF-1 and IGF-1R. Insulin resistant obese patients have increased insulin and IGF-1R levels as well as low IR and IGF-1 levels. It results in increased number of hybrid receptors in muscles (*110*). As seen in Fig 2, IR is composed of two extracellular α subunits and two intracellular β subunits linked together by disulfide bonds. Insulin binding to IR triggers a conformational change in the α subunits which brings the two β subunits into close proximity. This allows for cis and trans tyrosine phosphorylation of the β subunit and activation of IR tyrosine kinase activity. In this state, IR recruits and phosphorylates IRS-1 to 6. These substrates are common to all pathways, IRS-1 and 2 being the most important. Metabolic effects of insulin are mediated mostly through the PI3K pathway. PI3K allows for the production of phosphatidyl inositol-3,4,5 triphosphate which acts as a second messenger to activate phosphoinositide-dependent kinase 1. This serine/threonine kinase phosphorylates the serine protein kinases PKC and PKB (also named Akt). Akt/PKB allows for glycogen synthesis in the liver and muscles through inhibition of glycogen synthase kinase 3 activity. Akt decreases expression of PEPCK (phosphoenolpyruvate carboxykinase), G-6-Pase and others genes involved in glucose production through activation of the transcriptional repressor FOXO-1. Akt increases GLUT-4 translocation to the membrane and increases protein synthesis through mTOR (mammalian target of rapamycin) and inhibits apoptosis. GLUT-4 translocation is also triggered by PKC and the CAP/Cbl/TC10 pathway. In adipocytes, a recently discovered protein, AS160, links Akt to GLUT-4 translocation. Finally, Grb-2, Shc and SHP-2 activate the MAPK (mitogenic-activated protein kinase) pathway necessary for proliferation, growth, differentiation, apoptosis and protein synthesis (*93, 110*).

Thus, insulin signalling inhibits gluconeogenesis in liver, glycogenolysis in liver and muscles and FFA release from adipose tissue. It increases lipid synthesis in liver and adipocytes and glucose uptake in muscles and adipocytes through GLUT-4 (*110, 115*). Muscles remove 75% of the glucose from the blood (*116*). Uptake of glucose is the limiting step for glycogen synthesis in muscles (*117*). Liver and pancreas are permeable

to glucose through GLUT-2, which are constitutively found at the cell surface and are not regulated by insulin. Glucose entry is regulated by the glucose gradient. Insulin affects glucose entry in these organs by increasing intracellular glucose utilization, which consequently decreases intracellular glucose concentrations (*93*).

b) IR endocytocis

Regulation of insulin signalling is mostly mediated by insulin-stimulated endocytosis of the insulin-receptor complex. This process is used in the liver to clear plasma insulin and regulates the number of IRs located at the cell surface (*118*). IRs are specifically located in villi sections of the plasma membrane that are characterized by specific actin and lipidic organization. Once insulin has bound its receptor, the complex travels to internalization sites where it attaches to clathrin-coated pits (*119*). Internalization of the complex occurs with other receptors/molecules (*120*). Faure *et al.* recently proposed a new model of IR endocytosis where a complex formed of CEACAM1/β-catenin/SHP-1/Cdk2 facilitates IR accumulation at internalization sites through actin rearrangement. Upon binding to insulin, IR would be internalized with LRP1/SHP1/Cdk2 (personal communication from Dr. R.L. Faure). This is slightly different from the previous mechanism proposed by Carpentier *et al.* which postulated that insulin is important for transfer from villi to non-villi portions of the plasma membrane, but is not required for IR internalization once bound to clathrin-coated pits. Thus, insulin allows a rapid internalization of IR, which occurs constitutively at a slower rate (*121*).

Complexes are targeted to endosomes and IR autophosphorylation is required for this process (*122*). In endosomal insulin-receptor complexes, the IR tyrosine kinase is still active (*123*). It mediates signalling through interactions with molecules away from the plasma membrane such as IRS-1, PI3K and PKB (*124*). In addition, Rab5, a small GTPase important to endocytosis, is a mediator of IRS-1-PI3K interaction and activation (*125*). Some interactions can happen both at the plasma membrane and in the cytoplasm. However, it seems that acute signals are most often initiated at the membrane while long term ones emerge from endosomes (*126*). Acidification of the compartment allows dissociation of insulin from IR as well as conformational inactivation of IR kinase

activity (*127*). Free insulin is degraded sequentially by proteolysis (*128*). Unbound internalized IRs are dephosphorylated by PTP (phosphotyrosine phosphatases) surrounding endosomes (ER, perinuclear) and can no longer be rephosphorylated by insulin in endosomes (*129*). IRs are either degraded in lysosomes or recycled to the plasma membrane (*130, 131*). IRs must be dephosphorylated to recycle back to the plasma membrane (*132*). Recycled receptors are more sensitive to insulin than newly synthesized receptors (*133*). Processes that follow internalization are tightly regulated in part by PI3K and MAPK pathways (*134*). All these processes are accompanied by actin cytoskeleton rearrangements (*135*).

c) Insulin resistance mechanisms

Insulin resistance is defined at the systemic level by higher blood glucose for a given quantity of insulin. The gold standard for measuring insulin resistance is the laborious euglycemic hyperinsulinemic clamp study. Several alternative methods exist such as the measurement of fasting insulin levels (*136*). Insulin resistance leads to increased gluconeogenesis, which is an important factor explaining hyperglycemia and constant increase in insulin secretion from the pancreas. It also decreases glucose uptake from muscles and adipose tissue (*93*). Molecularly, insulin resistance is seen as a decrease in signalling downstream of IR (*137*). Mechanisms of insulin resistance represent a normal negative feedback mechanism that shuts down insulin signalling (*138*).

The most common cellular effect of insulin resistance is serine phosphorylation and/or decreased tyrosine phosphorylation of IR, IRS-1 and 2 (*110, 137, 139-141*). It is important to note that a reduction of IR autophosphorylation always translates into decreased kinase activity. However, it is possible to have normal phosphorylation with decreased IR activity (*137*). The major serine kinases implicated in IRS-1-mediated insulin resistance are JNK, IKKB and PKC (*93*). Serine phosphorylation results in decreased IRS-1 tyrosine phosphorylation and/or increased degradation. Serine phosphorylated IRS-1 can block binding to IR and/or binding to downstream molecules, or it can have an inhibitory effect on IR. The effect depends on the specific serine residue, and thus of the specific kinase, implicated. IR serine phosphorylation by kinases

such as JNK and PKC can lead to decreased IR autophosphorylation and/or decreased tyrosine kinase activity (*137, 142*). Several sources also affect other molecules in the PI3K/Akt pathway. It is important to note that insulin resistance affects the metabolic action of the insulin signalling pathway (*110*), but not the mitogenic cascade (*143*). Physical activity increases IR signalling independently of BMI (*144*), in part by increasing GLUT-4 translocation to the membrane (*145*). Hyperinsulinemia affects insulin signalling, but also decreases IR levels through reduced transcription and increased IR degradation (*92, 145, 146*).

In addition to phosphorylation-induced insulin resistance, hyperglycemia decreases insulin signalling through Ser/Thr glycosylation by increasing the flux through the hexosamine biosynthesis pathway (*147*). Hyperglycemia increases glycation, which is produced by a non-enzymatic reaction between protein free amino termini and glucose. In addition to diminishing insulin signalling, glycated groups are degraded into advanced glycation end-products, which are scavenged by their receptor (*148-150*). Oxidative stress enhances this degradation process and hyperglycemia downregulates soluble scavenger receptors. This process is implicated in problems related to diabetes (*151*).

Short term high fat diet (HFD) and high levels of circulating FFA, partly due to their intermediates, decrease the activity of several molecules downstream of IR (*149*). Saturated FFA increase the activity of the Munc18c protein, leading to decreased GLUT-4 translocation (*152*). HFD induces liver insulin resistance accompanied by normal peripheral insulin sensitivity, fasting glucose levels and basal hepatic glucose production. Liver insulin resistance was only seen in hyperinsulinemic euglycemic clamp studies (*141*). Ectopic fat activates JNK and MAPK and increases the amount of diacylglycerols which activates PKC (*142*). Adipose tissue overload increases the levels of fatty acid binding-protein 4, activating JNK and IKKβ (inhibitor of kappa B kinase) (*153*).

Inflammatory molecules such as TNF-α and IL-6 activate serine kinases to produce insulin resistance (*139, 154*). JNK further enhances this signalling by increasing the production of TNF-α (*92*). Salicylates, which are known anti-inflammatory agents,

inhibit IKKβ and decrease insulin resistance (*155*). In addition, JNK and IKKβ in liver, muscles and adipose tissue increase the expression of SOCS-1 and 3 (suppressor of cytokine signalling), which bind to IR and block access to IRS proteins (*156*). The levels of SOCS proteins are elevated in obesity-mediated insulin resistance (*157*). SOCS-6 also binds to IR (*158*). Another cytokine, MCP-1, decreases adipocyte glucose uptake through decreased IR tyrosine phosphorylation (*159*).

Increased expression and activity of PTP has also been observed in insulin-resistant muscles (*160*). The phosphatases PTEN and SHIP2 have been shown to inhibit insulin signalling by directly dephosphorylating IR and IRS-1 (*161*). PTP1B and LAR (leukocyte related-antigen) are overexpressed in obese patients and decrease after weight reduction in adipose tissue and muscle. However, the levels are lower in patients with T2DM (*162*). LAR and PTPα overexpression leads to insulin resistance, but their knockout has no effect on insulin sensitivity. Their *in vivo* effects are downstream of IR. The role of PTP1B is more evident as overexpression produces insulin resistance and deletion promotes insulin sensitivity (*163*). Recently, a SHP-1 defective mouse model demonstrated increased insulin sensitivity in liver and muscle due to increased tyrosine phosphorylation of IR, IRS-1 and 2 as well as increased activation of PI3K and Akt (*164*).

Exogenous NO and NO produced by iNOS (inducible nitric oxide synthase) in muscles decrease insulin signalling through nitrosation of cysteine residues in proteins such as IRβ, IRS-1 and Akt (*165*). iNOS is increased in insulin resistant muscle as well as in the context of T2DM, obesity and inflammation (*166*).

Endocytosis abnormalities translate into signalling and recycling problems. Decreased acidity in endosomes leads to decreased IR recycling and signalling (*167*). Increased life-time of insulin-receptor complexes in endosomes diminishes insulin degradation and IR recycling, which may trigger extensive signalling (*132*). Lower rates of IR internalization are accompanied by decreased amount of intracellular tyrosine phosphorylated IRs, which could be accompanied by different signalling (*168*). Glimeperide, a known hypoglycemic agent, increases dissociation and downstream processes of IR trafficking (*169*).

3. Adiponectin

Ad was discovered ten years ago simultaneously by four different groups. It was given several names such as Acrp30 (*170*), AdipoQ (*171*), apM1 (adipose tissue most abundant protein) (*172*) and GBP28 (gelatin-binding protein) (*173*). Ad represents approximately 0.01% of total protein in blood with concentrations between 5-10 μg/ml i.e. three times more elevated than leptin concentrations. It is one of two adipokines which are decreased in obesity (*174*). Low adiponectin levels are clinically associated with mutations in the *Ad* gene, MetS components such as T2DM, CVD, insulin resistance, obesity, hypertension and dyslipidemia, an increase in androgen/testosterone, oxidative stress, ectopic fat and steatosis (*175, 176*). Genetic studies demonstrate an inverse correlation between Ad levels and the number of MetS components present (*176*). Different *Ad* knockout models display characteristic of MetS (*177*). From these evidences, Ad is hypothesized as the underlying factor of MetS (*176*). In fact, Ad levels are most closely associated with one MetS profile, which exhibits obesity as the most important component followed equally by insulin resistance, dyslipidemia and hypertension (*178*). On the other hand, elevated Ad concentrations are found in patients with heart and renal failures. Weight loss, consumption of oil and soy and treatments with drugs such as TZD, ARB (angiotensin II receptor blockers) and ACEI (angiotensin-converting enzyme inhibitors) are also associated with increased Ad concentrations (*175*).

a) Gene expression

The *Ad* gene is located on chromosome 3q27 (*179*). Ad is mostly expressed in adipocytes (*171*). Adult transgenic mice overexpressing exogenous Ad in adipocytes show reduced Ad mRNA and protein in fat as well as in blood, indicating negative regulation of Ad on its own promoter (*180*). Ad expression is increased during adipocyte differentiation and during fasting. It is decreased by oxidative and ER stress. It is modulated by several transcription factors and by lipid content (*181, 182*). Ad increases with increased fat mass until a certain threshold. In obesity, Ad expression in adipocytes is negatively correlated with the amount of visceral fat, but not of subcutaneous fat (*183*). IL-6, TNF-α, IL-1β and PAI-1 from adipocytes as well as endothelin from endothelial cells decrease Ad expression (*184-186*). Insulin reduces Ad expression and blood levels of Ad are

inversely proportional to blood fasting insulin levels (*187*). Ad expression and secretion in adipocytes are regulated by several hormones (androgen, progesterone, oestrogen, glucocorticoids and prolactin), mostly at the post-transcriptional level (*188*). The *Ad* gene has a PPARγ response element in its promoter and PPARγ agonists such as TZD increase Ad levels (*189*). Under conditions of stress, Ad is expressed by hepatic parenchyma, hepatic endothelial and muscle cells (*190-192*). Ad is found in osteoblasts (*193*). Ad is located in the apical region of the oviduct epithelium before its secretion and its levels are regulated by sexual hormones (*194*). Ad is secreted by cardiac myocytes (*195*).

b) Protein

Ad is a 244 amino acid protein of approximately 30 kDa (*170*). It assembles into low molecular weight (LMW) trimers and hexamers as well as into high molecular weight (HMW) 12 and 18-mers (*196, 197*). It is composed of an N-terminal signal sequence, a variable domain, 22 collagen repeats required for oligomerization and a globular C-terminal domain sharing homology with the TNF-α and C1q families as well as with the globular domain of collagen type VIII and X (*153, 170, 173, 198*) (Figure 3). The blood contains mostly fAd in hexamers or in HMW forms (*199*). gAd is found in very small amounts in plasma and is probably produced by cleavage of fAd by monocyte and neutrophil leukocyte elastase (*198, 200*). It cannot form higher structures than trimers (*200*). Ad undergoes several post-translational modifications. Disulfide bonds between cysteines in the collagenous domain are required for formation of structures higher than trimers (*199*). Several proline and lysine residues in the variable and the collagenous domains are hydroxylated and hydroxy-lysines are further glycosylated (*201*). HMW complexes are more heavily glycosylated. Hydroxylation and glycosylation of four lysine residues in the collagenous domain are crucial for HMW complex formation and stability as well as for the insulin-sensitizing effect of Ad (*202-204*).

In most functions, HMW complexes are largely or totally responsible for the effects of Ad. Higher levels of HMW complexes are associated with better parameters of insulin sensitivity, abdominal fat and lipid profiles (*23, 175, 205*). LMW complexes are still important because they are, as HMW complexes, proportional to FA β-oxidation and

inversely proportional to carbohydrate oxidation (*206*). The proportion of HMW is higher in adipocytes than in blood. TZD, an insulin-sensitizing PPARγ agonist, increases the proportion of HMW complexes in blood (*207*).

Ad is secreted from adipocytes through intracellular vesicles distinct from those used by GLUT-4 and the endosomal marker transferrin receptor (*208*). This process is regulated differently in diverse fat pads and insulin increases Ad secretion through PI3K (*183, 208*). Blood Ad levels are not subject to acute regulation, but follow a circadian cycle showing an approximate 30% reduction at night (*209*). This cycle is lost in obesity and T2DM (*187*). After puberty, females have higher blood Ad levels as well as higher proportions of HMW complexes than males (*188, 199*).

The Ad clearance mechanism is unknown. Ad is found in urine (*199, 210*). Oligomers are highly stable in blood and do not dissociate with time or stimuli. Under basal conditions, HMW complexes have a longer half-life than LMW complexes, but their fate is unknown under stimulating conditions. One group hypothesized that after stimulation HMW complexes are reduced by proteolytic cleavage to produce gAd (*207*).

c) Adiponectin receptors

Two adiponectin receptors, AdipoR1 and R2, have been discovered, and share 67% homology. AdipoRs are integral membrane proteins with the C-terminus and the N-terminus located extracellularly and intracellularly, respectively. This topology is the opposite of the one usually found in seven transmembrane G protein-coupled receptors (*211*). However, AdipoRs do not seem to be coupled to G proteins since no differences were observed in intracellular cAMP, cGMP and Ca^{2+} upon stimulation (*211*). AdipoR2 is characterized by a smaller intracellular domain. AdipoR1 and R2 can form homo and hetero-oligomers. AdipoR1 has strong affinity for gAd and low affinity for fAd. AdipoR2 has intermediate affinity for both forms of Ad. They are highly conserved in mammals, mostly in their seven transmembrane domains (*211*).

Both receptors are expressed in multiple tissues. AdipoR1 is found in huge amounts in muscles, whereas AdipoR2 is mostly found in hepatocytes (*190, 211*). AdipoR1 is constitutively expressed in adipocytes, whereas AdipoR2 expression increases during adipocyte differentiation, partly due to growth hormone (*212*). AdipoR1 expression in the brain and AdipoR1 and 2 expression in muscle and liver increase during fasting period and rapidly return to normal upon refeeding (*213, 214*). Overexpression of exogenous Ad in adipocytes results in decreased AdipoR2, but not AdipoR1 levels. In addition, Ad knockout (ko) mice have increased AdipoR2 in fat, but not AdipoR1 (*180*). Insulin decreases their expression in muscle and liver (*213*). AdipoR1s are regulated by the amount of fat in adipocytes (*215*). Finally, low levels of AdipoRs were found in muscle, liver and adipose tissue of obese mice and were concurrent to decreased AMPK (AMP-activated protein kinase) activity (*213, 216*). Together with the observation of low Ad levels in obesity, the following vicious cycle was proposed. Obesity is also often accompanied by high insulin concentrations, which would further decrease AdipoR expression. Downregulation of AdipoR or "Ad resistance" would amplify the decrease in Ad signalling due to low Ad levels, causing additional insulin resistance and consequently hyperinsulinemia (*177*). AdipoRs are also found in monocytes, in pancreatic β cells, in smooth muscle and the in endothelium of the vascular system, in the adrenal cortex, in cardiac myocytes and in lymphocytes (*195, 217-220*).

AdipoRs have been recognized to mediate most of Ad's effects. In the liver, AMPK activation was attributed to AdipoR1, whereas AdipoR2 was associated with PPARα signalling (Figure 3). AdipoR2, but not R1, ko mice were hyperinsulinemic. Interestingly, AdipoR1 and R2 double ko mice were more insulin resistant than Ad knockout mice, suggesting the presence of other ligands, or of low receptor constitutive activity (*216*). Following Ad binding, the intracellular domain of AdipoR1 associates with the adaptor protein APPL, beginning the intracellular cascade (*221*).

Hexameric and HMW Ad bind to a member of the cadherin family of cell adhesion molecules, T-cadherin, in muscle, but not in the liver (Figure 3). Since T-cadherin lacks an intracellular domain, it is postulated that it acts as a co-receptor (*222*).

d) Functions

i. Insulin sensitizing hormone

In different *in vivo* settings, supplementation of fAd or gAd increases insulin sensitivity (*177*). These effects were observed with and without differences in weight and insulin levels, indicating an independent effect (*177*). In one case, insulin sensitivity was completely restored by infusion of both adiponectin and leptin, suggesting that these are the two most important hormones regarding insulin sensitivity (*223*). Different *Ad* ko mouse models are all characterized by insulin resistance, but to different degrees and under different conditions (*224*). These differences are probably due to different mouse genetic backgrounds (*175*). Results are more consistent with the overexpression of Ad than with its absence (*225*). The insulin-sensitizing role of Ad is also endorsed by several genetic studies demonstrating association between certain polymorphisms, low Ad levels, increased insulin resistance and risk of T2DM (*177*).

Intracellular analysis revealed different mediators of the effects of Ad. These were summarized by Kadowaki *et al* in their reviews (Figure 3) (*175, 177*). Ad binding to its receptors activates the AMPK and the PPARα pathways. Both fAd and gAd mediate effects in muscle, while only fAd has an effect in the liver. In muscle, AMPK and MAPK activation leads to increased GLUT-4 translocation and glucose uptake, as well as to increased β-oxidation through inhibition of acyl-CoA carboxylase. In liver, AMPK activation increases β-oxidation and decreases expression of enzymes involved in gluconeogenesis such as PEPCK and G6Pase. In both organs, β-oxidation is also stimulated by PPARα activation, in part through MAPK, and ensures low levels of ectopic fat. Increased glucose uptake in muscles, decreased glucose output from liver and decreased TG in tissues all improve insulin sensitivity. The AMPK activation seems to mediate its effect in a short term (< 6 h), whereas PPARα acts more on a long term scale (>6 h). gAd also increases glucose uptake through AMPK in adipocytes (*226*).

Ad is implicated in the regulation of body energy at the peripheral level through increased thermogenesis (*227*). Ad levels increase in the brain during fasting periods and, through AMPK, increase food intake, thermogenesis and insulin sensitivity (*214*).

ii. Cardiovascular protection

Overexpression of Ad decreases the size of atherosclerotic lesions in a known model of atherogenesis without changes in blood lipid and glucose concentrations (*228*). *Ad* ko mice are characterized by increased neointimal formation after injury (*229*). In addition, Ad binds lesions in the endothelium (*230*). These observations are explained by different molecular mechanisms. Ad inhibits phosphorylation of IKKβ and thus activation of NFκB signalling mediated by TNF-α (*231*). This represses the expression of adhesion molecules in the endothelium after injury. Ad also decreases foam cell formation through decreased expression of scavenger receptor class A-1 in macrophages, which results in decreased uptake of oxidized LDL (*232*). Ad reduces the proliferation and migration of smooth muscle cells induced by growth factors via decreased ERK signalling and sequestration of the platelet-derived growth factor BB (*177*). In addition, Ad up-regulates the production of IL-10, which increases TIMP-1 (tissue inhibitor of metalloproteinases-1) and stops lesion progression (*233*).

There is no independent association between Ad levels and CVD. An indirect link may exist through modulation of HDL levels. *Ad* tg+ and ko mice do not show differences in basal lipid levels in the blood. However, Ad tg+ females have increased lipid clearance after gavage (*234*). Ad, by increasing LPL and decreasing hepatic lipase activities, would positively modulate levels of plasma lipoproteins (*205*).

Ad increases blood vessel formation in two models of angiogenesis and *Ad* ko mice show decreased angiogenesis after ischemia (*235, 236*). NO is important in angiogenesis and vasodilation. Ad increases NO production by AdipoR-bearing endothelial cells in aorta, (*237*). Ad inhibits apoptosis of cardiac and endothelial cells (*238*). *Ad* ko mice are characterized by increased infarct size, apoptosis and TNF-α levels after an ischemia-reperfusion experiment (*236, 239*).

iii) Anti-inflammatory molecule

Ad inhibits secretion of the pro-inflammatory molecules IL-6, IL-8 and MCP-1 from adipocytes (*240*). It also increases IL-10 and IL-1R antagonist secretion by macrophages,

monocytes and dentritic cells and decreases production of IFN-γ (interferon gamma) by macrophages (*241*). gAd, through AdipoR1, inhibits NFκB signalling induced by Toll-like receptors in activated macrophages (*242*). Low Ad is associated with high levels of CRP in the blood and adipose tissue (*243*). Ad decreases the T cell allogenic reaction (*241*). LMW and HMW Ad induce cell apoptosis and decrease scavenger receptor expression in macrophages. After LPS activation, LMW Ad decreases IL-6 and increases IL-10 secretion by macrophage while gAd amplifies TNF-α secretion from macrophages, which, over a certain time, triggers IL-10 secretion and the shut down of the reaction (*244, 245*). Ad may reduce inflammatory events by directly binding to some chemokines via its globular domain (*246*). Induction of Ad expression in non-adipose tissues in response to stress could be an anti-inflammatory mechanism (*225*).

Ad protects against liver diseases such as NAFLD, which progress to the inflammatory stages of steatosis and fibrosis in different mouse models (*79*). In the liver, Ad inhibits TNF-α signalling, increases β-oxidation and decreases lipid synthesis through reduced expression of SREBP1c, which leads to a decrease in FAS (fatty acid synthase) and ACC (acetyl-CoA carboxylase). It is also associated with decreased levels of hepatic enzymes in the blood (*247, 248*).

iv) Adipocyte differentiation

Ad acts in an autocrine manner in the differentiation of adipocytes. Ad mRNA levels increase up to 100-fold in the middle of this process (*170, 171, 182*). Ad accelerates adipocyte differentiation, and increases lipid storage and glucose uptake by mature adipocytes (*234, 249*). This led to the hypothesis that Ad acts as a lipid sensor in adipocytes, specifying the space left for fat accumulation through adipocyte size (*249*).

v) Cancer prevention

The role of Ad in cancer is a new field and few clinical studies have been reported. Ad levels are negatively correlated with the risk of obesity/insulin resistance-related cancers such as endometrial, breast, acute myelogenous leukemia, colon, gastric and prostate cancers. In some cases, low levels of Ad were associated with higher tumour grades and

stages (*250*). Kelesidis *et al* proposed several mechanisms linking Ad and cancers. Low Ad is often associated with high insulin levels, which negatively regulates production of IGFBP-1 and 2 (insulin like growth factor binding protein) by the liver and tissues. This leads to higher levels of IGF-1 in plasma. Insulin and IGF-1 increase mitogenic and decrease apoptotic signals through their receptors. Ad also sequesters some growth factors (*250*).

Ad activates several cellular pathways, which can be linked to cancerous signalling. Ad signals through AMPK, which inhibits FAS. This enzyme was associated with colon, breast, prostate and ovarian cancers. AMPK also activates an inhibitor of mTOR, which is part of the PI3K pathway often constitutively active in cancers. mTOR itself was associated with colon, breast, prostate, liver and lung cancers. Ad inhibits the production of reactive oxygen species. Low amounts of these molecules may increase levels of NO, decreasing the amount of oxidized LDL and their activation of mitogenic pathways (*250*). Ad triggers endothelial cell apoptosis and inhibits endothelial proliferation and migration around tumours (*251*). Finally, Ad may signal through JNK and the transcription factor STAT3 to negatively regulate tumour growth (*250*).

e) Characteristics of the Ad transgenic (tg+) mouse model generated by Dr. P.E. Scherer

It is quite difficult to overexpress Ad in adipocytes due to the high quantity already present and to the feedback inhibition of Ad on itself and on its receptors (4). Dr. Scherer created an *Ad* tg+ mouse model, which elevates serum Ad through increased secretion and not expression. 50% of Ad produced in adipocytes is degraded. This tg+ model is characterized by the expression of a truncated transgene lacking 13 of the 22 collagen repeats. This transgene is under the control of the AP2 promoter and is expressed in low amounts specifically in adipocytes. It forms heterotrimers with the wildtype Ad monomers, which inhibit the degradation of wildtype homotrimers and lead to increased secretion of these functional homotrimers. The heterotrimers are never excreted. The distribution of HMW Ad vs LMW Ad is conserved. Detailed characteristics of this mouse model are described in Table 1 (*234*). Briefly, these mice are characterized by increased insulin sensitivity due to increased insulin hepatic inhibition of

gluconeogenesis. There is no difference in glucose uptake, glycolysis or glycogen synthesis. The *Ad* tg+ mice are resistant to diet-induced insulin resistance. Brown adipose tissue is increased in these mice in the interscapular and orbital regions. This phenotype increases with age and is stronger in females than in males. Females are sterile, and have increased lipid clearance and LPL activity (*234*).

4. Association of MetS with cancer

Presence of a MetS cluster (ie $\geq$ 3 components) is associated with increased incidence and death from colorectal cancer in men in three independent epidemiological studies comprising a total of 85 000 patients (*252-254*). It is also related to increased colon adenomas in men (*255*). The gender differences may be explained by hormone status and amount of visceral obesity (*256, 257*). One report linked MetS to increased breast cancer risk (*258*). The increased risk from MetS relative to those of individual risk factors is possibly explained by the fact that these risk factors have different carcinogenesis mechanisms (*256*).

Many epidemiological studies correlate the individual components of MetS to several cancers. The most defined are colorectal and breast cancers. Others include endometrial, esophageal, liver, gallbladder, stomach, kidney, prostate, pancreas and cervical cancers. Obesity, insulin resistance/hyperinsulinemia/T2DM/hyperglycemia, inflammation and low HDL levels are independently associated with increased risk of several of these cancers (*256*). The molecular mechanisms explaining these epidemiological associations include increased ROS, hormone levels (oestrogen, IGF-1, insulin, adipocytokines) and energy substrate concentrations. These would respectively damage DNA, increase proliferation and angiogenesis as well as decrease apoptosis and supply energetic fuel to highly metabolic cancerous cells (*256*).

The L-SACC1 mouse model, which overexpresses a dominant negative form of the CEACAM1 molecule specifically in the liver, clearly demonstrates several characteristics of MetS (see section below). Preliminary data indicated a similar phenotype for the *Ceacam1* ko mouse model (*259*). In addition, CEACAM1 is downregulated in early

stages of several cancers (see below). These two mouse models are thus interesting to study MetS molecular mechanisms and their relation to cancers.

B) The CEACAM1 molecule

CEACAMs (CEA-related cell adhesion molecule) are a class of molecules belonging to the CEA (carcinoembryonic antigen) family and to the Ig (immunoglobulin) superfamily. They are found only in mammals (*260*). CEACAM1 is the most conserved molecule among species in this family (*260*). The CEA family contains 18 genes and 11 pseudogenes located on chromosome 19q13.2. The family is divided into PSG (pregnancy-specific glycoprotein) and CEACAM branches (*261*). CEACAM1 was given its name in 1999. It was previously identified as biliary glycoprotein, BGP1, TM-CEA, CD66a, Bgp1, mCEA1, mmCGM1a, MHVR, bb-1, Cell-CAM105, C-CAM, C-CAMn, gp110, pp120, HA4, ecto-ATPase, CBATP, depending on the cells and species in which it was discovered and the function studied by different research groups (*260*).

1. Gene expression

The *Ceacam1* gene is found in humans, mice, rats, cows, dogs, elephants and opossums. In rodents, there are two different alleles named a and b, and mice have two homologous genes identified *Ceacam1* and *Ceacam2* (*260, 262*). Most inbred mice have the "a" allele (*263*). The *Ceacam1* gene contains nine exons and eight introns (*264*). It encodes for one N-terminal IgV (variable) and three IgC2-type (constant A1, B1, A2) extracellular domains, a transmembrane domain and a cytoplasmic domain (*265, 266*). It produces up to 12 different protein isoforms by alternative splicing. Expression of the *Ceacam1* gene is highly conserved between species and is found in epithelial cells, in myeloid cells and lymphocytes, in hepatocytes and in the endothelium of microvessels (*267-269*). The *Ceacam1* gene is expressed in maternal tissues surrounding the embryo and in the placenta and has a specific pattern of expression in the embryo throughout gestation (*270*). The *Ceacam1* promoter is activated by the transcription factors USF and HNF-4, that respectively mediate anti-proliferative and liver-specific gene expression (*271*). *Ceacam1* mRNA and protein levels are increased by IFN-γ in epithelial cells through

interaction of interferon regulatory factor-1 with the *Ceacam1* promoter, but are decreased in macrophages (*272, 273*). The androgen receptor directly increases *Ceacam1* promoter activity (*274*).

2. Protein structure

The CEACAM1 protein is composed of 519 aa (*275*). The functional differences between isoforms containing different numbers of constant extracellular IgC domains are unknown (*276*). The intracellular domain is either long (L) with 71-73 aa or short (S) with 10 aa. Insertion of exon 7 generates the L domain (*264, 277*). High molecular weight complexes may form through activity of the transglutaminase enzyme on the L domain (*278*). Naming of splicing isoforms is done by a number indicating the number of Ig extracellular domains followed by the letter L or S for the intracellular domain. Mice express the CEACAM1-4S, -4L, -2L and -2S isoforms and humans eleven different isoforms (*260*). Soluble CEACAM1 isoforms, lacking the transmembrane domain have also been characterized and are found in different biological fluids. They block homo/heterophilic binding with membrane CEACAM1 (*279, 280*). The most characterized isoform is the CEACAM1a-4L and we will focus mainly on this one (Figures 4 and 5).

CEACAM1 is heavily glycosylated, with up to 50% of its molecular weight accounted for by sugars (*275*). It contains 16 possible asparagine sites for N-glycosylation, but no O-glycosylation sites (*275*). In hepatocytes, the sugar coat is formed by complex N-glycans with sialic acid residues and high-mannose N-glycans (*281, 282*). In neutrophils and endothelial cells, CEACAM1 is characterized by Lewis^x and sialyl Lewis^x epitopes (*283, 284*). CEACAM1 in neutrophils contains high-mannose N-glycans with fucose residues and galactoside moieties (*285*). The N-terminal binding site for most pathogens and for homo/heterophilic interactions is devoid of carbohydrate residues (*286*). In cultured fibroblasts, most of the L isoform is highly glycosylated and considered mature, whereas 50% of the S isoform is immature and degraded in lysosomes (*287*).

3. Signalling

CEACAM1 is present at the surface of epithelial cells in homodimers. These structures are disrupted by increased intracellular Ca^{2+} concentrations and subsequent calmodulin binding to the membrane-proximal domain and possibly by phosphorylation (*265, 288, 289*). Cis-homodimers are involved in few extracellular and intracellular interactions due to steric hindrance (*289, 290*). The two most important factors in determining binding partners of CEACAM1-L are the L/S ratio and extracellular homotypic binding. L/S ratios change with cell signalling (*291-293*). In the long cytoplasmic tail, two tyrosines (Y488 and Y513 (515 in mouse)) are positioned within an ITIM (immunoreceptor tyrosine-based inhibitory motif) and at least one serine (S503) out of the 17 present in kinase consensus sequences are often phosphorylated (*294*). C-terminal amino acids and phosphorylation of tyrosines are required for interaction with the tyrosine phosphatases SHP-1 and SHP-2 (*295, 296*). These tyrosines can be phosphorylated by Src-like kinases or the insulin or EGF (epidermal growth factor) receptors and, once phosphorylated, can bind other kinases of this family and lead to their activation (*297, 298*). The CEACAM1 intracellular domain binds to tropomyosin and actin, explaining concordant cytoskeleton rearrangement in most CEACAM1 functions (*299*). The phosphorylated Y488 of the L domain has been shown to interact with the cytoskeleton component paxillin and with integrinβ3 (*300, 301*). From these facts and T cell experiments, Gray-Owen and Blumberg proposed a mechanism of action for CEACAM1-L in T cells (Figure 4). Since signalling from CEACAM1 is similar in different cell types, this model can be modified to be applied in other systems.

4. Functions

a) Intercellular adhesion and migration

CEACAM1 mediates Ca^{2+}-independent homophilic and heterophilic intercellular adhesion through binding of its N-terminal domains (*277, 290, 302*). CEACAM1 also interacts with CEA and CEACAM6 (*290*). In epithelial cells, CEACAM1-L is recruited to intercellular contact sites through Rho-like GTPases, where it associates with polymerized actin intracellularly and with another CEACAM1 molecule extracellularly (*303*). Lateral, but not apical, distribution of CEACAM1-L in polarized epithelial cells is

maintained only by intercellular adhesion in adherens junctions. CEACAM1-S is only apical and mostly in the bound state (*304, 305*). Homotypic intercellular adhesion is performed in the trans conformation and the strength of the interaction increases with the number of IgC2 domains (*286, 306*). Phosphorylation of the L cytoplasmic domain is not required for intercellular adhesion (*307*). Cleavage of the L domain by caspase 3 during the apoptosis process increases the strength of intercellular adhesion (*308*).

CEACAM1-L promotes migration. However, its association with the cytoskeleton component filamin-5 inhibits migration (*309*). Association between phosphorylated Y488 of CEACAM1-L and integrinβ3 may be involved in cell invasion (*300*).

b) Angiogenic factor

CEACAM1 was observed in newly formed microvessels found in normal tissues undergoing constitutive proliferation/regeneration, in hypoxic tissues, in wound healing and in tumours, but not in large vessels from which they originate (*284, 310-312*). Its expression is increased by TNF-α (*313*). VEGF (vascular epidermal growth factor) increases CEACAM1 mRNA and protein levels in endothelial cells and in the medium of cultured cells (*312, 314*). Soluble CEACAM1 increases proliferation and chemotaxis of endothelial cell as well as formation of microvessels *in vitro*. It increased the vascular density in an *in vivo* model of angiogenesis (*314*). At the molecular level, overexpression of CEACAM1 in endothelial cells increases mRNA levels of several angiogenic factors as well as protein levels of VEGF (*311*). CEACAM1 seems to act downstream of VEGF and their effects are additive (*314*). Indeed, different *Ceacam1* mouse models confirmed the role of CEACAM1 in invasion of extracellular matrices, formation of the endothelial tube, integrity of capillaries and interactions with accessory cells. S503 and Y488 in the L domain are necessary for these activities. In initiation of neoangiogenesis, CEACAM1 is involved in cytoskeleton rearrangement and in interaction with extracellular matrix integrins, leading to migration of endothelial cells (*315*). However, *Ceacam1-/-* mice do not show vascularization problems during development (*316*).

c) Bacterial and viral receptor

The protein produced by the *Ceacam1a* allele is a receptor for the mouse hepatitis virus and *Ceacam1-/-* mice are resistant to infections by this virus (*262, 316*). In humans, the CEACAM1 sugar coat allows binding of *E. coli* and *Salmonella* bacteria (*317, 318*). Several strains of *Neisseria* bacteria bind CEACAM1 on epithelial, phagocytic cells and lymphocytes through their Opa protein (*313, 319*). CEACAM1 is also bound by *Haemophilus influenzae* and *Moxarella catarrhalis* (*276*). Most pathogens bind to the N-terminal variable domain. The apical localization of CEACAM1 in mucosal epithelium makes it a good entry site for pathogens (*320*). Through different mechanisms, mostly inhibitory, pathogen binding to CEACAM1 is a resistance mechanism against the host immune system.

d) Regulation of immune cells

The amount of CEACAM1 on the surface of T lymphocytes is low in CD4+ T cells and absent on CD8+, γδ and intestinal intraepithelial lymphocytes (*276*). CEACAM1 is transported from intracellular compartments to the cell surface upon activation. This event happens in the first 30 minutes, with similar kinetics as the activation marker CD69 and before the major inhibitory molecule CTLA-4 (cytotoxic T-lymphocyte antigen 4) (*276*). Activation can be triggered by cytokines (IL-2, IL-7, IL-15), ligation of the T cell receptor or chronic inflammation (*276*). Several studies revealed an inhibitory role for CEACAM1-L on T cell proliferation, cytokine secretion and cytotoxic function (*276*). However, *Ceacam1-/-* mice show only a very small increase in proliferation and cytokine production and only at very high stimuli concentrations (*321*). In addition to its role downstream the T cell receptor, CEACAM1 binds to the IL-2 receptor, inhibits signalling downstream of it and downregulates its expression (*322*). Only two studies demonstrate CEACAM1-induced hyperproliferation, which could be a real function under specific conditions or experimental artefacts (*276*).

B cell receptor stimulation changes the ratio of L to S isoforms, but the two studies on cell proliferation gave opposite results (*294, 323*). CEACAM1 is up-regulated during B cell development through binding of early B cell factor to *Ceacam1* promoter (*324*). The

presence of CEACAM1-L at the surface of natural killer cells is induced by activation and inhibits their cytotoxic function (*276*). Upregulation of CEACAM1 expression in some cancers would decreased tumour immunosurveillance by this mechanism and explain the association with poor prognosis and increased invasiveness (*276*). Overexpression of CEACAM1 is observed in melanomas, lung adenocarcinomas, non-small cell and squamous cell lung cancers, in gastric carcinomas, as well as in highly metastatic colon tumour cells (*325-330*). CEA-CEACAM1 interactions also inhibit natural killer cell cytotoxicity (*306*). The first report on CEACAM1 in dentritic cells shows a role in maturation and antigen presentation through an increase in cytokines (*331*). In contrast to rodents, human leukocytes are devoid of the S isoform (*332*). The role of the S isoform in the immune system is unknown, but seems stimulatory (*276*).

e) Suppression of tumour growth

CEACAM1 inhibits tumour epithelial cell proliferation when the ratio of L vs S isoforms is kept at a physiological level (*291, 333, 334*). Phosphorylation of S503 and Y488 is required for this effect, but not extracellular homophilic interaction (*333-335*). Part of the inhibitory function is mediated by the association of ITIM in the L domain with SHP-1 tyrosine phosphatase (*295*). CEACAM1 also has a positive effect on apoptosis in enterocytes (*336*). CEACAM1-4S is implicated in epithelial apoptosis during lumen formation in mammary glands (*337*). Introduction of CEACAM1-4S to breast tumour cells lacking CEACAM1 reverts them to their normal state (*337*). Serine and threonine residues are important for this morphogenic event (*338*). The effect of CEACAM1 on cell proliferation is dependent upon the state of the cell. In highly dividing adherent cells reaching confluence, CEACAM1 is implicated in growth contact inhibition. However, in non-confluent, suspension and/or low growth factor cells, CEACAM1 amplifies the growth factor proliferation response. This is done through modulation of ERK1/2 (extracellular signal-regulated kinase) kinases and the cell cycle inhibitor p27 (*339, 340*).

CEACAM1 expression levels are reduced in hepatocellular, prostate, 30% of breast, endometrial, bladder, kidney, thyroid and colorectal cancers (*341-346*). In fact, its levels start to decrease in pre-cancerous stages and this increases their tumorigenic potential

(*347, 348*). In colon cancer, it is reduced in aberrant crypt foci and in hyperplastic polyps to the same extent as in adenomas and carcinomas. This event happens before known mutations in the *Apc (Adenomatous polyposis coli)* gene (*336*). This reduction is in part explained by an augmentation in the transcriptional repressor Sp2, which interacts with the *Ceacam1* promoter and recruits histone deacetylase (*349*). CEACAM1 levels in tumour cells are inversely proportional to stages and grades of the tumour. Low levels of CEACAM1 correlate with disappearance of cell polarity (*341, 347, 350*). In prostate and bladder cancers, the downregulation of CEACAM1 in tumour epithelial cells increases angiogenesis through VEGF secretion and CEACAM1 up-regulation in tumour microvessels (*345, 351*).

Ceacam1-/- mice do not normally develop tumours and have normal lifespans (*316*). However, upon chemical carcinogen induction, they show increased colon tumour numbers and size due to increased cellular proliferation and decreased apoptosis. Normal tissue surrounding these tumours is characterized by decreased levels of cell-cycle inhibitors p21 and p27 as well as decreased apoptosis (*352*). In $Apc^{1638N/+}$ mice prone to intestinal tumour development, *Ceacam1-/-* mice also demonstrate multiplicity, but the effect is far greater on the size and stage of tumours. This is mainly due to decreased apoptosis. No difference in the proliferation of the intestinal crypt cells is observed. Increased β-catenin translocation to the nucleus with decreased degradation as well as increased transcription of downstream targets such as c-Myc and Cyclin D1 in *Ceacam1 -/-* mice suggest an effect of CEACAM1 on the Wnt signalling pathway (personal communication from Dr. N. Beauchemin).

f) Metabolic regulation

i. Insulin receptor recycling

In 1985, Taylor *et al* was the first group to identify a protein of MW 120 kDa in insulin receptor preparations. This protein, called pp120, was mostly tyrosine phosphorylated only in the presence of insulin, with some delay in comparison to insulin receptor autophosphorylation. In the absence of insulin, only phospho-serine residues were observed and their amount decreased as insulin increased. Absence of co-

immunoprecipitation revealed weak or indirect interaction. Its localization to hepatic microsomes suggested a membrane glycoprotein (*353, 354*). This protein was later formally identified as the CEACAM1 protein (*260*). Most of the studies in that field were performed by researchers from the same group.

Only the CEACAM1-L isoform is phosphorylated in the presence of insulin and mutational analyses revealed that Tyr488 and Ser503, but not Tyr513, in the cytoplasmic tail of CEACAM1-L are required. Amino acid consensus sequence analysis suggested that Ser503 is phosphorylated by a cAMP-dependent kinase. Phosphorylation of this residue is a pre-requisite for Tyr488 phosphorylation and decreases after insulin treatment (*355*). Tyr513 apparently regulates the dephosphorylation of the Ser503 residue. A plausible mechanism would be conformational change induced by sustained Tyr488 phosphorylation, which allows recruitment of an unknown serine phosphatase (*356*). The extra-cellular domain of CEACAM1-L is not necessary for its insulin-mediated phosphorylation (*355*) nor for IR endocytocis (*357*). CEACAM1-L is phosphorylated on Tyr488 by the C-terminus of the β subunit of the insulin receptor. The autophosphorylation of IR on Tyr1316 is crucial for phosphorylation of CEACAM1-L. The fact that the IR Tyr1316 residue is replaced by phenylalanine 1310 in IGF-1R explains why CEACAM1-L is only phosphorylated by IR. This event is responsible for the decreased mitogenic activity of IR in comparison to IGF-1R. Mutation of Tyr1316 to phenylalanine in IR does not affect insulin affinity for its receptor nor IR autophosphorylation (*358*). CEACAM1-L is the first substrate demonstrating selectivity of the IR and the IGF-1R. CEACAM1-L is not phosphorylated by the IGF-1R (*359*), in part due to its extracellular domain (*358*). IGF-1R is not endocytosed by CEACAM1-L (*360*). CEACAM1-L is also phosphorylated by EGFR upon EGF binding in hepatocytes (*361, 362*).

This insulin specific phosphorylation of CEACAM1-L increases the internalization of the insulin receptor. This is postulated to happen through clathrin-coated pit-mediated endocytosis since amino acid sequences around both tyrosines constitute recognition motifs for the adaptor protein AP-2 (*363*). Moreover, CEACAM1-L co-localizes with

another adaptor in this complex, α-adaptin. CEACAM1-L seems to be endocytosed with the insulin receptor since its surface localisation quantified by biotin labeling decreases only following insulin-stimulated phosphorylation (*364*). However, the same group previously observed no difference in IR endocytosis kinetics in conditions of decreased CEACAM1 expression, but saw an increase in IR accumulation at the cell surface (*355*). In addition, Fiset *et al* recently noted no difference in the amount of CEACAM1-L found in the hepatic endosomes/Golgi fraction after insulin treatment (personal communication from Dr. R.L. Faure). Phosphorylated Tyr960 in the juxtamembrane domain of IR is required for its endocytosis (*360*). CEACAM1-L is phosphorylated by both isoforms of the IR, IR-A and IR-B. However, it targets almost exclusively the high insulin affinity IR-A to endocytosis (*365*), even if IR-B is the most abundant form in the liver (*366*). The IR-A specific removal was postulated to prevent IR downregulation in the presence of high insulin concentrations in the portal vein (*367*). Phosphorylated CEACAM1-L does not interact directly with the IR, but insulin increases co-immunoprecipitation with four proteins. Two of them are tyrosine phosphorylated and this phosphorylation is drastically decreased in the CEACAM1-L Tyr488Phe unphosphorylable mutant. Choice *et al* postulated that CEACAM1-L recruits these two molecules to allow their phosphorylation by the IR (*364*).

Amino acid sequences surrounding both tyrosines are characterized by consensus sequences which allow interaction with SH2 domain containing proteins (*355*). SHP-1, which is highly expressed mostly in the cytosol but also in the nucleus of hepatocytes, was implicated in negative regulation of insulin signalling. Dominant negative SHP-1 mutants expressed in mouse liver increase insulin clearance through endosomal degradation. SHP-1 co-precipitates with CEACAM1-L, IR and the p85 subunit of PI3 kinase and dephosphorylates them *in vitro*. In presence of catalytically inactive SHP-1, dominant negative SHP-1 or shRNA against SHP-1, there is at least a three-fold increase in CEACAM1-L tyrosine (probably Tyr488) phosphorylation prior to and after insulin stimulation. This indicates that SHP-1 is a player in the CEACAM1 effect on insulin clearance and downregulation of growth and proliferation through the PI3 kinase/Akt pathway (*164, 296*). This was further confirmed recently in Dr. R.L. Faure's laboratory.

Analyses of rat livers did not reveal differences in phosphorylation, kinetics, complexes or amount of many proteins in the endosomes/Golgi fraction after insulin treatment. These changes were observed, however, in the presence of tyrosine phosphatase inhibitor or defective SHP-1. This indicates a rapid and tight regulation of IR downstream signalling by SHP-1 and other tyrosine phosphatases. From fractionation and co-immunoprecipitation experiments, this group proposed a model of IR endocytosis. At the plasma membrane, CEACAM1-L associates with β-catenin in the SHP-1/Cdk2/cyclinE complex to rearrange the actin cystoskeleton and form complete IR internalization sites. Upon insulin binding to IR, the endocytic receptor shuttling protein LRP1 displaces β-catenin from the complex and binds to IR, triggering its internalization. Thus, CEACAM1 would facilitate IR endocytosis, but would not be endocytosed with it (personal communication from Dr. R.L. Faure). Phosphorylation of Tyr63 in the cytosolic domain of LRP1 could also allow it to bind to Shc in endosomes (*368, 369*).

In addition to its role in insulin clearance, CEACAM1-L is implicated in the downregulation of mitogenic insulin signalling. Its phosphorylation by the IR is required for this effect (*359*). Tyr960 in the IR, which is also essential for IR endocytosis, partly mediates mitogenic signal following insulin binding as a Tyr960Phe IR mutant shows decreased mitogenesis. Presence of CEACAM1-L, both with wt and mutant Tyr960Phe IRs, drastically decreased the mitogenic effect of insulin, showing that the CEACAM1 effect is not only mediated by its role in IR endocytosis. Soni *et al* proposed a role for CEACAM1-L in sequestering SHP-2, which binds the phosphorylated Tyr1322 in the IR (*370, 371*) and to valine residue around the Tyr513 of CEACAM1-L in epithelial cells (*296*). CEACAM1-L would block SHP-2 binding to IR, which would decrease mitogenic signalling (*358*).

Poy *et al* showed that the molecule Shc binds to Tyr488 of CEACAM1-L through its SH2 domain and to the IR at pTyr960 through its phosphotyrosine binding domain. Recruitment of Shc to the plasma membrane by CEACAM1-L allows Shc to compete with IRS-1 for binding and phosphorylation by the IR. Interaction of Shc with CEACAM1-L decreases the interaction between IRS-1 and the p85 subunit of the PI3

kinase and leads to subsequent downregulation of the Akt pathway. Binding of Shc to CEACAM1-L also decreases signalling through the RAS/MAP kinase pathway by diminishing the tightness of the interaction between Grb2 and the IR. Both pathways are implicated in cell proliferation and growth. Akt is involved in the anti-apoptotic effect of insulin, and it is not known if CEACAM1-L signalling through this pathway increases cell death (*372*).

ii. Downregulation of FAS

CEACAM1-L seems also to be implicated in acute regulation of fat metabolism. Insulin is known to decrease TG output from the liver after a meal and this process is not seen in hyperinsulinemic patients (*373, 374*). Najjar *et al* proposed a mechanism to explain this observation. They found that the phosphorylated Tyr488 of CEACAM1-L interacts with the enzyme FAS following insulin binding to its receptor. This association downregulates the FAS enzymatic activity in a way that follows the biphasic mode of insulin secretion after a meal. This acute process is dependent on IR signalling since models of insulin resistance such as L-SACC1 mice (see below) and ob/ob obese mice do not show this phenomenon. Instead, FAS levels and activity are elevated during fasting in these mouse models. Levels do not vary with insulin output, but activity is further increased after refeeding. This was also seen in *Ceacam1* -/- mice, which were first shown to be hyperinsulinemic (↑ 3X) at two months of age. The downregulation of FAS required the expression of CEACAM1-L, as primary hepatocytes from the *Ceacam1* ko mice show no *in vitro* decrease in FAS following insulin signalling. This phenotype can be rescued by transfecting wildtype but not Ser503Ala CEACAM1-L cDNA (*259*). In addition, mice with inactive SHP-1 have elevated phosphorylation of CEACAM1-L and are characterized by a smaller amount of adipose tissue and blood TG (*164*). The summary of proposed mechanisms mediating CEACAM1-L effect in insulin signalling is illustrated in Figure 5.

iii. The L-SACC1 mouse model

To further support the role of CEACAM1-L in regulating insulin metabolism, a mouse model over-expressing a Ser503Ala dominant negative CEACAM1-L molecule in the

liver was produced in the laboratory of Dr. S.M.Najjar. Each allele contains six copies of a rat transgene which encodes for CEACAM1-L with a non-phosphorylable alanine residue at position 503. This blocks tyrosine phosphorylation of CEACAM1-L by IR and subsequent regulation. The transgene expression is driven by the human apolipoprotein A-1 liver-specific promoter. There were no phenotypic difference between the homozygous wildtype and the heterozygous mice. Thus, the L-SACC1 model consists of mice homozygous for the transgene.

The mouse demonstrates several characteristics associated with MetS and insulin resistance such as hyperinsulinemia, increased visceral adiposity, glucose intolerance, elevated FFA and TG in blood and elevated TG in the liver. Since FAS activity as well as tissue fatty acid biosynthesis are normal in male fed mice, excess free fatty acids have been postulated to come from increased lipolysis in adipose tissue (*367*). However, another study showed that L-SACC1 female mice have higher liver FAS activity during fasting and after refeeding (*259*). Park *et al* observed an increase in FAS protein levels, but did not look at its activity. There was no difference in the expression of lipoprotein lipase (LPL) in the liver and in the total body of these male mice, indicating unaltered lipolysis from adipose tissue (*375*). Thus, there is uncertainty about the source of excess fatty acids driving the excess synthesis of TG. These mice have normal food consumption (*376*). It was proposed that their hyperinsulinemia springs from reduced insulin clearance and leads, with elevated FFA, to major hepatic and minor peripheral (muscle and adipose tissue) insulin resistance, hyperglycemia and glucose intolerance (*375-377*). Females develop insulin resistance slightly later than males, which is characteristic of increased insulin sensitivity in females vs males.

C) Research hypothesis

As previously stated, the MetS cluster and individual components are associated in epidemiological studies with several cancers including colorectal cancer. However, these pathologies share several environmental cofounder effects (*378*). In addition to the epidemiological data, tumour induction in obese/high fat diet rat models or in presence of

chronic insulin injections have shown a direct link between insulin levels and increased colon cancer (*379*). *Ceacam1-/-* mice were at first characterized by a three fold increase in blood insulin levels (*259*). Fasting hyperinsulinemia is a secondary effect of insulin resistance and consequently is a good index. Hyperinsulinemic euglycemic clamp studies have now confirmed the presence of insulin resistance in *Ceacam1-/-* mice (Dr. Marette, Appendix 2). *Ceacam1-/-* mice do not develop colon and intestinal tumours even in old age, but demonstrate increased multiplicity and progression of tumours in models of carcinogenesis N (*352*)(personal communication from Dr. N. Beauchemin). This indicates a role for CEACAM1 in the progression, but not in the initiation of colon cancer.

The goal of this project was to determine to what extent hyperinsulinemia and insulin resistance contribute to the increased progression of colon/intestinal tumours in *Ceacam1-/-* mice. The plan was to reverse the insulin resistance by mating *Ceacam1-/-* mice with tg+ mice overexpressing the insulin-sensitizing hormone adiponectin. It was to be followed by tumour induction and quantitative and qualitative tumour analysis in different *Ceacam1 (CC1) : Ad* genotypes. We chose this particular *Ad* tg+ model because it overexpresses HMW fAd, which is the major circulating form available in plasma, at levels comparable to TZD treatment. It targets liver, which is the main location of CEACAM1 action in metabolism. Using endogenously produced Ad ensures correct post-translational modifications. A decrease of tumour number, size and/or stage in *CC1-/-* : *Ad* tg+ mice in comparison to *Ceacam1-/-* mice would assign a role of insulin resistance in the progression of colon cancer devoid of cofounders.

The first step consisted of transferring the *Ad* tg+ mice from the FVB to the C57Bl/6 background such as to equate their background with the *Ceacam1-/-* mice, and to assess the extent of characteristic similarities between both strains. Following the confirmation of transfer, metabolic parameter studies would define the extent of insulin resistance and metabolic syndrome components in the different genotypes. Upon rescue of the insulin resistance of *Ceacam1-/-* mice by overexpression of adiponectin, tumour induction could be started. My role in this project covered evaluation of transfer and metabolic

parameters, on which the decision of inducing tumours or not will be based. Upon a positive decision, these results would allow a better comprehensive view of the mechanism explaining the absence or presence of differences in tumour induction.

Figure 1. Schematic view of interactions between MetS components

This figure has been drawn from a lipocentric view. However, it illustrates a complete portrait, which also allows starting from insulin resistance in different organs or from increased inflammation. Increased adipose mass or insulin resistance increases secretion of FFA, and pro-inflammatory and pro-atherogenic cytokines from adipocytes. The anti-inflammatory and insulin-sensitizing adipokine, adiponectin, is also decreased. Adipose tissue activated macrophages also secrete inflammatory factors. These decrease insulin sensitivity in the liver, muscle and adipose tissue, leading to decreased glucose uptake, increased ectopic fat, and inhibition of gluconeogenesis and glycogenolysis in the liver. This creates hyperglycemia, which with FFA, increase insulin secretion from the pancreas, leading to hyperinsulinemia. Under these conditions, the liver produces pro-atherogenic and inflammatory molecules. This is accompanied by an abnormal blood lipid profile. This environment also participates in hypertension.

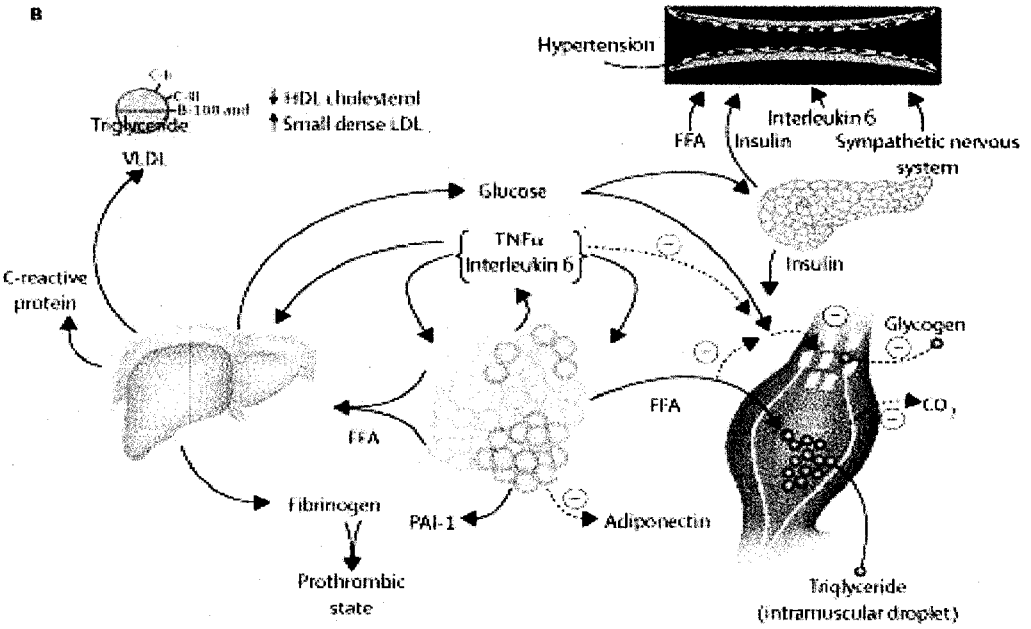

"Reprinted from The Lancet, Vol 365, Robert H. Eckel, Scott M. Grundy, Paul Z.Zimmet, The metabolic syndrome, Pages 1415-1428, Copyright (2005), with permission from Elsevier"

Figure 2. Intracellular insulin signalling

Insulin binding to its receptor triggers a large intracellular response activating several molecular pathways. Only IR is specific to insulin. Activated IRs recruit several molecules to the membrane such as IRS proteins, Shc and CAP. The PI3K pathway mediates most of the metabolic effects, such as increased GLUT-4 membrane translocation in muscles and adipose tissue, increased glycogen synthesis in muscles and liver and inhibition of liver gluconeogenesis. It also participates in cell survival mechanisms and protein synthesis required for growth. CAP/Cbl/TC10 pathway also helps in GLUT-4 translocation. Cell proliferation, growth and differentiation are mostly controlled by the MAP kinase pathway downstream of Shc and Grb2.

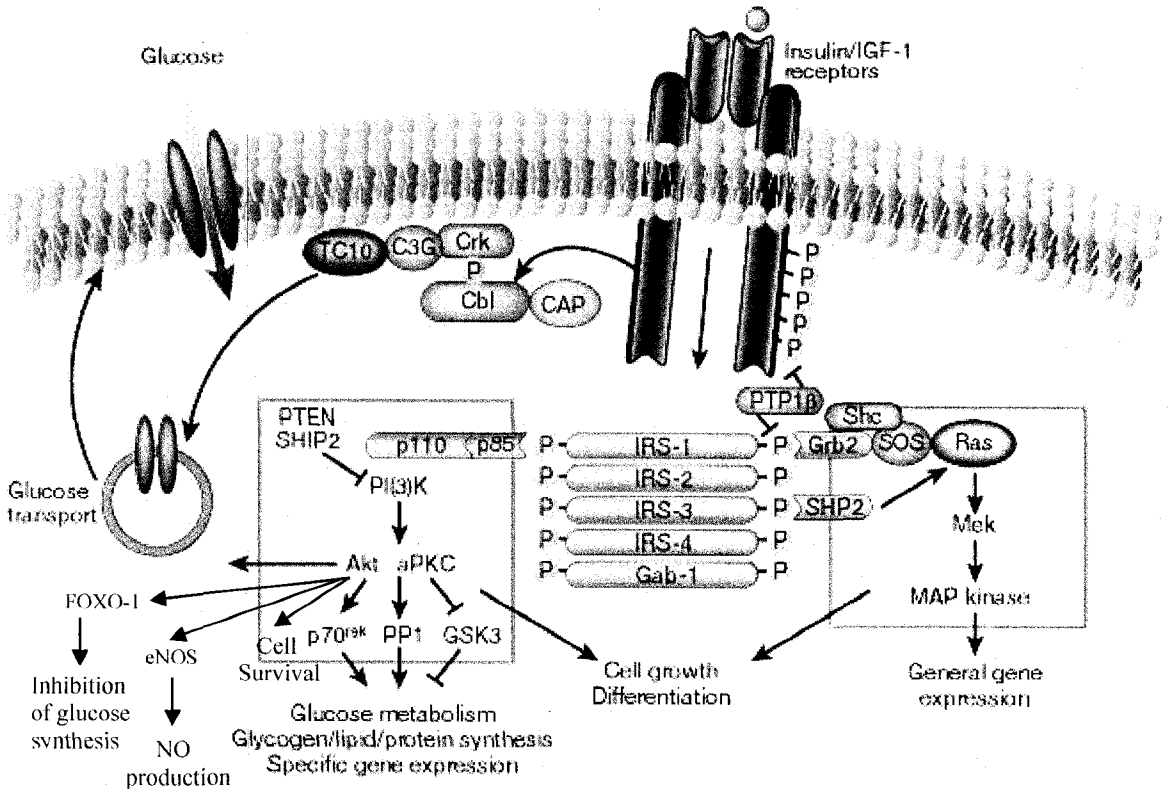

Adapted by permission from Macmillan Publishers Ltd : NATURE, Saltiel AR, Kahn CR. Insulin signalling and the regulation of glucose and lipid metabolism. Nature. 414 : Pages 799-806, Copyright (2001).

Figure 3. Intracellular adiponectin signalling mediating its insulin-sensitizing property

Full-length adiponectin is composed of a globular C-terminal domain and a collagenous domain allowing formation of hexamers and HMW isoforms. Globular adiponectin is formed by trimers of the C-terminal domain only. AdipoR1 is mostly found in muscle and is strongly bound by gAd. AdipoR2 has intermediate affinity for fAd and gAd and is mostly expressed in the liver. AdipoR1 seems more ubiquitous, whereas AdipoR2 is more tightly regulated. Adiponectin activates the AMPK pathway in the short term and the PPAR-α pathway in the long term. In muscle, both fAd and gAd bind to AdipoR1. It activates both AMPK and MAPK, which increases glucose uptake and β-oxidation. In the liver, fAd binding to AdipoR1 and AdipoR2 activates AMPK/MAPK and PPAR-α, respectively. It increases inhibition of gluconeogenesis and β-oxidation through activation of the AMPK pathway. Activation of PPAR-α in both tissues, partially through MAPK, also increases lipid β-oxidation. Hexamers and HMW adiponectin also bind to T-cadherin in muscle, but the implication of this interaction is unknown.

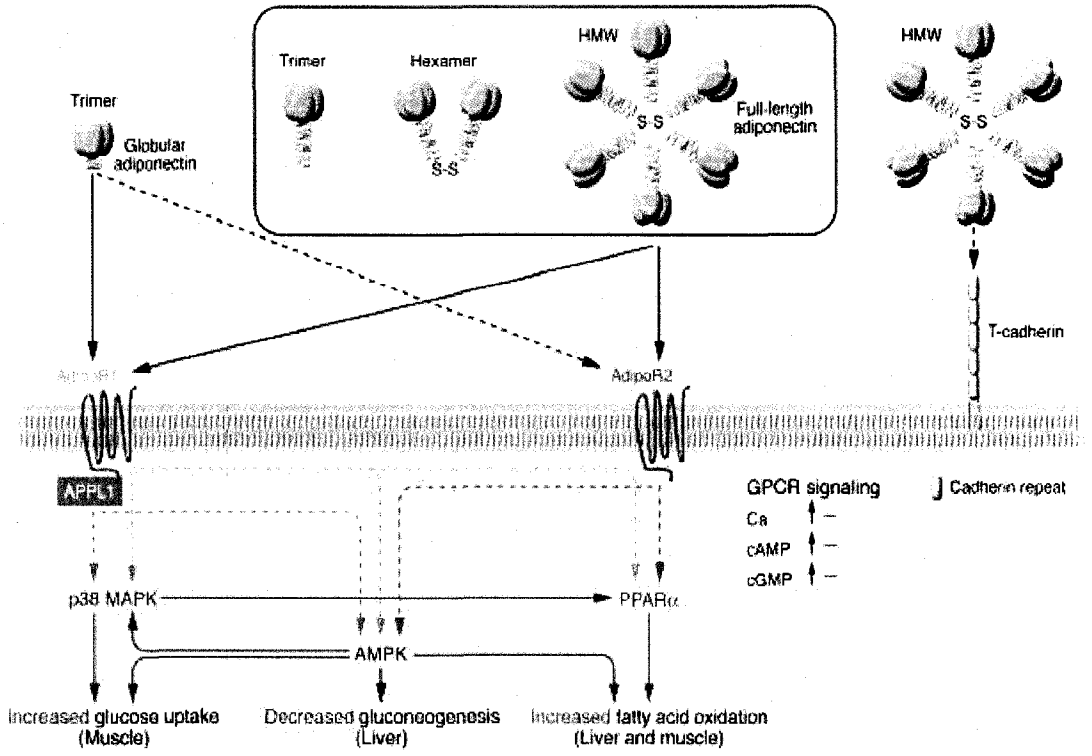

Reprinted from Kadowaki T et al. Adiponectin and adiponectin receptors in insulin resistance, diabetes, and the metabolic syndrome. The Journal of Clinical Investigation. Vol 116 (7). July 2006. Pages 1784-1792. With permission of Copibe©

This figure was adapted from Kadowaki T, Yamauchi T. Adiponectin and Adiponectin Receptors. Endocrine Reviews. Vol 26 (3). 2005. Pages 439-451. Copyright 2005, The Endocrine Society.

Figure 4. Implication of CEACAM1 in signal transduction

This figure represents CEACAM1 participation in signalling downstream of the activated T cell receptor. However, this model can be applied to other cell types by changing CEACAM1 expression and the names of serine/threonine and tyrosine kinases. CEACAM1 often associates and recruits the same effector molecules independently of the cell type. In resting T lymphocytes, CEACAM1 is mostly intracellular, with few CEACAM1 molecules at the surface in the form of cis-dimer. The CEACAM1-L isoform associates with the adaptors AP-1 and 2 intracytoplasmically, which ensures its constant recycling. T cell receptor stimulation activates Src kinases, phospholipase C (PLC), PKC and ZAP70 (serine/threonine and tyrosine kinases). PLC increases intracellular calcium concentrations, leading to dimer dissociation. ZAP-70, through Rho GTPases, induces cytoskeleton rearrangement. Binding of the CEACAM1 cytoplasmic tail to actin allows its recruitment to the immunological synapse (site of action). Monomers are phosphorylated by PKC on serine residues, which facilitates tyrosine phosphorylation by Src kinases. Tyrosine phosphorylation blocks AP1 and 2 binding and allows CEACAM1 surface accumulation. Trans binding between CEACAM1 on opposite cell surfaces permits Shc association with CEACAM1-L, which reduces activation of the MAPK pathway. Phosphorylation of both ITIMs allows association with SHP-1, which decreases downstream signalling through dephosphorylation of Src, ZAP70 and MAP kinases. With time, SHP-1 also dephosphorylates CEACAM1-L ITIMs, which restores interaction with adaptor proteins and recycling (*276*).

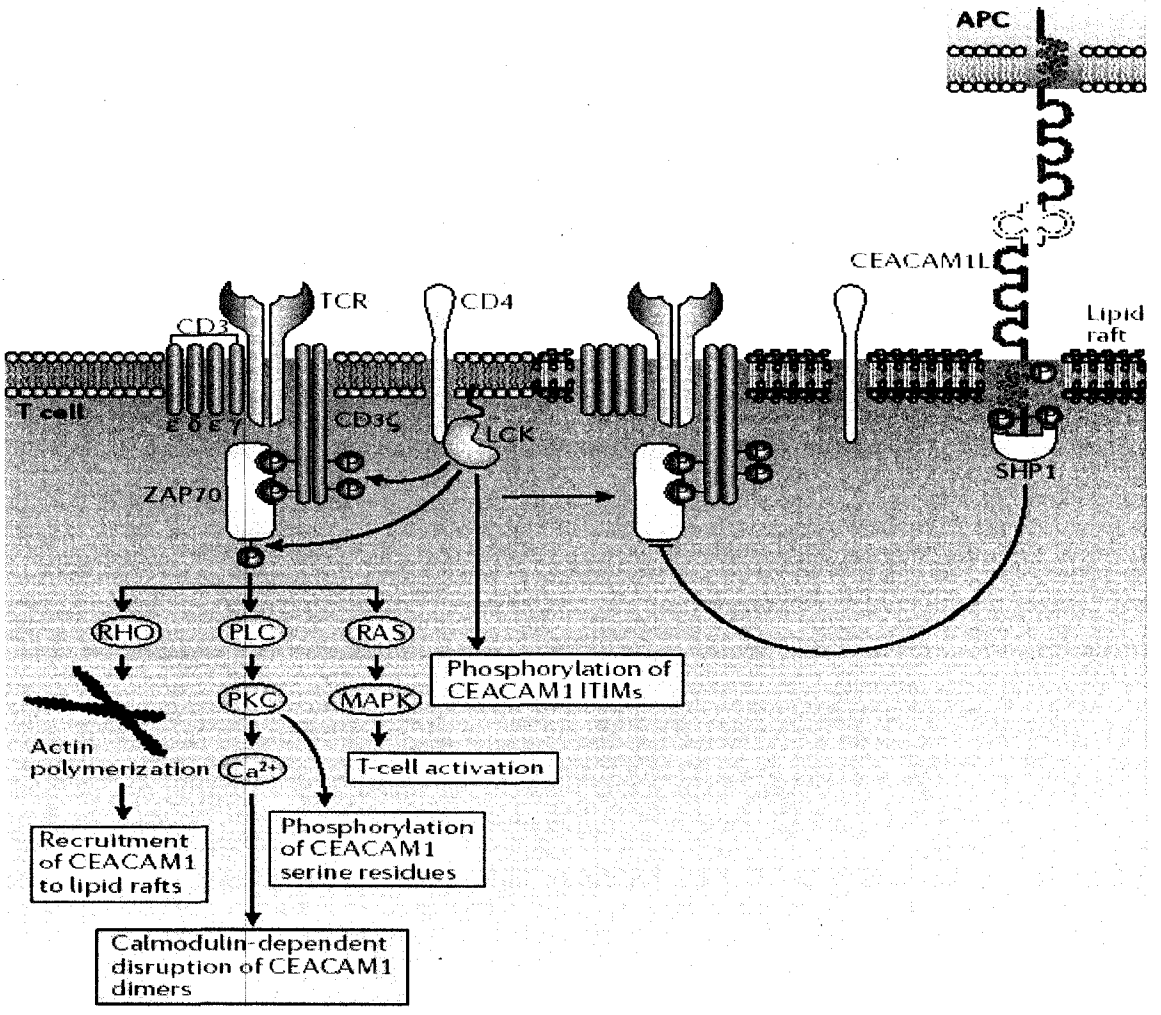

Reprinted by permission from Macmillan Publishers Ltd: NATURE REVIEWS IMMUNOLOGY, Gray-Owen SD, Blumberg RS. CEACAM1: contact-dependent control of immunity. Nature Reviews Immunology. Vol 6 (6). 2006. Pages 433-446. Copyright (2006).

FIGURE 5. Proposed mechanisms of CEACAM1-L effect in insulin signalling

CEACAM1 is phosphorylated on S503. It complexes with β-catenin, SHP-1 and Cdk2/CyclinE to mediate events required for formation of IR internalization sites. Upon binding of insulin to its receptor and subsequent IR autophosphorylation, IR phosphorylates CEACAM1-L Y488 residue. Shc binds to both CEACAM1-L and IR. CEACAM1-L binding by Shc competes with the Grb2-SOS interaction and downregulates the MAP kinase pathway, whereas Shc binding to IR competes with that of IRS-1 for IR phosphorylation and decreases signals through the PI3-kinase pathway. Possible CEACAM1-L binding to SHP-2 would also decrease signals through the MAP kinase pathway by competing with its binding to IR. These events lead to decreased mitogenic and growth signals. Activated IR associates and is endocytosed in clathrin coated pits with LRP1, SHP-1, Cdk-2/CyclinE and possibly Shc. This leads to receptor recycling and insulin degradation. β-catenin is probably released from the complex by tyrosine/serine phosphorylation. CEACAM1-L's phosphorylated Y488 residue can then bind and downregulate FAS, leading to decreased lipogenesis. CEACAM1-L is dephosphorylated by SHP-1.

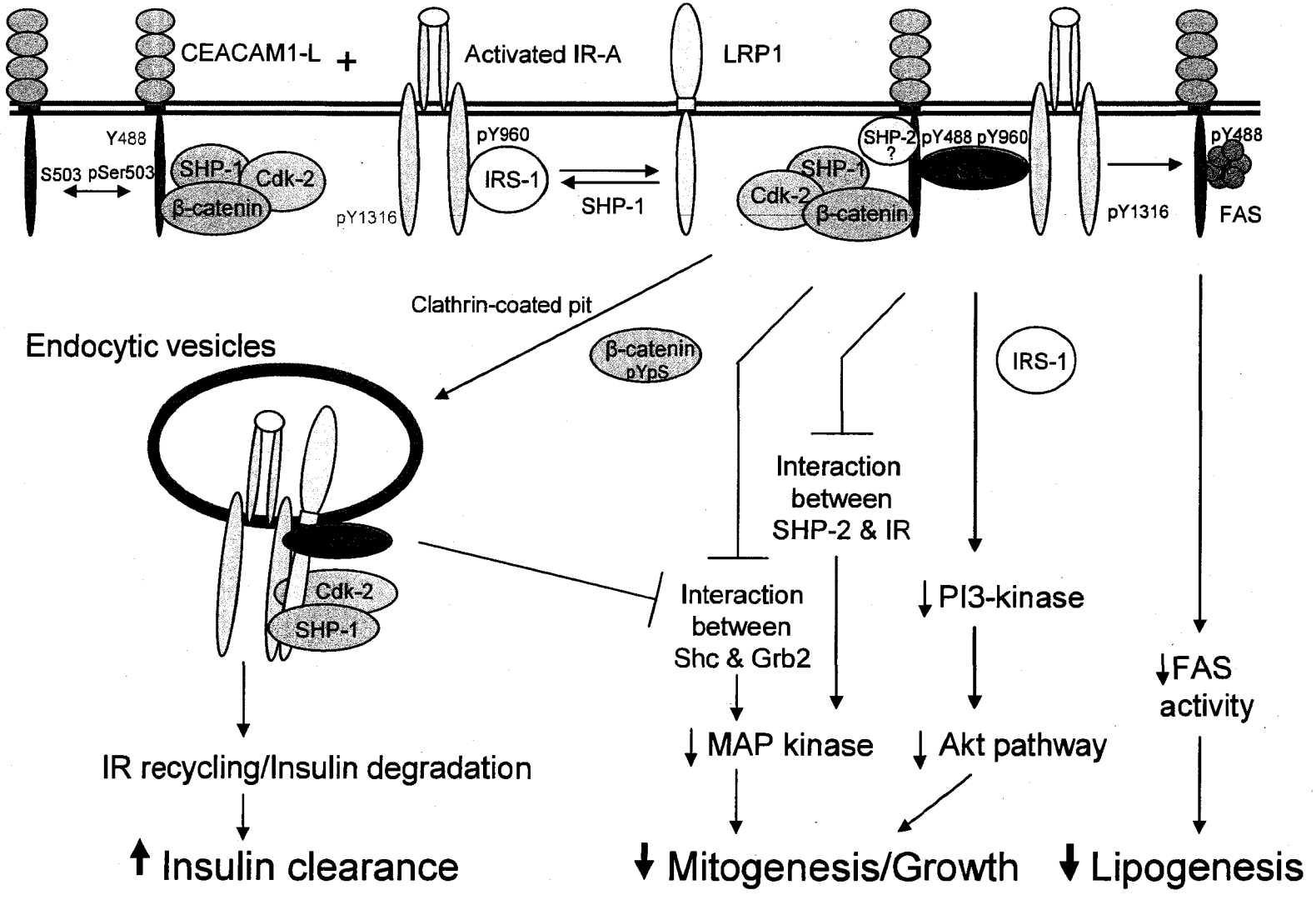
CEACAM1-L
+
Activated IR-A
LRP1
Y488
S503 pSer503
SHP-1
Cdk-2
β-catenin
pY1316
pY960
IRS-1
SHP-1
SHP-2
?
pY488 pY960
SHP-1
Cdk-2
β-catenin
pY1316
pY488
FAS
Clathrin-coated pit
Endocytic vesicles
β-catenin
pYpS
IRS-1
Interaction
between
SHP-2 & IR
Cdk-2
SHP-1
Interaction
between
Shc & Grb2
PI3-kinase
FAS
activity
IR recycling/Insulin degradation
MAP kinase
Akt pathway
Insulin clearance
Mitogenesis/Growth
Lipogenesis

Table 1. Adiponectin transgenic mouse model described by Dr.Scherer's laboratory

ORGANS	CHARACTERISTICS	PHENOTYPE[1] (*234*)		Age (months)
		MALE	FEMALE	
Body			Infertile	
	Weight	ND		0-12
			ND	0-4
			↑ (15%)	4-(12)
	Weight on HFD	ND	↑ (15%)	7
	% total fat	ND	↑ 2X	6-8
	Food intake		ND	6-8
	Energy expenditure		ND	6-8
	Respiratory quotient		ND	6-8
	Glucose uptake (clamp)	ND	ND	6-18
Liver	Hepatic glucose production (clamp)	↑	↑	6-8
	AMPK protein level (basal-fasted)	ND	ND	6-8
	AMPK phosphorylation (basal-fasted)	ND	ND	6-8
	AMPK phosphorylation time (clamp)	↑	↑	6-8
Blood	Ad clearance	ND	ND	
	Ad boost at puberty	ND	ND	0.5-2
	Ad level in female vs male (ratio of 2-3)	ND	ND	
	Ad	**↑ 3X**	**↑ 3X**	**0-12**
	HMW Ad distribution	ND	ND	4-6
	TNF-α	ND	ND	6-8
	Glucocorticoids	ND	ND	6-8
	Growth hormone	ND	ND	6-8
	Tyroid stimulating hormone	ND	ND	6-8
	Leptin	ND	ND	6-8
	Prolactin	↑ 2X	↑ 2X	6-8
	Fasting TG and non-esterified FA	ND	ND	6-8
	Fed (gavage) TG and non-esterified FA	ND	↓	6-8
	Fed and **fasted glucose**	**ND**	**ND**	**6-8**
	Fed and fasted FA	ND	ND	6-8
	Fed and fasted cholesterol	ND	ND	6-8

	Fed lactate	ND	ND	6-8
	Insulin after insulin injections (clamp)	↓ 50%	↓ 50%	6-8
	Glucose after OGTT on HFD	ND	↓	6
	Insulin after OGTT on HFD	↓	↓	6
BAT (subcutaneous)				
	LPL activity	↑ 2X	↑ 2X	6-8
	Caveolin-1 protein level	↑	↑	4
Interscapular	Ad mRNA	ND	ND	
	Ad protein	↑	↑	4
	Mass		↑	**12**
		↑		**>20**
Orbital	Ad mRNA	ND	ND	
	Mass	↑ (delayed vs females)	↑	12
WAT (subcutaneous)				
Inguinal	Ad mRNA	ND	ND	
	Ad protein	↑	↑	4
Mammary	Ad mRNA		ND	
	Ad protein		↑	4
	Caveolin-1 protein		↑	4
WAT (visceral)				
Epididymal	Ad mRNA	ND		
	Ad protein	↑	-	4
	LPL activity	ND		6-8
Perimetrial (uterine)	Ad mRNA		ND	
	Ad protein	-	↓	4
	Caveolin-1 protein		↓	4
	LPL activity		↑ 3.5X	6-8
Abdominal	Ad mRNA	ND	ND	
	LPL activity	↑ 0.5X	↑ 4X	6-8
	PPARγ2 mRNA	↑	↑↑	
	Resistin mRNA	↑	↑	
	ADP/ATP translocator	↑	↑	
	Dicarboxylate transporter	↑	↑	
Perirenal	LPL activity	ND	↑ 3X	6-8

[1] Phenotype = adiponectin tg+ vs wildtype

II. MATERIALS AND METHODS

Generation of genetically modified mice

Ceacam1 -/- mice were generated in our laboratory. The detailed procedure and genotyping are described in a previous publication (*352*). Briefly, the first two exons of the *Ceacam1* gene were replaced by a cassette containing the TK (thymidine kinase) promoter and the *neo*^{r} (neomycine resistance) gene, removing the initiator ATG codon. This leads to the total absence of *Ceacam1* gene expression in all tissues. Mice were produced on the 129/SV background and transferred in C57Bl/6 mice.

Adiponectin transgenic mice were kindly provided by Dr. P.E. Scherer (Department of Cell Biology, Albert Einstein College of Medecine, New York). The generation of these mice has been described (*234*). In summary, the transgene contains the ap2 adipocyte-specific promoter regulating the transcription of the *Ad* gene lacking the sequence representing 13 of the Gly-X-Y collagen repeats. This transgenic protein forms heterotrimers with full-length proteins, inhibiting the degradation of wildtype homotrimers which results in a three-fold increase in wildtype homotrimer secretion. These mice have been produced on a FVB background.

The *Ad* transgene was transferred from the FVB to the C57Bl/6 background by mating FVB tg+ mice with C57Bl/6 mice. The backcross was increased by mating the progeny with C57Bl/6 mice. Most of the tg+ mice have a light brown fur color. This method yields wt and transgenic mice for the *Ad* gene that are wildtype for the *Ceacam1* gene. C57Bl/6 tg+ mice were further mated with mice heterozygous or homozygous knockout for the *Ceacam1* gene to generate mice +/- : wt, -/- : wt, +/- : tg+ and -/- : tg+ (*CC1 : Ad*). Experiments were performed on backcrosses 3 and 4 for C57Bl/6.

Genotyping

Small tail fragments were obtained from 2-3 week- old mice. The DNA was isolated by adding 300 µl of 50 mM NaOH, heating at 100°C for 20 min followed by neutralization with 25 µl of 1 M Tris buffer pH 8.0. The mixture was centrifuged for 1 min at 13 000

rpm and the supernatant removed and frozen in a new tube at -20°C. DNA was genotyped by polymerase chain reaction (PCR) with *Ceacam1*-specific oligonucleotides (PN5 and PN8) as well as with *neo*^{r}-specific oligonucleotides. The *Ceacam1* wildtype and knockout genes are recognized on agarose gel by a 250 bp and a 550bp fragment, respectively (*352*).

Both FVB and C57Bl/6 mice were genotyped for the presence of the *Ad* transgene with the same PCR protocol, which consists of a modified version of the original protocol from Dr. Scherer's laboratory. DNA was isolated as per the *Ceacam1* mice. Adipo30 (GTTCCTCTTAATCCTGCCCATC) and Adipo30r (CCCGGAATGTT GCAGTAGAACTTG) are two internal primers specific for the transgene. The master mix consists of 1X Taq complete buffer, 200μM of dNTP, 0.5 unit of Taq polymerase, 0.5μM of Adipo30 and Adipo30r in water. 1μl of genomic DNA is added to 10 ul of master mix. The thermocycler program starts with 5 min at 94°C followed by 30 cycles formed by 30 s at 94°C, 45 s at 64°C and 30 s at 72°C. The program is terminated with 10 min at 72°C. The transgene is recognized by the presence of a 363 bp fragment on agarose gel.

Mouse bleeding and tissue collection

All animal procedures conformed to the standards of the Canadian Council on Animal Care. Mice were kept in a sterile environment equipped with an automatic 12 hours light/dark cycle changing at 7:00 am and pm. The mice were fed on a normal chow diet (Harlan Teklad Rodent Diet (W) 8604). Experiments were performed on 6 month-old mice. All mice were fasted 5 h prior to any manipulation i.e. from 8:00 am to 1:00 pm. Mice were first gently immobilized in a paper towel, their tail dipped in warm water and blood was collected from the tail vein. The first drop was used for glucose measurements with a glucose oxidase glucometer (One Touch Ultra, LifeScan Inc, BC, Canada) and exceeding blood (approximately 10-20 μl) was collected using a heparinized capillary (Fischer Scientific, Ontario, Canada). Mice were then anesthetised with approximately 2 μl/g of rodent cocktail containing 50 mg/ml ketamine (Vetalar, Bioniche), 5 mg/ml xylazine (AnaSed, Novopharm), 1 mg/ml acepromazine (Atravet, Ayerst) and 15% v/v

saline 0.9%. After weighing the mice, peripheral blood (300-400 µl) was removed by retro-orbital bleeding using half a heparinized capillary. Tail and retro-orbital blood was immediately placed on ice. A cardiac puncture was performed with a 1 ml syringe using a 25G needle (BD Fischer Scientific, Ontario, Canada). The blood was left to coagulate at room temperature for 20 min and then placed on ice. All samples were centrifuged 10 min at 10 000 rpm at 4°C. The serum was kept at -80°C for further analysis. The mice were sacrificed by cervical dislocation. Interscapular fat (subcutaneous brown adipose tissue (BAT)), inguinal fat (subcutaneous white adipose tissue (WAT)), gonadal fat (abdominal WAT) and liver were removed, weighed and immediately placed on dry ice. Muscles from both arms were also taken and frozen on dry ice. All tissues were stored at -80°C.

Serum analyses

Adiponectin and insulin were quantified from tail and retro-orbital sera, respectively using radioimmunoassay kits (RIA) (Linco Research, St-Charles, Missouri, USA). After validation of expected adiponectin levels by a RIA partly designed by Dr. Scherer, the adiponectin was measured by enzyme-linked immunosorbent assay (ELISA) (R&D Systems, Minneapolis, USA).

Adiponectin quantification in fat

The following protocol was obtained from Dr. Scherer's laboratory. Quantification was done from female inguinal and perimetrial fat. 1 ml of 20mM Tris pH 8.0 containing 1X protease inhibitors (Roche complete tablet, Roche Diagnostics, Indianapolis, IN, USA) was added to 0.2 g of frozen fat on ice. Tissue was homogenized with a manual homogenizer on ice. The homogenate was centrifuged for 3 min at 13 000 rpm at 4°C. The fat cake at the surface was removed and Triton X-100 was added to the supernatant to a final concentration of 1%. After re-suspension, the solution was centrifuged for 5 min at 13 000 rpm at 4°C. The supernatant was transferred to a new tube and protein content was measured by BCA assay (Pierce, Rockford, IL, USA). Samples were mixed with equal volumes of 3X sample buffer, run on a 12.5% acrylamide gel and transfered to a PVDF (polyvinylidene fluoride) membrane (Millipore, MA, USA). The membrane was

blocked with 5% fat-free milk solution overnight at 4 °C. The adiponectin was detected with a 1/5000 dilution of the rabbit polyclonal mAcrp30 N-terminus antibody (Dr. Scherer's laboratory) in milk for two hours at room temperature, followed by a 1/5000 dilution of anti-rabbit IgG coupled to horseradish peroxidase (GE Healthcare, NJ, USA) in milk for 1 h at room temperature. Detection was performed with chemoluminescence plus reagent (PerkinElmer, Boston, MA, USA) for 1 min. The membrane was stripped with 62.5 mM Tris pH 7.5 solution containing 2% SDS (sodium dodecyl sulphate) and 100mM β-mercaptoethanol at 45 °C for 30 min. The membrane was thoroughly washed and re-blocked in milk for 1 h at room temperature. It was incubated with rabbit actin antibody (Sigma, St-Louis, Missouri, USA) (1/1000) in milk overnight at 4 °C. The protein was detected with anti-rabbit IgG coupled to horseradish peroxidase (1/2000) in milk for 1 h at room temperature followed by chemoluminescence reagent for 1 min.

Statistical analysis

Males and females were analysed separately. All results are presented as mean ± SE. Differences between different genotypes were assessed by the Student's t-test. Since there was no difference in mouse weight between different genotypes, the tissue weight was normalized against the mouse weight using the ratio of one to the other. P-values < 0.05 indicate statistical significance.

III. RESULTS

A) Transfer of the Ad tg+ phenotype from the FVB to the C57Bl/6 background

Entering "mouse strain comparison" and "mouse strain metabolism comparison" as key words in Pubmed gives 1980 and 847 entries respectively. It is thus clear that mouse strains (inbred or outbred) have an effect on experimental design and results. These differences concern susceptibility to cancer, infections and diseases as well as morphology, metabolism, behaviour, etc. More precisely, the effect of a high fat diet on weight gain and fat accumulation in nine mouse strains was studied. Some strains, as the C57Bl/6 mouse, were highly susceptible, whereas three strains demonstrated resistance (*380*). C57Bl/6 mice were also susceptible to the development of T2DM caused by obesity (*381, 382*). C57Bl/6 and AKR mice both develop dietary obesity. However, for the same weight, C57Bl/6 mice are more glucose intolerant and less insulin resistant than AKR mice (*383*). Thus, obesity and diabetes incidence and manifestations differ between mouse strains. Consequently, it was important for us to compare the *Ad* tg+ mouse model characteristics observed in mixed C57Bl/6-FVB (further called C57Bl/6) to the initial description in pure FVB mice. It will allow correct interpretation of *Ceacam1* -/- phenotype rescue by the *Ad* transgene.

The *Ad* tg+ FVB mice were kindly provided by Dr. P.E.Scherer. This mouse model has been extensively described (*234*). Detailed characteristics are grouped in Table 1. The parameters highlighted in bold represent the characteristics chosen to assess transfer from the FVB to the C57Bl/6 background. All characteristics were examined after a five hour fast in approximately 6 month-old mice. Most of the parameters in Dr. Scherer's paper were studied in mice between 6 and 8 months of age. Serum Ad levels do not change after 5 months of age (*234*).

1. Transfer of the *Ad* transgene

The presence of the transgene was assessed by polymerase chain reaction. Figure 1 illustrates the presence of the transgene in both FVB and C57Bl/6 as a band of approximately 360 bp. In both strains, wt mice yield a negative response. The transgene was not lost or modified during the transfer.

2. Ad levels in inguinal and perimetrial fat

In the original description of the mouse model, adiponectin levels in tg+ mice were elevated in interscapular, inguinal, epididymal and mammary fat pads, but were decreased in perimetrial fat (*234*). No precise ratios were given. Indeed, we observed an increase in adiponectin levels in inguinal fat and a decrease in perimetrial fat of tg+ females, both on the FVB and on the C57Bl/6 backgrounds (Figure 2). Thus, the transgene led to a similar effect on adiponectin levels in visceral and subcutaneous fat pads in both strains, indicating similar levels of expression.

3. Macroscopic parameters

As in humans, male mice weigh more than female mice. It was previously observed that FVB *Ad* tg+ mice, both females and males, did not show a significant increase in total body weight at 6 months of age in comparison to their wt littermates. *Ad* tg+ females were, however, slightly heavier as they aged due to an increase in interscapular fat. This difference reaches significance at 8 months. At 6 months of age, we did not observe a significant difference in mouse weight between wt and *Ad* tg+ FVB mice, neither in females nor in males, confirming Dr. Scherer's observations. On the C57Bl/6 background, *Ad* tg+ males weigh slightly, but significantly, less than wt males. No differences were seen in C57Bl/6 females (Figure 3A).

Livers and different fat deposits were collected and weighed, in order to examine fat distribution in these mice. Ratios of organ weight / body weight were first calculated to normalize for differences in individual weight and slight differences in age (data not shown). This was based on the assumption that no differences in weight exist between wt and *Ad* tg+ mice. However, since a difference was observed between wt and *Ad* tg+ males on the C57Bl/6 background and between different *CC1 : Ad* genotypes in females (see below), net organ weights were used for further characterization. Macroscopic profiles were comparable between ratios and raw data, with only few differences in statistical significance. Since it is known that FVB and C57Bl/6 strains show morphological differences, p-values were only calculated for the same background. The goal here was to test if characteristic profiles were similar enough to assign to the

C57Bl/6 *Ad* tg+ mice the features described by Dr. Scherer in the FVB mice. We wanted to transfer the global phenotype, not the absolute values.

There was no mention of liver weight in the original paper. The livers of *Ad* tg+ FVB mice were on the average smaller than the wt ones, but this was significant only for males. This difference was amplified on the C57Bl/6 background and both sexes showed significance (Figure 3B). Notably, in this case, the ratio difference in FVB females was significant. The liver weights on both backgrounds were similar.

The initial characterization of the *Ad* tg+ mouse in the FVB background noted an accumulation of interscapular fat (BAT) in females starting at 4 months of age, which contributed to the increase in body weight. This phenotype was delayed in males and was clearly seen only in mice older than 20 months. At 6 months of age, we observed in both females and males a significant increase in interscapular fat in *Ad* tg+ mice, both on the FVB and on the C57Bl/6 backgrounds (Figure 3C). Wildtype mice showed similar amounts of interscapular fat in both backgrounds. However, interscapular fat accumulation was more elevated in the tg+ FVB compared to the C57Bl/6 background. This was more evident in females. With respect to this, Dr. Scherer described a rare phenotype in his *Ad* tg+ FVB mice that consists of an increase in the BAT in the orbital cavity in all female mice of one year. This leads to axial proptosis, i.e. pushing of the ocular globe outside of the cavity. We observed this phenotype in some FVB female mice at 8 months of age. This phenotype was obvious enough to be noticed by the animal care attendants (Figure 4). This characteristic was not observed in C57Bl/6 mouse at this age.

It was mentioned in the description of the *Ad* tg+ mouse model (FVB), that except for the interscapular fat, there were no macroscopic and weight differences in any other fat pad tested. However, the decrease in the amount of gonadal fat (visceral WAT) in the tg+ mice (either epididymal for males or perimetrial for females) was drastic in comparison to wt ones (Figure 3D). This phenotype was further used with the increase in interscapular fat to confirm mouse genotypes. Weights were comparable between FVB and C57Bl/6

mice, except that wt C57Bl/6 females have less than half the amount of uterine fat than wt FVB mice. The differences between wt and *Ad* tg+ on the C57Bl/6 background were still significant.

The quantity of inguinal fat was the same for wt and *Ad* tg+ males in both backgrounds. In females, the tg+ FVB mice are characterized by a significant increase in this subcutaneous WAT that is absent in the C57Bl/6 mice (Figure 3E).

In summary, even though we observed some characteristics on the FVB background that were not originally described, most macroscopic features were as apparent on the C57Bl/6 background as compared to the FVB background. Small differences in statistical significance were observed in male body weights, in female liver weights and in female inguinal fat weights, but the profiles were essentially the same.

4. Serum Ad levels

Dr. Scherer's laboratory measured tail vein peripheral blood adiponectin levels by radioactive iodine Western blotting. The absolute levels in 6 month-old FVB mice were approximately 15 μg/ml for wt males, 30 μg/ml for *Ad* tg+ males, 25 μg/ml for wt females and 80 μg/ml for tg+ females. It has previously been shown that female mice have approximately three times more adiponectin in their blood than males (*188*). Ratios of adiponectin expressed by wt and tg+ mice used to characterize the model are found in the left part of Figure 5A. The most important characteristic is the 2-3 fold increase in adiponectin level in tg+ mice in comparison to wt mice, with the ratio being more elevated in females than in males.

The adiponectin levels quantified here by RIA are slightly lower in both sexes, genotypes and backgrounds than the ones measured by Dr. Scherer's laboratory (Figure 5B). However, the different ratios are almost perfectly reproduced on the FVB background, with a ratio of tg+ / wt of 3.6 for males and 3.7 for females (Figure 5A, middle column), being slightly higher than the original ones. On the C57Bl/6 background, the adiponectin levels were slightly increased in comparison to the FVB ones. The different

augmentations led to changes in some ratios i.e. a smaller M tg+/ wt (2.8) ratio, a bigger F tg+/ wt (4.4) ratio and a smaller F wt/ M wt ratio. The 0.7 differences still maintain the ratios in the good range. Hence, the model almost perfectly transferred from the FVB to the C57Bl/6 background relative to adiponectin serum levels.

5. Serum insulin levels

Fasting insulin levels on standard chow in the *Ad* tg+ mouse model were not previously examined. However, oral glucose tolerance test were performed on these mice after 6 months on a high fat diet. At time 0, before glucose gavage, there was no difference in the insulin levels between wt and tg+ females. However, wt males displayed levels 2.5 times higher than their tg+ littermates. In light of these results, we would not expect to see differences in females on a standard chow. The male profile was unpredictable. On standard diet, both males and females on the FVB background showed no difference in serum insulin levels after a 5 h fast. Absolute blood insulin levels were comparable between FVB and C57Bl/6 mice, except for C57Bl/6 males which had highly elevated and variable levels. Thus, insulin levels in *Ad* tg+ C57Bl/6 males were 4 times lower than in wt males and were similar to the phenotype observed on the high fat diet. However, both backgrounds showed decreased insulin levels in *Ad* tg+ males, but these were significant only in C57Bl/6 mice. No differences were observed for females on the C57Bl/6 background (Figure 6A). In summary, the phenotype transferred well from one background to the other in females. The differences seen in males were significant, but were not an obstacle to the use of this model.

The general conclusion concerning the transfer of the *Ad* transgene from the FVB to the C57Bl/6 background is the following: the phenotype observed between wt and *Ad* tg+ mice is comparable and the *Ad* tg+ C57Bl/6 mice share the same characteristics as original FVB mice. These mice can thus be used for further experiments implicating this mouse model.

B) Phenotypes on different *CC1 : Ad* genotypes in C57Bl/6 mice

1. Macroscopic parameters

Another student in our laboratory observed a small, but significant, increase in weight in 6 month-old *Ceacam1* -/- mice. Dr. Scherer's studies showed that, on a HFD, both wt and *Ad* tg+ mice gain weight to the same extent. The phenotype seen on regular chow is conserved on the high fat diet, i.e. no differences between males as well as differences between females becoming significant at 8 months. In 6 month-old mice, we would expect to observe a slight increase in weight in mice with the *Ceacam1-/-* genotype, independently of the *Ad* genotype. No differences between wt and ko mice were observed here, neither in males nor females. In males, there were no differences between different genotypes, except that seen between wt and tg+ mice. The *Ceacam1* background did not produce an effect on weight. Surprisingly, in females, differences in weights between different *Ceacam1* genotypes appeared only on the *Ad* tg+ background. *CC1* +/- : *Ad* tg+ and *CC1* -/- : *Ad* tg+ mice have the same weight and were both slightly, but significantly, heavier than the *CC1* +/+ : *Ad* tg+ mice. In addition, *CC1* -/- : *Ad* tg+ female mice weigh significantly more than *CC1* -/- : *Ad* wt and *CC1* +/+ : *Ad* wt mice (Figure 7A). In summary, deletion of the *Ceacam1* gene affects body weight mainly in females of the *Ad* tg+ background.

CEACAM1 associates with the enzyme fatty acid synthase in the liver (*259*). *Ceacam1-/-* females are characterized by fatty livers at one year-old (personal communication from Dr. N. Beauchemin). In addition, CEACAM1 downregulates mitogenic signals following insulin binding in hepatocytes (*372*). L-SACC tg+ mice expressing a dominant negative CEACAM1L protein in livers and *Ceacam1-/-* mice were shown to be hyperinsulinemic (*259, 375-377*). Thus, *Ceacam1-/-* mice would be expected to present heavier livers. Despite all this, my fellow student Nelly Leung did not observe a significant difference in liver weight at six months. However, she observed an increase in perimetrial fat in females at this age. The effects of different *Ceacam1* genotypes on interscapular and inguinal fat weights have not been previously described. In this study, no differences were observed between different *Ceacam1* genotypes in males and females or on the *Ad*

wt and the *Ad* tg+ backgrounds. The differences previously mentioned between wt and *Ad* tg+ mice (see above) were still observed and the *Ceacam1* genotype did not significantly alter these differences. For example, *CC1* -/- : *Ad* wt mice have heavier livers than *CC1* +/+ : *Ad* tg+, *CC1* +/- : *Ad* tg+ and *CC1* -/- : *Ad* tg+ mice. This was seen for all macroscopic features (liver, interscapular fat, gonadal fat and inguinal fat) (Figure 7 B-E).

In summary, the partial or total deletion of CEACAM1 did not translate into significant differences in male body weight and in interscapular, gonadal and inguinal fat weights in both sexes. The only differences were observed in the female body weight on the *Ad* tg+ background, where *Ceacam1* heterozygous and knockout mice were heavier than wt mice. This increase could not be explained alone by any of the macroscopic parameters examined in this study.

2. Serum adiponectin levels

Ceacam1-/- mice displayed some characteristics of the metabolic syndrome, which is associated with lower adiponectin levels (*175, 384*)(personal communication Dr. N. Beauchemin). Thus, it was postulated that serum adiponectin levels from *Ceacam1*-/- mice would be lower than in wt mice. Indeed, preliminary tests indicated lower adiponectin values in these mice. Several mice were tested first with the RIA (Figure 5C top). However, since it was more convenient, adiponectin levels in other mice were quantified using an ELISA assay (Figure 5C bottom). However, this method is less sensitive and seems affected by other factors. Adiponectin profiles for different *CC1 : Ad* genotypes is the same in males by RIA and by ELISA. The absolute amount is the same for *Ad* wt mice for both techniques, but the levels for *Ad* tg+ mice are approximately 10µg/ml lower in the ELISA. There were no differences between *Ceacam1* +/+ and -/- mice on the *Ad* wt background. However, on the *Ad* tg+ background, there were increases in adiponectin levels as CEACAM1 levels decreased, which creates a significant difference between *CC1* +/+ : *Ad* tg+ and *CC1* -/- : *Ad* tg+ mice. In females, the ELISA detected half the amount of the RIA in the wt and a third in the tg+ mice. Thus, the ratios are not conserved. There were slight differences in profiles between RIA

and ELISA in the *Ad* tg+ background. As in males, there were significant differences between *CC1* +/+ : *Ad* tg+ and *CC1*-/- : *Ad* tg+ in the ELISA. However, it was not seen by RIA. Even though many more mouse sera were measured by ELISA than by RIA, supplementary tests with the RIA will be needed to validate this. In females and in males, as for macroscopic parameters, the differences seen between the *Ad* wt and the *Ad* tg+ genotypes were conserved and passed over *Ceacam1* genotypes. In summary, differences in adiponectin levels between different *Ceacam1* genotypes are observed only on the *Ad* tg+ background, with *Ceacam1* knockout mice having more elevated levels than wt ones.

3. Serum insulin levels

L-SACC1 and *Ceacam1*-/- mice were shown to be hyperinsulinemic, with insulin levels 3 times more elevated than in wt mice (*259, 375-377*). Dr. Scherer's experiment with mice on a HFD indicated a decrease in insulin levels in males. Thus, the hypothesis was that overexpressing adiponectin would return the insulin levels to normal in *Ceacam1* -/- male mice by increasing sensitivity to the hormone. Given the significant number of mice tested, the *Ad* transgene lowers the insulin levels in both sexes, independently of the *Ceacam1* genotype. To our surprise, the absence of the CEACAM1 protein led to a decrease in blood insulin levels in both sexes and on both *Ad* genotypes. However, the differences are significant only in *Ad* tg+ males (Figure 6B). The insulin profiles were exactly the inverse of the adiponectin profiles obtained by RIA, indicating a major role of adiponectin in this phenotype. In conclusion, this raises a controversy about insulin levels in *Ceacam1* -/- mice. In this study, deletion of the *Ceacam1* gene results in significantly lower levels of insulin in *Ad* tg+ males only.

4. Blood glucose levels

No data was available on fasting blood glucose levels in the *Ceacam1*-/- mice. However, L-SACC1 mice expressing a dominant negative CEACAM1 mutant specifically in the liver had the same glucose levels in blood as wildtype mice following an overnight fast. In addition, after 6 months on a HFD, no differences in glucose levels in both sexes were seen after a 5h fast in *Ad* tg+ mice. Thus, we would not expect to see a difference in glucose levels, neither between *Ceacam1* genotypes nor between *Ad* genotypes. Indeed,

the *Ceacam1* genotype did not present any differences. The expression of the *Ad* transgene induced a subtle reduction in glucose levels. In males and in females, *Ceacam1* knockout mice had higher glucose levels than *Ceacam1* wt and knockout mice on the *Ad* tg+ background. In females, wt mice also had higher glucose levels than *Ceacam1* wt and knockout mice on the *Ad* tg+ background. The *CC1*+/- : *Ad* tg+ mice were not involved, probably due to the low number of mice (Figure 6C). In summary, as predicted, no differences were found in glucose levels between *Ceacam1* genotypes and overexpression of adiponectin lowered glucose levels in certain cases.

Figure 1. Genotyping of *Ad* tg+ mice by PCR. The presence of the transgene is indicated by the presence of a band of approximately 360 bp. Lanes of wt mice are left blank. FVB (top) and C57Bl/6 (bottom) mice are showed for comparison.

FVB

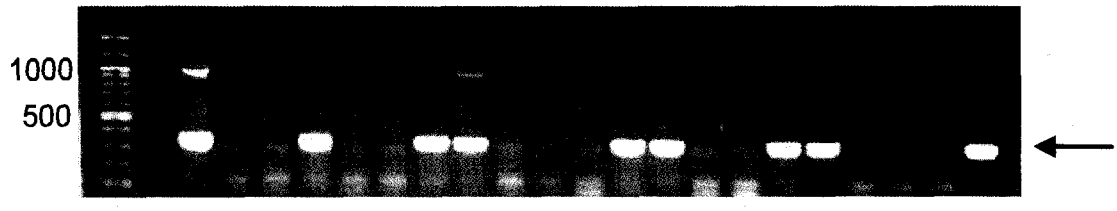
100 bp ladder
- control
+ control
1000
500

C57Bl/6

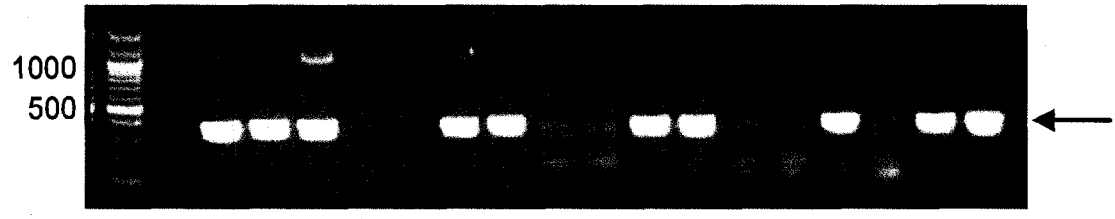
100 bp ladder
- control
+ control
1000
500

Figure 2. Adiponectin levels in A) inguinal and B) perimetrial fat. Fat depots from 6 month-old females were homogenized and adiponectin detected by Western blotting. FVB (left) and C57Bl/6 (right) levels are showed.

A

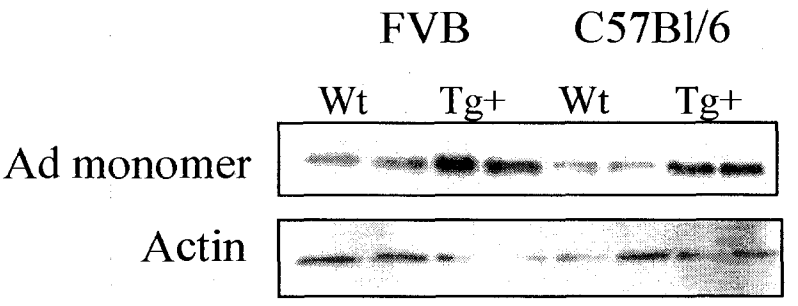

Ratios	FVB	C57Bl/6
Tg+ / Wt (net)	1.6	1.8
Tg+ / Wt (normalized for actin)	3.8	5.4

B

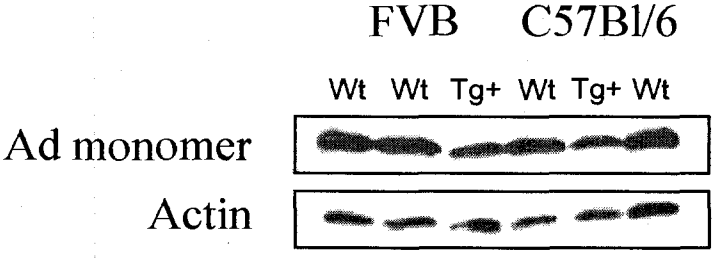

Ratios	FVB	C57Bl/6
Tg+ / Wt (net)	0.6	0.6
Tg+ / Wt (normalized for actin)	0.6	0.7

Figure 3. Comparison of macroscopic features of 6 month-old wt (blue) and *Ad* tg+ (orange) mice sacrificed and dissected after a 5 hour fast between FVB (left graph) and C57Bl/6 (right graph) strains. Males (left) were separated from females (right) for all analyses. A) Body weights B) Liver weights C) Interscapular fat weights D) Gonadal fat weights E) Inguinal fat weights. Values are expressed as average ± standard error with the number of mice indicated under each column. * is indicating a p-value < 0.05.

A

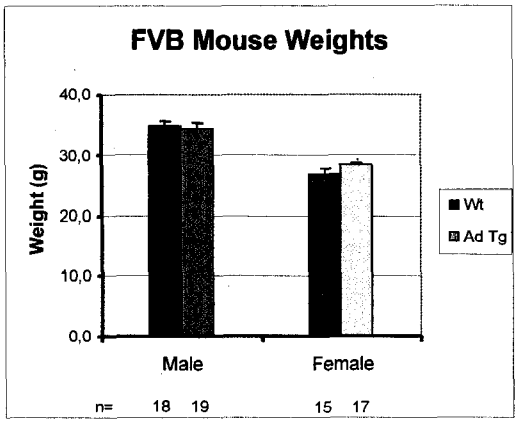
FVB Mouse Weights
Weight (g)
40,0
30,0
20,0
10,0
0,0
Male
Female
n= 18 19 15 17
Wt
Ad Tg

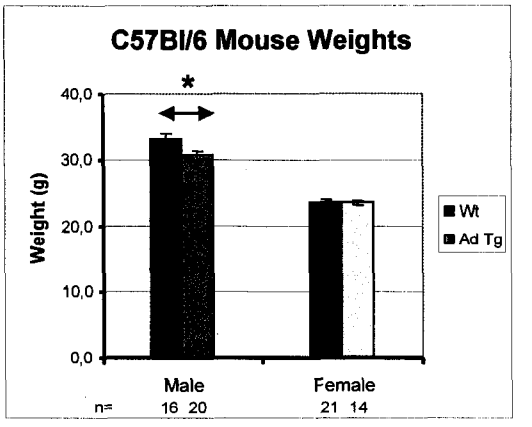
C57Bl/6 Mouse Weights
*
Weight (g)
40,0
30,0
20,0
10,0
0,0
Male
Female
n= 16 20 21 14
Wt
Ad Tg

B

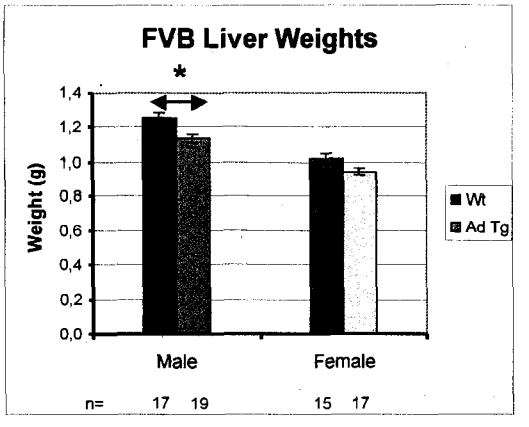
FVB Liver Weights
*
Weight (g)
1,4
1,2
1,0
0,8
0,6
0,4
0,2
0,0
Male
Female
n= 17 19 15 17
Wt
Ad Tg

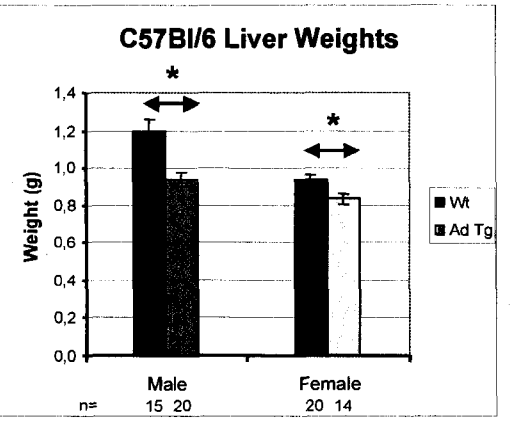
C57Bl/6 Liver Weights
*
*
Weight (g)
1,4
1,2
1,0
0,8
0,6
0,4
0,2
0,0
Male
Female
n= 15 20 20 14
Wt
Ad Tg

C

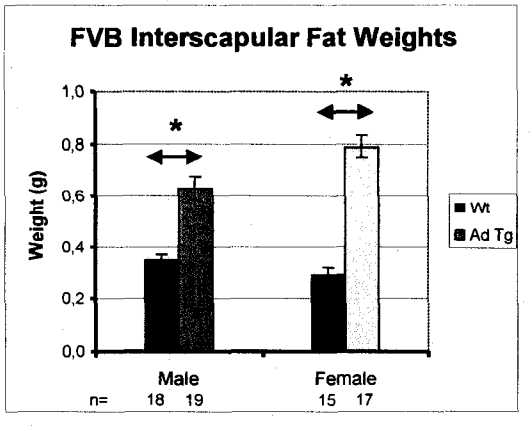
FVB Interscapular Fat Weights
*
*
Weight (g)
1,0
0,8
0,6
0,4
0,2
0,0
Male
Female
n= 18 19 15 17
Wt
Ad Tg

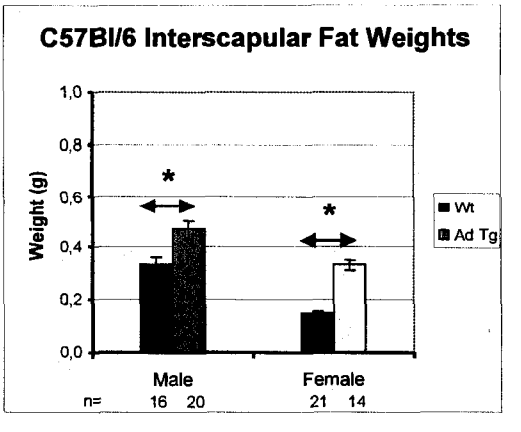
C57Bl/6 Interscapular Fat Weights
*
*
Weight (g)
1,0
0,8
0,6
0,4
0,2
0,0
Male
Female
n= 16 20 21 14
Wt
Ad Tg

D

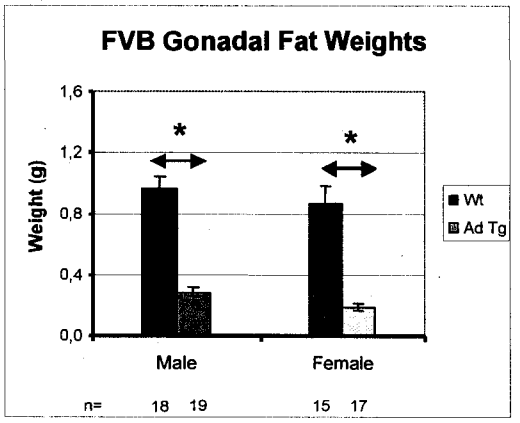
FVB Gonadal Fat Weights
Weight (g)
1,6
1,2
0,8
0,4
0,0
*
*
Male
Female
n= 18 19 15 17
Wt
Ad Tg

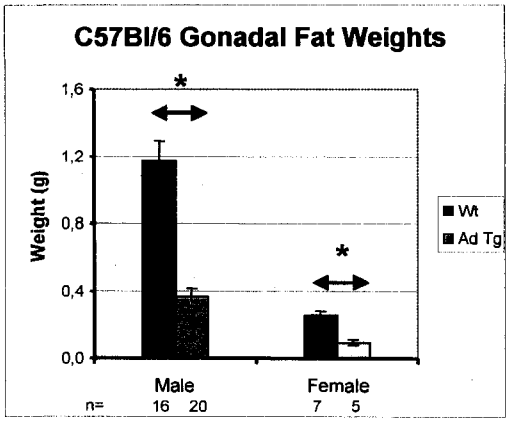
C57Bl/6 Gonadal Fat Weights
Weight (g)
1,6
1,2
0,8
0,4
0,0
*
*
Male
Female
n= 16 20 7 5
Wt
Ad Tg

E

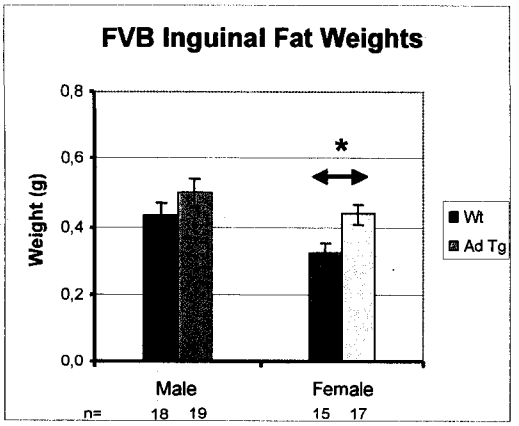
FVB Inguinal Fat Weights
Weight (g)
0,8
0,6
0,4
0,2
0,0
*
Male
Female
n= 18 19 15 17
Wt
Ad Tg

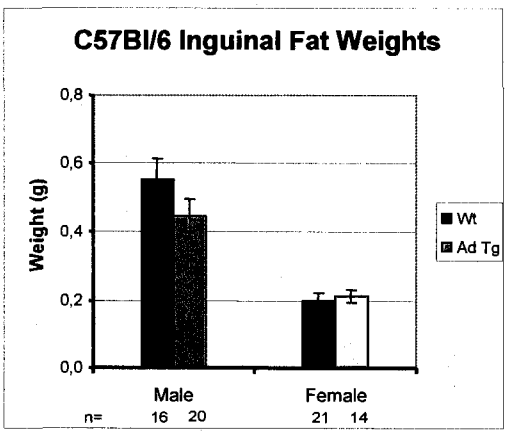
C57Bl/6 Inguinal Fat Weights
Weight (g)
0,8
0,6
0,4
0,2
0,0
Male
Female
n= 16 20 21 14
Wt
Ad Tg

Figure 4. Picture of BAT accumulation in Ad tg+ females with age. In order from left to right : *Ad* tg+ at 8 months, *Ad* wt at 8 months, *Ad* tg+ at 2 1/2 months, *Ad* wt at 2 1/2 months. In the older tg+ mouse, increased interscapular fat formed a bump (thin arrow) and accumulation of orbital BAT (bold arrows) pushes the globe outside of the cavity.

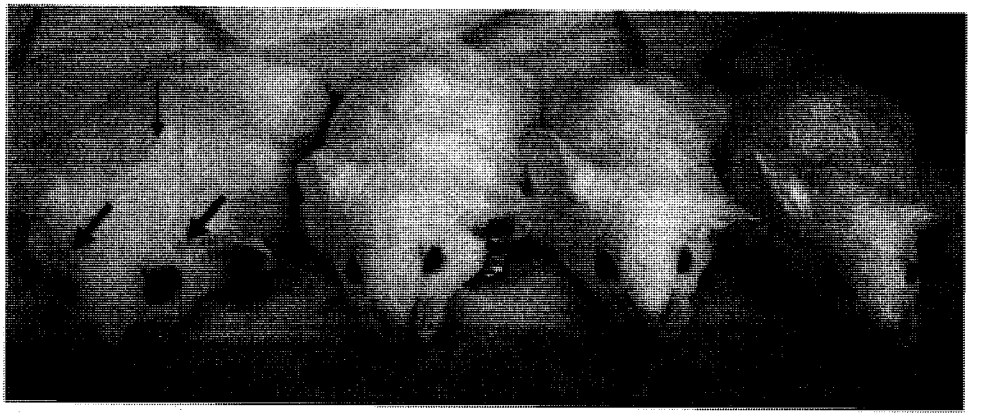

Figure 5. Serum adiponectin levels. A) Comparative table of different adiponectin ratios in Dr. Scherer's FVB tg+ mice and in our FVB tg+ and C57Bl/6 tg+ mice. B) Comparison of adiponectin levels in wt (blue) and *Ad* tg+ (orange) mice between the FVB (left graph) and the C57Bl/6 (right graph) backgrounds. C) Adiponectin levels in different *CC1 : Ad* genotypes on the C57Bl/6 background measured by RIA (top) or ELISA (bottom). Males are shown in the left part of the graphs and females in the right part. Mice were 6 months old. Fasting was for 5 hours prior to bleeding. Values represent average ± standard error with the number of mice written under each column.
*, p-value < 0.05.

A

	Dr.P.E.Scherer	Observed	
Ratios	FVB	FVB	C57Bl/6
M tg+ / M wt	2-3	3.6	2.8
F tg+ / F wt	2-3	3.7	4.4
M tg+ / F wt	1	1.3	1.5
F tg+ / M tg+	3	2.8	3.0
F wt / M wt	3	2.7	2.0

B

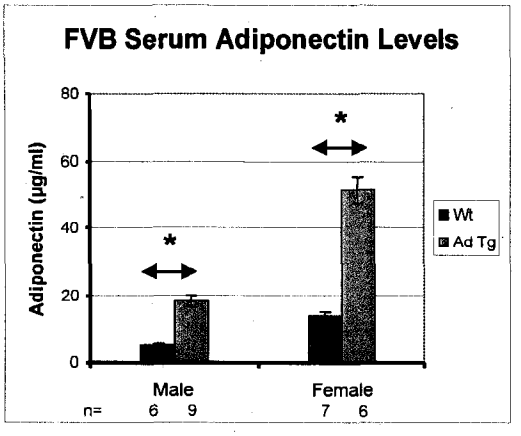

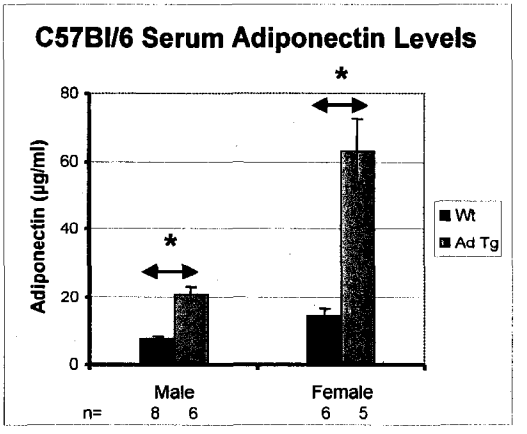

C

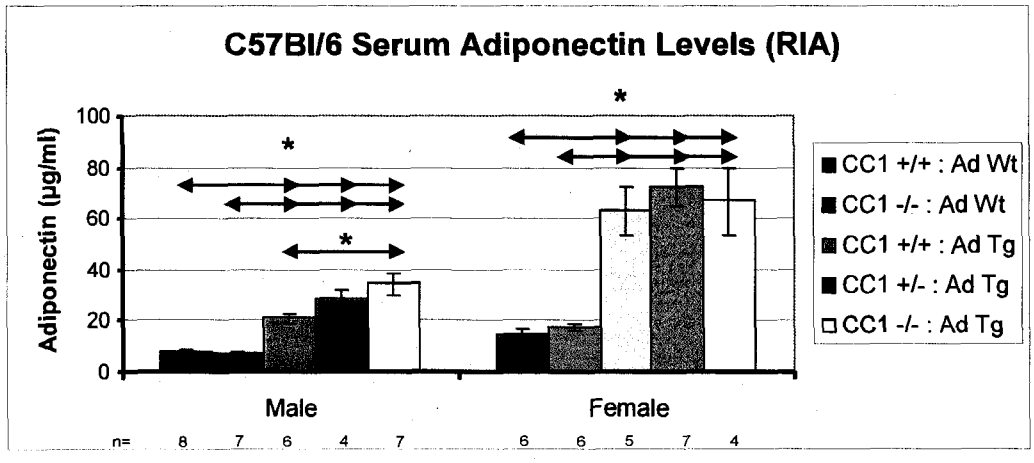
C57Bl/6 Serum Adiponectin Levels (RIA)
Adiponectin (µg/ml)
100
80
60
40
20
0
*
*
*
Male
Female
n= 8 7 6 4 7 6 6 5 7 4
CC1 +/+ : Ad Wt
CC1 -/- : Ad Wt
CC1 +/+ : Ad Tg
CC1 +/- : Ad Tg
CC1 -/- : Ad Tg

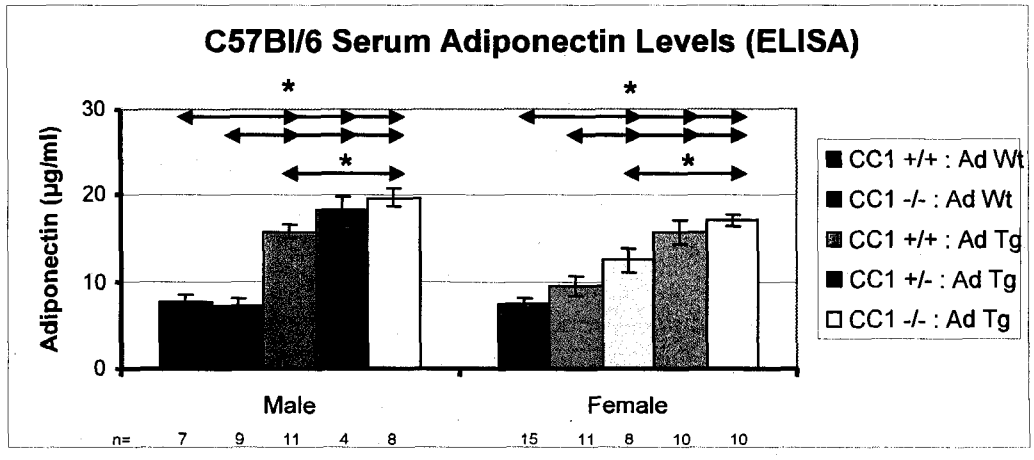
C57Bl/6 Serum Adiponectin Levels (ELISA)
Adiponectin (µg/ml)
30
20
10
0
*
*
*
*
Male
Female
n= 7 9 11 4 8 15 11 8 10 10
CC1 +/+ : Ad Wt
CC1 -/- : Ad Wt
CC1 +/+ : Ad Tg
CC1 +/- : Ad Tg
CC1 -/- : Ad Tg

Figure 6. Serum insulin and blood glucose levels. A) Insulin levels in wt (blue) and *Ad* tg+ (orange) mice in FVB (left graph) and in C57Bl/6 (right graph) strains. B) Effect of different *CC1 : Ad* genotypes on insulin levels in the C57Bl/6 background. C) Blood glucose levels in C57Bl/6 6 month-old mice with different *CC1 : Ad* genotypes. Data are shown for fasting 6 month-old males (left) and females (right) separately and indicate average ± standard error. The number of mice per genotype is specified under each bar. *, p-value < 0.05.

A

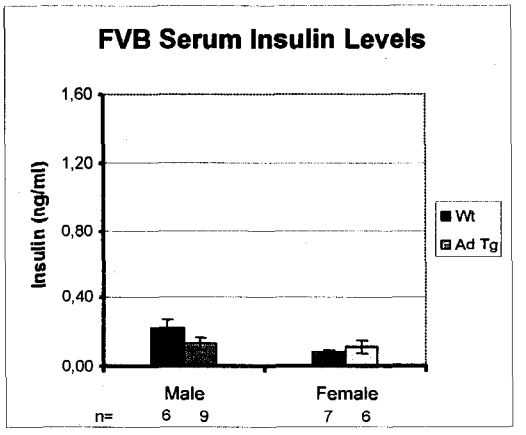
FVB Serum Insulin Levels
Insulin (ng/ml)
1,60
1,20
0,80
0,40
0,00
Wt
Ad Tg
Male
Female
n= 6 9 7 6

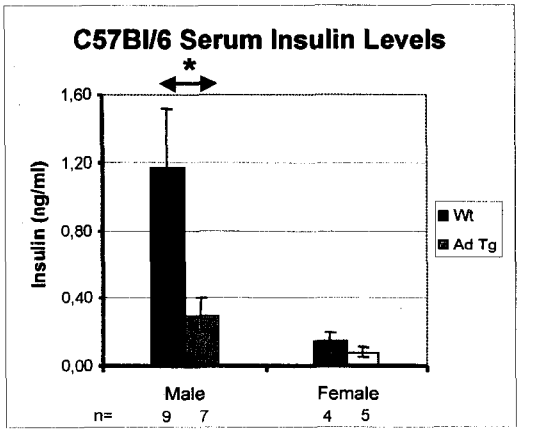
C57Bl/6 Serum Insulin Levels
*
Insulin (ng/ml)
1,60
1,20
0,80
0,40
0,00
Wt
Ad Tg
Male
Female
n= 9 7 4 5

B

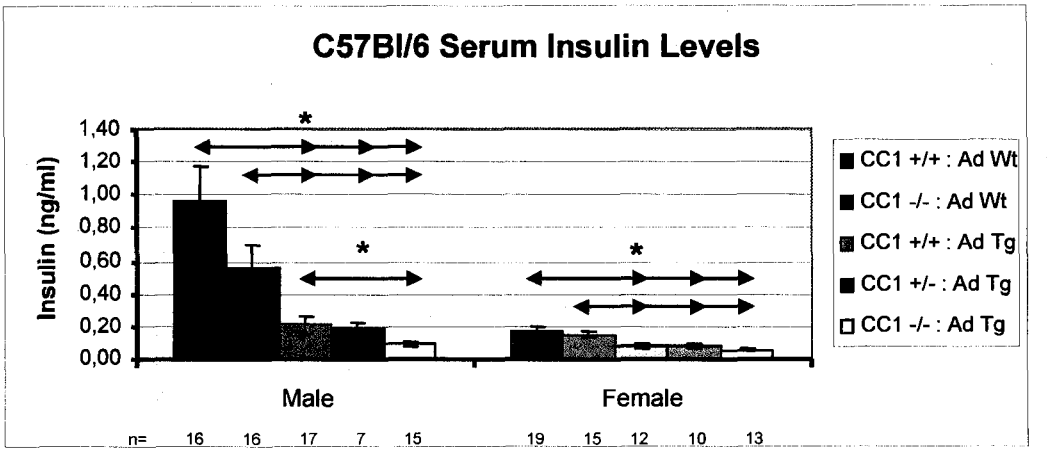
C57Bl/6 Serum Insulin Levels
Insulin (ng/ml)
1,40
1,20
1,00
0,80
0,60
0,40
0,20
0,00
*
CC1 +/+ : Ad Wt
CC1 -/- : Ad Wt
CC1 +/+ : Ad Tg
CC1 +/- : Ad Tg
CC1 -/- : Ad Tg
Male
Female
n= 16 16 17 7 15 19 15 12 10 13

C

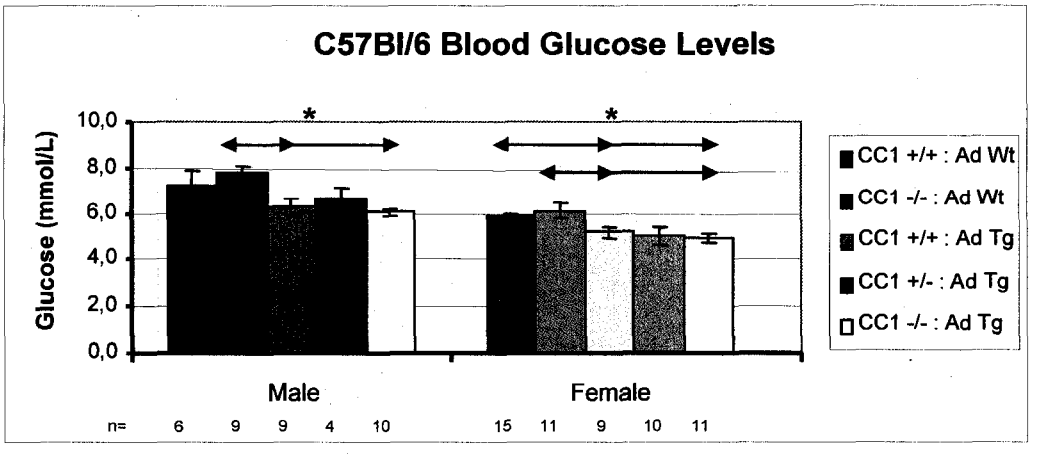
C57Bl/6 Blood Glucose Levels
Glucose (mmol/L)
10,0
8,0
6,0
4,0
2,0
0,0
*
CC1 +/+ : Ad Wt
CC1 -/- : Ad Wt
CC1 +/+ : Ad Tg
CC1 +/- : Ad Tg
CC1 -/- : Ad Tg
Male
Female
n= 6 9 9 4 10 15 11 9 10 11

Figure 7. Effect of different *CC1 : Ad* genotypes on macroscopic parameters in C57Bl/6 mice. A) Body weights, B) Liver weights, C) Interscapular weights, D) Gonadal weights, E) Inguinal weights. Male (left) and female (right) mice were analyzed at 6 months after a 5 hours fast. Data are shown as average ± standard error. The mice number per average is indicated under the appropriate column. *, p-value < 0.05.

A

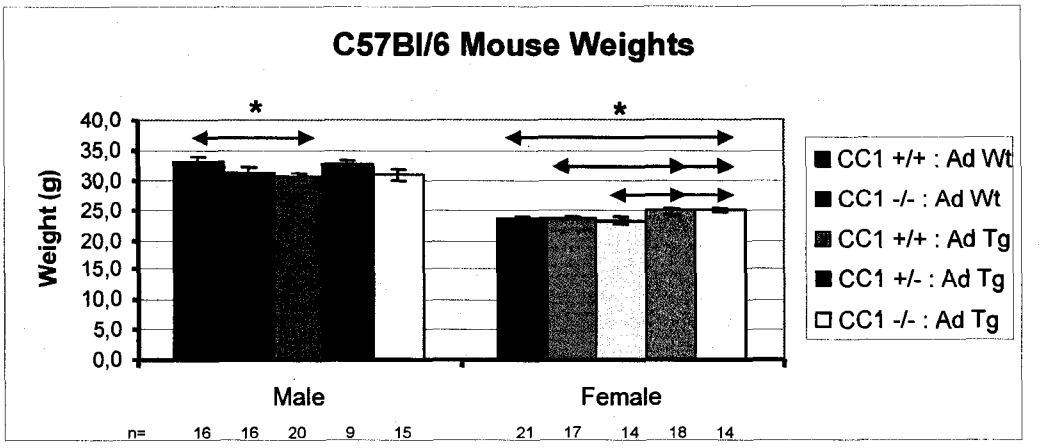
C57Bl/6 Mouse Weights
Weight (g)
40,0
35,0
30,0
25,0
20,0
15,0
10,0
5,0
0,0
*
*
Male
Female
n= 16 16 20 9 15 21 17 14 18 14
CC1 +/+ : Ad Wt
CC1 -/- : Ad Wt
CC1 +/+ : Ad Tg
CC1 +/- : Ad Tg
CC1 -/- : Ad Tg

B

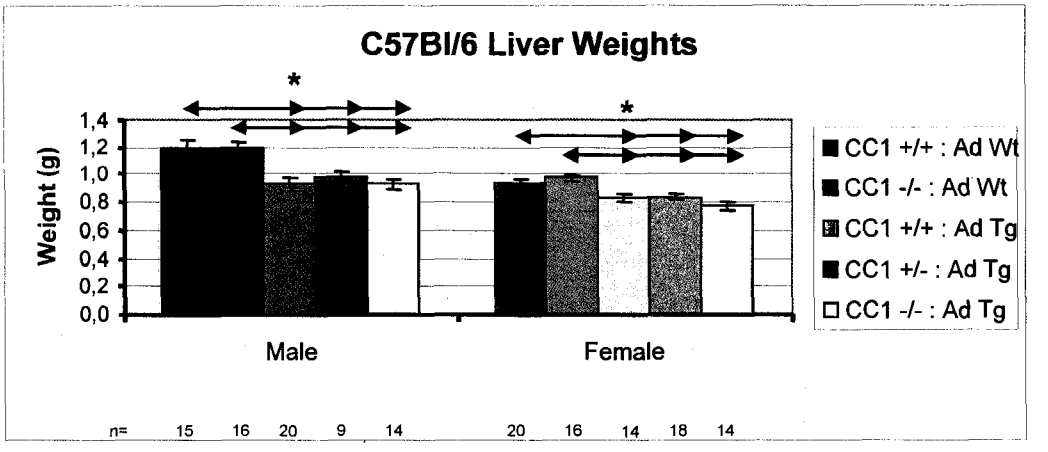
C57Bl/6 Liver Weights
Weight (g)
1,4
1,2
1,0
0,8
0,6
0,4
0,2
0,0
*
*
Male
Female
n= 15 16 20 9 14 20 16 14 18 14
CC1 +/+ : Ad Wt
CC1 -/- : Ad Wt
CC1 +/+ : Ad Tg
CC1 +/- : Ad Tg
CC1 -/- : Ad Tg

C

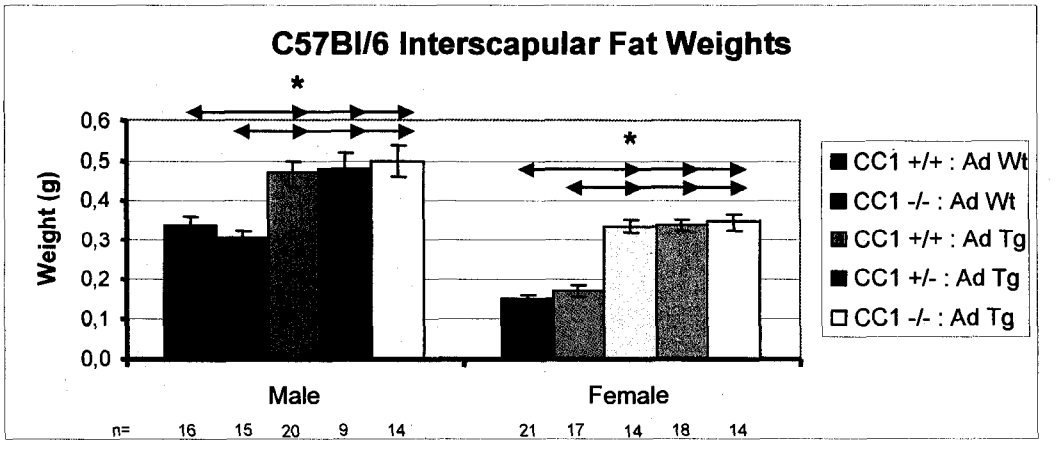
C57Bl/6 Interscapular Fat Weights
Weight (g)
0,6
0,5
0,4
0,3
0,2
0,1
0,0
*
*
Male
Female
n= 16 15 20 9 14 21 17 14 18 14
CC1 +/+ : Ad Wt
CC1 -/- : Ad Wt
CC1 +/+ : Ad Tg
CC1 +/- : Ad Tg
CC1 -/- : Ad Tg

D

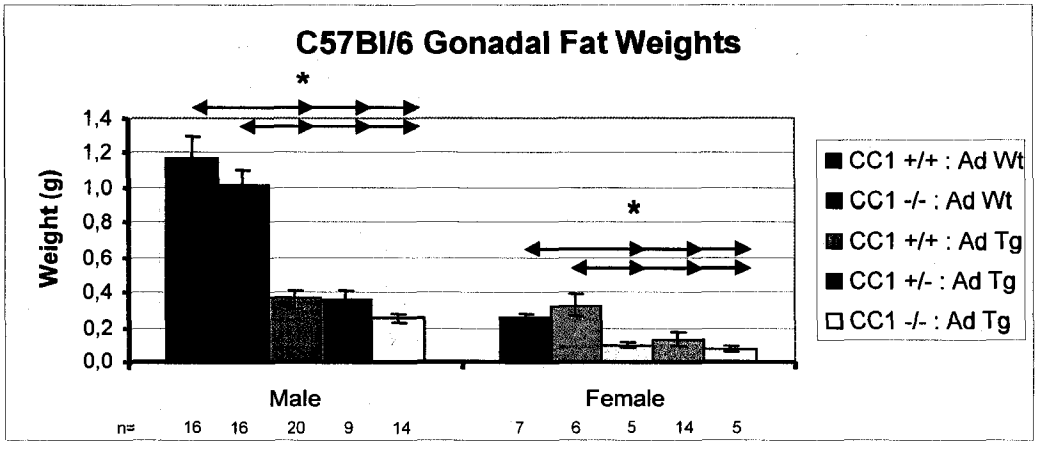
C57Bl/6 Gonadal Fat Weights
*
*
Weight (g)
1,4
1,2
1,0
0,8
0,6
0,4
0,2
0,0
Male
Female
n=
16 16 20 9 14
7 6 5 14 5
CC1 +/+ : Ad Wt
CC1 -/- : Ad Wt
CC1 +/+ : Ad Tg
CC1 +/- : Ad Tg
CC1 -/- : Ad Tg

E

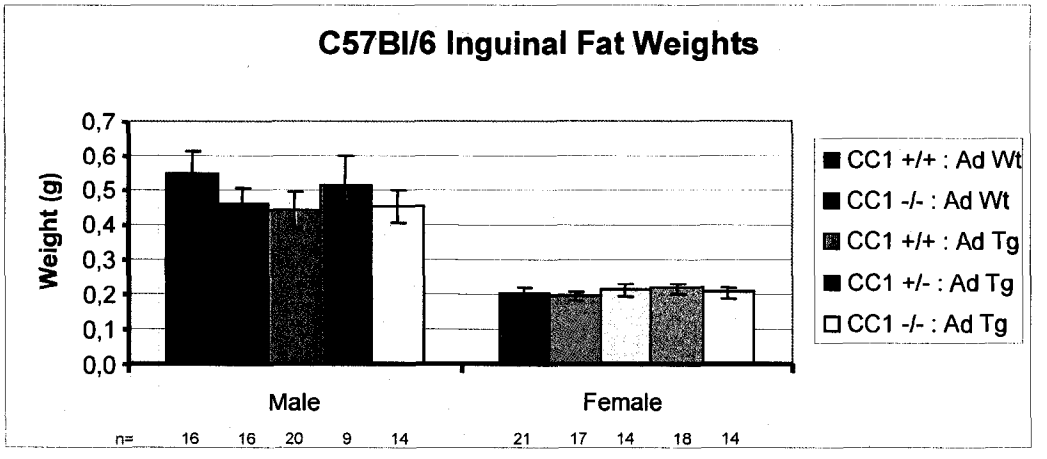
C57Bl/6 Inguinal Fat Weights
Weight (g)
0,7
0,6
0,5
0,4
0,3
0,2
0,1
0,0
Male
Female
n=
16 16 20 9 14
21 17 14 18 14
CC1 +/+ : Ad Wt
CC1 -/- : Ad Wt
CC1 +/+ : Ad Tg
CC1 +/- : Ad Tg
CC1 -/- : Ad Tg

IV. DISCUSSION

A) Transfer of the *Ad* transgene from the FVB to the C57Bl/6 background

The first goal of this work was to gauge whether by backcrossing the *Ad* tg+ mice onto the C57Bl/6 background, the phenotypes of these tg+ mice would still be present. The *Ad* transgene was correctly transferred from one strain to the other, as shown by genotyping. The net tg+ / wt ratios corresponding to the levels of Ad protein in inguinal (subcutaneous) and in perimetrial (visceral) fat pads of female mice are conserved between FVB and C57Bl/6 backgrounds. To ensure equal loading, level normalization was done with actin. The normalized and net levels are equal in perimetrial fat, but not in inguinal fat. However, the problem seems to be at the level of the actin protein in the Western blot, as normalization increases the tg+ / wt ratio. The faint signal in three consecutive columns seems to indicate a defect in the blot.

At the macroscopic level, *Ad* tg+ C57Bl/6 males, but not FVB's, weigh significantly less than their wt counterparts. No difference in weight was observed in females. The liver weight differences were amplified on the C57Bl/6 background and both genders showed significant differences, whereas only males showed significant differences in the FVB background. C57Bl/6 wt males had more epidydimal fat than FVB's. Insulin levels in C57Bl/6 wt males were four times those of FVB wt males. Insulin levels were similar in females and in tg+ males and no differences were observed between wt and tg+ mice. These results probably illustrate the predisposition of C57Bl/6 mice for obesity-linked insulin resistance in comparison to the FVB mice as well as the decrease insulin control of males over females (*380, 382, 385, 386*).

Both strains were characterized by a significant increase in interscapular fat accumulation in *Ad* tg+ mice. However, the levels were two times higher in FVB mice. Wt FVB females also had twice more interscapular fat than C57Bl/6 females. Some FVB *Ad* tg+ females developed axial proptosis, i.e. protusion of the eye outside of the cavity, due to increased BAT in the orbital cavity at 8 months of age. This was never observed in

C57Bl/6 mice. Since accumulation of BAT is also a manifestation of the PPARγ-agonist TZD, it could be postulated that the FVB-related increased sensitivity to insulin seems to be mediated in part by signalling through PPARγ (*234*).

Both strains showed significant reduction in gonadal fat in the *Ad* tg+ mice. However, C57Bl/6 wt females had approximately half the amount of perimetrial fat as FVB females. FVB *Ad* tg+ females displayed a significant increase in inguinal fat. This difference was not seen in FVB males or in the C57Bl/6 background for either gender. C57Bl/6 mice seem to show a lesser fat re-distribution between visceral and subcutaneous fat. More precisely, *Ad* tg+ FVB female mice had a bigger increase compared to wt mice in interscapular, inguinal and orbital fat than the *Ad* tg+ C57Bl/6 mice. This difference could be due to a lower amount of gonadal fat in female wt C57Bl/6 mice, presenting a smaller reservoir of visceral fat to redistribute to subcutaneous fat.

Serum Ad levels were similar in both strains. The small differences in serum Ad concentration lead to variations in tg+ / wt ratios, but these ratios stayed within the correct range and did not seem to affect the phenotype. Thus, the transgene transfer led to similar circulating Ad levels in both strains.

In summary, the *Ad* transgene was correctly transferred, similarly expressed and Ad was secreted into the circulation to a similar extent in both strains. Similar levels of secretion indicate comparable levels of Ad degradation in adipocytes. The small differences in statistical significance or absolute values between the two strains reflect predisposition of C57Bl/6 mice to insulin resistance (*380, 382, 385*). The characteristics described for the Ad tg+ FVB mice in Dr.Scherer's paper can thus be extended to our *Ad* tg+ C57Bl/6 mice.

A point to address is the portion of the FVB genome left in our mixed C57Bl/6-FVB (called C57Bl/6) mice in the backcrosses 3 and 4 used for these experiments. Preliminary studies and metabolism parameters of the *Ceacam1-/-* mice described by one of my colleagues were all performed on higher C57Bl/6 backcrosses (personal communication

from Dr. N. Beauchemin). At backcrosses 3 and 4, there are 12 and 6% of the FVB genome left, respectively. This remaining portion could translate into slightly decreased insulin resistance characteristics in comparison to higher C57Bl/6 backcrossed mice. The influence this low backcrossing may have on parameter differences between genotypes is unknown.

The association of the agouti coat color (light brown fur) with the transgenic genotype in mixed C57Bl/6-FVB mice for so many backcrosses is special. At backcrosses 3 and 4, most of the mice should be black, following the amount of C57Bl/6 genome transferred (i.e. 88% at backcross 3 and 94% at backcross 4). This indicates that the locus responsible for the agouti colour is close to that of the transgene and segregates with it. Close loci usually separate after 20-22 generations, when the line is considered pure.

B) Rescue of the *Ceacam1-/-* mouse model phenotype by overexpression of adiponectin

The second goal of this work was to examine if Ad overexpression would permit to limit the insulin resistance seen in *Ceacam1-/-* mice. In this study, *Ceacam1-/-* 6 month-old mice, both females and males, are not characterized by increased total body weight. However, my colleague Nelly Leung saw a significant increase. The partial or total ablation of the CEACAM1 molecule increases body weight here only in the most insulin sensitive environment, i.e in *Ad* tg+ females. The *Ceacam1* genotype did not affect liver, inguinal, interscapular and gonadal fat weights, neither in the wt nor in the *Ad* tg+ background. The increased body weight in *CC1* +/- and -/- : *Ad* tg+ mice relative to the *CC*1 +/+ : *Ad* tg+ mice could be due to an increase in other fat pads (for example, retroorbital, omental, mesenteric, subcutaneous). In fact, these mice showed a trend towards increased interscapular BAT and decreased blood glucose. Since *Ceacam1-/-* mice are characterized by hepatic insulin resistance, but normal peripheral glucose uptake (personal communication from Dr. A. Marette), it is also possible that on an ultra-sensitive background, the excess glucose production by the *Ceacam1-/-* liver is removed from the blood by the muscles and transformed into glycogen, leading to heavier muscles.

Muscles remove approximately 75% of the blood's glucose (*116*). This could be verified by weighing frozen muscles or by sectioning them and staining them with periodic acid-Schiff reagent for glycogen content.

We measured Ad levels using two different assays i.e RIA and ELISA. There is no difference in circulating Ad levels between *Ceacam1* genotypes on the *Ad* wt background at 6 months of age. In *Ad* tg+ males, *Ceacam1-/-* mice displayed higher Ad levels than wt mice. A difference was also seen in females on the *Ad* tg+ background by ELISA, but not by RIA. It is known that fasting circulating Ad levels are inversely proportional to fasting plasma insulin levels due to the regulation of Ad expression by insulin (*187*). Indeed, no differences in *Ceacam1* genotypes were observed relative to insulin levels, except in males on the *Ad* tg+ background where ko mice showed lower insulin levels. No differences were observed in females either. In addition, several abnormalities were observed in the ELISA, such as lower Ad levels and incorrect ratios between genotypes. Thus, even though more mice were tested by ELISA, more credit should be given to RIA results.

The lower detection in the ELISA can be due to several factors. First, RIAs were created to measure levels in serum/plasma, whereas ELISA is more suitable for culture supernatants. Serum samples contain many more interfering proteins. Fetal calf serum should have been added to the sample (and standard) diluent, even with a 1/10000 dilution factor. R&D Systems strongly suggests another kit for measuring Ad in serum, which is called Quantikine, but it is considerably more expensive. Absorbance situated in the middle of the standard curve, different maximal values and the differences between genotypes refute the saturation hypothesis. The inconsistent Ad detection between sexes and genotypes is puzzling. Prolactin is elevated 2-fold in *Ad* tg+ mice and is the only hormone varying with the genotype. However, levels are higher in males than females. Levels of other hormones such a glucocorticoids, growth hormone, thyroid stimulating hormone and leptin are comparable between wt and *Ad* tg+ mice (*234*). Even though the ELISA technique revealed some weaknesses, it allowed us to rapidly sample a huge

number of mice. Given that profiles are almost all conserved from RIA comparison, it also permited observation of the effect of the *Ceacam1* deletion on circulating Ad levels. Insulin values are lower than the normal fasting range of 0.5-2 ng/ml, even though mice were only fasted for 5 h. These values were in the lowest range of the curve, at the limit of sensitivity of the kit. With the actual values, the use of the ultra-sensitive RIA insulin kit would have given more precise results.

In summary, since there was no difference observed between wt and *Ceacam1-/-* mice in the parameters examined in this study, overexpression of Ad did not appear to rescue the *Ceacam1-/-* phenotype. Inversely, in some parameters, it created a phenotype in the *Ceacam1-/-* mice. However, a definitive test to perform for quantifying insulin resistance is the hyperinsulinemic euglycemic clamp assay and this will be evaluated as soon as possible.

C) Description of the metabolic parameters of the *Ceacam1-/-* mouse model (Table 2)

1. Complete description

My results demonstrate that *Ceacam1-/-* mice have normal insulin, adiponectin and glucose fasting blood levels as well as normal macroscopic parameters (total body weight, liver weight, white and brown adipose tissue weight (gonadal, inguinal, interscapular). The insulin and glucose levels as well as the epidydimal and liver weights were confirmed by one of my colleagues. However, she saw an elevation in total body and perimetrial fat weights. It has been shown by Najjar *et al.* that *Ceacam1-/-* mice were hyperinsulinemic, with insulin levels 3 times more elevated than in wt mice at 2 months of age (*259*). Different fasting periods and bleeding procedures as well as measurements by four different investigators in three different groups collaborating with our laboratory have not reproduced these results. However, Dr. Marette's laboratory has recently shown that *Ceacam1-/-* female mice are slightly hyperinsulinemic after a 5 hour fast and this hyperinsulinemic state is exacerbated in the postprandial state. The *Ceacam1-/-* males do not show this same difference (Appendix 1B).

The *Ceacam1-/-* phenotype is described in detail in Table 2. Most of the results were produced by my colleague N. Leung and by Dr. Marette's laboratory. In addition to my results, some results come from our collaborators Dr. Lévy and Dr. Savard. These results are presently unpublished. Briefly, significant differences were mostly observed at 6-12 months of age, indicating an increase in phenotype with age. This is consistent with increased MetS prevalence with age (*26*). In 12 month-old females, *Ceacam1-/-* mice demonstrated increased weight and liver steatosis as well as decreased blood TG, HDL and cholesterol levels. Total and esterified liver cholesterol levels were increased. Leptin was increased. 12 month-old males showed increased liver enzymes in serum. 6 month-old *Ceacam1-/-* males are insulin resistant only when this is measured by the hyperinsulinemic euglycemic clamp technique (Appendix 2). This is accompanied by increased liver glucose production after insulin infusion, due to a reduced capacity of insulin to suppress basal glucose production. Glucose uptake was not affected. Levels of different blood lipids were also decreased after a glucose or insulin boost. However, *Ceacam1-/-* mice show a reduction of the inhibition of hepatic FAS after insulin injection (*259*). In addition, chips analysis of *Ceacam1-/-* mice DNA revealed modification of several genes implicated in metabolism. Notably, all enzymes implicated in lipogenesis downstream of SREBP1c were upregulated, except for the acetyl CoA carboxylase. This exception can probably be explained by the fact that this enzyme is a highly regulated rate-determining step in lipogenesis and accords the absence of increased blood TG and FFA levels in *Ceacam1-/-* mice. The differences observed between *Ceacam1* wt and ko mice were mostly kept on a HFD, except for the elevation of liver enzymes in male *Ceacam1-/-* serum which was lost.

Differences in weight were observed by my colleague in both genders when mice were followed over a long period of time as well as when mice were weighed once at 6 months of age. I did not observe differences in weight in females or in males after having weighed mice once at 6 months of age. These inconsistencies seem to indicate that the weak *Ceacam1-/-* phenotype would be translated into a MetS component without overt disease. In humans, patients with similar traits would be considered in the upper limit of the normal range. In humans, insulin resistance diagnosed in slightly overweight people

is called primary insulin resistance (*53*). The *Ceacam1-/-* phenotype displays several characteristics of metabolically obese normal-weight (MONW) patients. Despite normal BMI, these subjects are characterized by insulin resistance, increased abdominal fat, light increase in TG and cholesterol blood levels, higher blood pressure and lower energy use during exercise. Some of them are not glucose intolerant (*387*). MONW patients do not show lower Ad levels in blood (*388*). Several studies have estimated the percentage of insulin resistance in normal weight people between 10-20% (*387*).

The phenotype of the *Ceacam1-/-* mice is comparable to the effect of a short-term HFD, characterized by impaired hepatic insulin sensitivity, absence of peripheral insulin resitance, normal glucose levels and normal basal hepatic glucose production. Insulin resistance was only observed by the clamp technique (*141*). It is possible to find insulin resistance without hyperinsulinemia, even if the cause and effect are physiologically related one to the other. A European study on non-obese patients, found that both (hperinsulinemia and insulin resistance) were diagnosed in only 60% of patients with one or the other diagnostic. Patients with insulin resistance only were characterized by increased abdominal adiposity, increased lipolysis, TG and hepatic glucose production (*136*). Increased hepatic glucose production due to insulin resistance could be reinforced by measuring the levels of gluconeogenic enzymes in the liver. Since the phenotype of the *Ceacam1-/-* mice is really weak in the basal state, we could examine at the post-prandial and exercise states. These mice may have a reduced capacity to adapt rapidly to different stimuli. It is known that postprandial hyperinsulinemia develops before fasting hyperinsulinemia (*43*). In addition, mice with liver-specific ablation of IR show severe hepatic insulin resistance, but normal peripheral insulin sensitivity. Their phenotype is more evident in the fed state than in the fasted state (*389*).

Given the mild hepatic insulin resistance of the *Ceacam1-/-* mice, it is not surprising that adiponectin levels were not different. In addition, Ad levels are more closely correlated with obesity components of MetS than with insulin resistance (*178*). Since HMW Ad is associated with increased insulin sensitivity, it would be interesting to quantify serum levels of different Ad molecular complexes (*23*). ELISA kits exist to measure different

Ad isoforms in humans, but not in mice (*390*). However, these could be separated and quantified using a velocity sedimentation technique in a sucrose gradient (*234*).

Hepatic TG levels are closely associated with hepatic insulin resistance (*46*). The fact that fatty liver and steatosis are the first liver problems to occur in insulin resistance indicates the presence or future appearance of MetS components in *Ceacam1-/-* females (*48*). Steatosis in females is not associated with higher levels of blood hepatic enzymes, whereas these enzymes are elevated in males which do not show increased steatosis (*247*). Measure of alanine aminotransferase did not correlate closely to NAFLD prevalence, often underestimating it. Men are usually more predisposed to NAFLD (*391-393*).

How does ablation of the *Ceacam*1 gene lead to hepatic insulin resistance and the associated phenotype? Endocytosis is not required for initiation and direct termination of IR signalling. However, it stops signalling by removing insulin from its receptor, tightly regulating the duration of insulin signalling (*394*). The deletion of the *Ceacam1* gene decreases endocytosis of IR, but not enough to trigger blood insulin build up. Short term insulin signalling is activated from IRs located at the plasma membrane (*126*). The following hypothesis can be proposed: the decreased endocytosis increases insulin signalling time, which leads to serine phosphorylation of molecules downstream of IR, triggering insulin resistance. It is possible that females and males react differently to this decreased endocytosis and/or insulin resistance, as they control glucose and insulin levels differently. For example, Ad overexpression in this study created significant differences in insulin and Ad levels between *Ceacam*1 wt and ko males, but triggered an increase in body weight in *Ceacam1-/-* females. It would be important to examine the insulin signalling downstream of IR in the *Ceacam1-/-* mice, both in males and in females. Serine phosphorylation of downstream IR targets in males could lead to increased cytokine production and creation of a low-grade inflammatory environment. It would lead to liver damage at one year of age, with concomitant elevation in liver enzymes in blood. Alkaline phosphatase and asparagine aminotransferase are more closely associated with bile canaliculi and hepatocytes problems respectively (*389*). A

collaborator is currently measuring the levels of pro-inflammatory cytokines in the liver of *Ceacam1* wt and ko mice. At 12 months of age, mice devoid of IRs specifically in the liver show lipid accumulation in hepatocytes as well as larger mitochondria, indicative of oxidative stress (*389*). This can be looked at in the *Ceacam1-/-* mice.

Females are more insulin sensitive and better regulate insulin signalling (*386*). They could be less affected by increased insulin signalling. The CEACAM1-mediated downregulation of FAS activity after insulin triggering has not been directly verified in males. It is possible that this mechanism is more important in females due to their increased insulin sensitivity. Deletion of the *Ceacam1* gene would lead to more apparent phenotypes in females than in males, leading to development of fatty liver. This would add to the increased signalling through SREBP-1c in the absence of CEACAM1. It is also possible that the SREBP pathways are more highly activated in female than in male *Ceacam1-/-* mice. The increase in hepatic fat content would reinforce insulin resistance. The decrease in TG, cholesterol and HDL in the serum of *Ceacam1-/-* females would indicate a reduced ability of insulin to trigger their synthesis. Normal serum FFA indicate normal lipolysis in adipose tissue and thus strengthen the fact that *Ceacam1-/-* mice are not characterized by peripheral insulin resistance, even at 12 months (*389*). Measuring insulin resistance in females by the clamp technique will be of great value in interpreting these results. The presence of fatty liver in *Ceacam1-/-* females, but not in males, can also be explained by the elevation in leptin specifically in these mice (personal communication Dr. N. Beauchemin). Leptin decreases ectopic fat, but often, an increase in leptin with normal adipose tissue weight is indicative of leptin resistance, which is related to insulin resistance (*73*).

IL-18 is implicated in atherosclerosis, graft-vs-host disease and hepatitis, but also in satiety (*395*). It could be a factor explaining hyperphagy in both *Ceacam1-/-* males and females, despite normal leptin levels in males.

2. Comparison of the *Ceacam1-/-* and L-SACC1 tg+ mouse models

L-SACC1 mice were produced by liver-specific overexpression of a dominant negative CEACAM1 molecule and are characterized by hyperinsulinemia, increased visceral adiposity, glucose intolerance, high levels of blood FFA and TG and liver TG. They have normal glucose uptake. Most of the parameters were observed in young mice (3 months) and the phenotype decreased with age. No difference in insulin secretion was seen. This phenotype is associated with decreased hepatic insulin clearance and increased hepatic insulin resistance.

The phenotype of the L-SACC1 mouse model is definitively more pronounced than the *Ceacam1-/-* phenotype. Thus, the L-SACC1 phenotype is not only the result of the loss of a functional CEACAM1 molecule. One hypothesis is that the presence of the non-functional CEACAM1 molecule is quenching CEACAM1-independent IR endocytosis pathways, reducing insulin clearance to a greater extent. For example, this molecule could quench the recycling of the highly abundant IR-B in the liver (*366*). A 30 fold overexpression of a highly glycosylated membrane protein as a dominant negative mutant could greatly reduce access to internalization sites, whereas deletion of the CEACAM1 protein would not produce this effect. Measurements of insulin clearance in *Ceacam1-/-* mice will definitively answer this question. The ratio of C-peptide over insulin serum levels is a good index of insulin clearance. C-peptide is produced by proteolytic cleavage of pro-insulin and is thus equal to insulin production. However, it is removed from the circulation by the kidney independently of IR (*396*). Quantifying the number of IRs at the cell surface and IR internalization in primary hepatocytes of *Ceacam1-/-* mice would assess the degree of reduction of IR endocytosis in these mice.

Another hypothesis is ER stress created in hepatocytes by the overexpression of a highly glycosylated mutant secretory proteins. ER stress is accompanied by increased CRP and inflammation. CRP is increased in L-SACC1. It would be interesting to quantify inflammation markers such as TNF-α and IL-6 in serum of L-SACC1 mice. The factors against the ER stress hypothesis are absence of increased fatty acid synthesis in the liver and absence of reduced IR downstream signalling. This hypothesis could be tested by

measuring the phosphorylation of two key markers of ER stress, PERK (PKR like ER kinase) and eIF2α (translation initiator factor 2), in the liver of L-SACC1 mice. Increased phosphorylation indicates ER stress (*397*).

It is also possible that hyperinsulinemia in *Ceacam1-/-* mice is prevented by increased clearance due to the absence of recruitment of SHP-1 complexes (SHP-1/Cdk2/cyclin E) to the plasma membrane. Expression of inactive SHP-1 in hepatocytes has been shown to increase insulin-IR endosomal degradation (*164*). This could be due to elevated CEACAM1 phosphorylation, but also to increased phosphorylation of other proteins leading to increased clearance. In L-SACC1 mice, SHP-1 could still be recruited to the plasma membrane by the few remaining functional CEACAM1 molecules.

D) Tumour induction

Due to the lack of differences I observed in metabolic parameters (total and organ weight, hormones and glucose levels) between wt and *Ceacam1-/-* mice, I would not induce tumours in *CC1 : Ad* mice. First, the most recognized hypothesis linking Ad, MetS and cancers is based on hyperinsulinemia (*250*). However, our mice do not display profound fasting hyperinsulinemia. Second, epidemiological studies saw a link between MetS and colon cancer only in men (*252-254*). My colleague did not observe a sexual dimorphism in the incidence and progression of intestinal and colon cancers in *Ceacam1-/-* mice (*352*)(personal communication Dr. N. Beauchemin). This suggests that the mild insulin resistance and the different metabolic manifestations between males and females, do not affect tumour progression. Third, IR and CEACAM1 are both found in the intestine and in the colon (*398*). The role of CEACAM1 in intestinal IR endocytosis has not yet been studied. However, it has been shown that colon tumours express higher IR levels (*398*). If insulin signalling does play a role in the development of colon cancer in *Ceacam1-/-* mice, it could also be due to reduced IR endocytosis in this organ and to decreased inhibition of mitogenic IR signalling in the absence of CEACAM1. Fourth, confirmation from the hyperinsulinemic euglycemic clamp is needed, but it is highly possible that the increased insulin sensitivity created by overexpression of Ad will be much higher than

what is needed to rescue the *Ceacam1-/-* insulin resistance. Inducing tumours in these mice would probably inform us about the role of insulin resistance in colon cancer through Ad, but not the role of *Ceacam1-/-* insulin resistance. In addition, overexpression of Ad created new differences between *Ceacam1* wt and ko mice for some parameters, such as insulin and adiponectin serum levels. This would complicate the analysis.

On the other hand, Dr. Marette has recently observed postprandial hyperinsulinemia in *Ceacam1-/-* females (Appendix 1B). Postprandial insulin levels will thus be measured in females with different *CC1 : Ad* genotypes. Upon normalization of postprandial insulin levels by overexpression of Ad, tumours will be induced by the chemical carcinogen azoxymethane in *CC1 : Ad* females.

In addition, it would be interesting to look at the effect of a global increase in insulin sensitivity on tumour induction and progression in the colon. Adiponectin receptors are not expressed in the colon and the intestine, avoiding direct anti-carcinogenesis action of adiponectin (*225*). Low Ad levels in humans have already been associated with lower grades and stages of tumours (*250*).

E) Future directions

We are currently waiting to test mice with different *CC1 : Ad* genotypes by hyperinsulinemic euglycemic clamps to examine if hepatic insulin resistance is reversed by overexpression of Ad. This will also tell us about insulin resistance in *Ceacam1-/-* females, which has not yet been measured. This technique is laborious and requires expertise. Only few laboratories in North America perform this experiment in mice. Our mice will be sent to Dr.André Marette's laboratory (Université Laval, Québec, Canada).

Fatty liver with steatosis was observed in *Ceacam1-/-* mice at 12 months of age (personal communication Dr. N .Beauchemin). Ad rescues NAFLD and AFLD in different mouse models (*79*). Pieces of livers from all 6 month-old mice dissected in this project were fixed in formalin and paraffin-embedded. We are now sectioning these samples and

staining them with hematoxilin and eosin. They will be sent to a pathologist, which will evaluate the extent of hepatocyte ballooning, a stage preceding overt steatosis. Quantification of Ad in serum of *Ceacam1-/-* mice at 12 months of age will also give insight into the relation between Ad and fatty liver in this model.

Ceacam1-/- livers are characterized by overexpression of several enzymes involved in lipid synthesis downstream of SREBP1c (personal communication from Dr. N. Beauchemin). mRNAs are now being isolated from frozen livers with different *CC1 : Ad* genotypes to quantify the expression of FAS and acetyl-CoA carboxylase.

Even though the levels of different lipids are not elevated in the basal state, difficulty in inserting catheters in *Ceacam1-/-* arteries in the clamp technique was observed (personal communication from Dr. A. Marette). In addition, CEACAM1 expression in platelets has been shown to inhibit interaction with collagen (personal communication from Dr. D.E. Jackson). Since it has been shown that *Ceacam1-/-* mice have normal vascularization but deficient neovascularization, examining the levels of atherosclerosis may give us novel information. Given the anti-atherogenic role of Ad (*228*), we will shortly be isolating the aorta from different *CC1 : Ad* genotypes, fixing them and sending them to a pathologist for atherosclerosis lesion grading. Asymmetric dimethylarginine could also be measured as a sign of endothelial dysfunction (*67*).

Even though *Ceacam1-/-* mice do not have different Ad levels in blood and CEACAM1 is not expressed in adipocytes, one of our collaborators, Dr. R. Savard, has observed decreased Ad and increased leptin secretion from mature adipocytes derived from *Ceacam1* heterozygous parametrial fat. This was also observed in C57Bl/6 mice fed with a HFD in which blood Ad levels were normal despite reduction in gonadal fat levels. It was postulated that other fat pads may compensate. However, AdipoR levels were different in liver and muscles (*399*). Adiponectin levels in blood could also be normalized by secretion from liver endothelium and parenchyma under stress (in this case fatty liver) conditions (*191*). A larger number of *Ceacam1-/-* mature adipocytes have GLUT-4 at their surface, but the quantity of GLUT-4 on each cell is decreased. This

phenotype was shown to be rescued by overexpression of Ad (personal communication from Dr. R. Savard). GLUT-4 is used as a marker of insulin resistance and adipocyte differentiation. The absence of differences in pre-adipocytes seems to indicate de-differentiation and not a differentiation problem. TNF-α directly regulates expression of differentiation genes such as adiponectin in adipocytes (*74*). This pro-inflammatory molecule is also implicated in insulin resistance, atherosclerosis and inflammation. TNF-α in the liver also augments fatty liver by increased activation of SREBP1c (*78*). This molecule is promising and should be quantified in blood, liver and adipose tissues. In addition to adipocytes, TNF-α is mostly produced by macrophages (*79*). It would also be interesting to quantify the expression levels of AdipoR1 and R2 in muscles, liver and fat in different *CC1 : Ad* mice. Presence of mature adipocytes with reduced differentiation markers is often observed with adipocyte hypertrophy caused by increased lipid storage in patients with obesity and subsequent insulin resistance (*11*). Dr. Savard's team is now measuring the size of parametrial adipocytes in different *CC1 : Ad* mice. Even in non-obese patients, inflammatory molecules such as TNF-α, IL-6 and CRP are more elevated and are associated with larger adipocytes (*400*). However, a recent study observed a higher amount of small adipocytes concomitant to reduced GLUT4 and Ad in insulin-resistant patients, after normalizing for BMI (*401*). In all these experiments, we expect a rescue of the *Ceacam1-/-* phenotype by Ad.

Although recent work greatly increases the understanding of the metabolic effects of the *Ceacam1-/-* deletion, it raises several avenues for further investigations. Briefly, the *Ceacam1-/-* metabolic phenotype is mild, increases with age, differs between females and males and is centered in the liver. Other experiments, mostly the hyperinsulinemic euglycemic clamp, are needed to confirm it, but overexpression of Ad seems to consist of a treatment too strong to correct *Ceacam1-/-* metabolic abnormalities. From the present information, the *Ceacam1-/-* metabolic phenotype is too mild to look at its implication in colon cancer. However, the recent observation of postprandial hyperinsulinemia in *Ceacam1-/-* females may lead to reconsideration of this decision. A complete understanding of the physiological and molecular portrait is still needed and reflects the complex inter-relationships between MetS components in the human population.

Table 2. Metabolic parameters of the *Ceacam1-/-* mouse model

ORGANS	CHARACTERISTICS	PHENOTYPE[1]			Age (months)
		MALE	FEMALE	MIXED	
Whole body	Weight	↑	↑	↑	6
		=	↑ 1.5X	↑	12
		↑ 10-15%	↑ 10-15%	ND	7
	Food consumption	↑ 10-20%	↑ 10-20%	ND	2
Liver	Weight	=	=	=	6
		=	=	=	12
	Cholesterol	ND	ND	↑ 1.5X	12
	Esterified cholesterol	ND	ND	↑ 2X	12
	Steatosis	=	↑ 1.5X	ND	12
	Structure	ND	ND	=	5
	Fat content (histology)	ND	ND	↑	12-14
	Hepatic glucose production (clamp)	↑ 3X	ND	ND	6
	Inhibition of basal hepatic production (clamp)	↓	ND	ND	6
	Glucose uptake (clamp)	=	ND	ND	6
	FAS activity (after insulin) (*259*)	ND	↑	ND	2
Blood	Leptin	=	↑ 2X	ND	?
	Ad	=	=	ND	6
	FFA	=	=	ND	6 and 12
	TG	=	=	=	6
		=	↓ 60%	↓30%	12
	HDL	=	=	=	6
		=	↓ 50%	↓20%	12
	Cholesterol	=	=	=	6
		=	↓ 40%	↓15%	12
	C15-C18 (after glucose gavage)	↓	ND	ND	3
	Esterified / non-esterified FA (after glucose gavage)	↓	ND	ND	3
	C16-C22 (after insulin)	↓	ND	ND	3
	Total lipid (after insulin)	↓	ND	ND	3
	Fasting blood glucose	=	TD ↓	=	6
		=	=	=	12
	Fasting insulin	=	=	=	6 and 12

	OGTT (glucose and insulin)	=	ND	ND	2 and 3
	ITT	=	ND	ND	3
	Alanine aminotransferase	=	=	=	6
		↑ 2X	=	↑ 2X	12
	Asparagine aminotransferase	↑ 1.3X	=	TD↑	6
		TD↑	=	TD↑	12
	Alkaline phosphatase	↑ 1.2X	=	=	6
		↑ 1.3X	=	↑TD	12
Fat					
Gonadal	Weight	↑ 2X	TD↑	↑ 1.5X	6
		↑ 1.5X	=	↑ 1.3X	12
	GLUT-4 on each adipocytes	ND	↓	ND	6
	Number of adipocytes with GLUT-4s	ND	↑	ND	6
Interscapular	Weight	=	=	ND	6
Inguinal	Weight	=	=	ND	6
Kidney	Function	ND	ND	=	3

[1] Phenotype = *Ceacam1* ko vs wt

1. M. Tjepkema, in *Health Reports*. (Statistics Canada, 2006), vol. 17 (3), pp. 9-26.
2. M. Shields. (Statistics Canada, 2006), vol. 17(3), pp. 27-42.
3. . (Public Health Agency of Canada. National Diabetes Surveillance System).
4. C. G. S. Murphy KA, O'Dwyer A for the Population Health Impact of Diseases in Canada (PHI). (Statistics Canada, 2005).
5. E. Arias, R. N. Anderson, H. C. Kung, S. L. Murphy, K. D. Kochanek, *Natl Vital Stat Rep* **52**, 1 (Sep 18, 2003).
6. D. E. Laaksonen *et al.*, *Am J Epidemiol* **156**, 1070 (Dec 1, 2002).
7. E. S. Ford, *Diabetes Care* **28**, 1769 (Jul, 2005).
8. E. Kylin, *Zentralblatt fuer Innere Medizin* **44**, 105 (1923).
9. G. M. Reaven, *Nutrition* **13**, 65; discussion 64 (Jan, 1997).
10. R. A. DeFronzo, E. Ferrannini, *Diabetes Care* **14**, 173 (Mar, 1991).
11. M. Teran-Garcia, C. Bouchard, *Appl Physiol Nutr Metab* **32**, 89 (Feb, 2007).
12. S. Desroches, B. Lamarche, *Appl Physiol Nutr Metab* **32**, 23 (Feb, 2007).
13. B. J. Shen *et al.*, *Am J Epidemiol* **157**, 701 (Apr 15, 2003).
14. E. Ferrannini *et al.*, *J Clin Endocrinol Metab* (May 15, 2007).
15. S. M. Grundy *et al.*, *Circulation* **112**, 2735 (Oct 25, 2005).
16. C. I. Ardern, I. Janssen, *Appl Physiol Nutr Metab* **32**, 33 (Feb, 2007).
17. G. M. Reaven, *Curr Atheroscler Rep* **5**, 364 (Sep, 2003).
18. J. P. Despres, *Int J Obes Relat Metab Disord* **27 Suppl 3**, S22 (Dec, 2003).
19. F. Leyva *et al.*, *Arterioscler Thromb Vasc Biol* **18**, 928 (Jun, 1998).
20. T. E. Graham *et al.*, *N Engl J Med* **354**, 2552 (Jun 15, 2006).
21. A. Xu *et al.*, *Clin Chem* **52**, 405 (Mar, 2006).
22. C. Menzaghi *et al.*, *J Clin Endocrinol Metab* **91**, 2792 (Jul, 2006).
23. C. Lara-Castro, N. Luo, P. Wallace, R. L. Klein, W. T. Garvey, *Diabetes* **55**, 249 (Jan, 2006).
24. R. Kahn, J. Buse, E. Ferrannini, M. Stern, *Diabetes Care* **28**, 2289 (Sep, 2005).
25. E. S. Ford, W. H. Giles, W. H. Dietz, *Jama* **287**, 356 (Jan 16, 2002).
26. E. S. Ford, W. H. Giles, A. H. Mokdad, *Diabetes Care* **27**, 2444 (Oct, 2004).
27. S. D. de Ferranti, K. Gauvreau, D. S. Ludwig, J. W. Newburger, N. Rifai, *Clin Chem* **52**, 1325 (Jul, 2006).
28. W. H. Organization, S. Geneva, Ed. (2000).
29. L. H. Opie, *Circulation* **115**, e32 (Jan 23, 2007).
30. S. R. Srinivasan, M. G. Frontini, G. S. Berenson, *Metabolism* **52**, 443 (Apr, 2003).
31. H. Ulmer, C. Kelleher, G. Diem, H. Concin, *Eur Heart J* **24**, 1004 (Jun, 2003).
32. K. J. Hunt, G. Heiss, P. D. Sholinsky, M. A. Province, *Genet Epidemiol* **19**, 395 (Dec, 2000).
33. E. Ravussin, M. E. Valencia, J. Esparza, P. H. Bennett, L. O. Schulz, *Diabetes Care* **17**, 1067 (Sep, 1994).
34. S. Francke *et al.*, *Hum Mol Genet* **10**, 2751 (Nov 15, 2001).
35. K. G. Alberti, P. Zimmet, J. Shaw, *Lancet* **366**, 1059 (Sep 24-30, 2005).
36. L. Palaniappan *et al.*, *Diabetes Care* **27**, 788 (Mar, 2004).
37. C. Weyer *et al.*, *Mol Genet Metab* **72**, 231 (Mar, 2001).
38. K. A. Jandeleit-Dahm, C. Tikellis, C. M. Reid, C. I. Johnston, M. E. Cooper, *J Hypertens* **23**, 463 (Mar, 2005).
39. M. Krssak *et al.*, *Diabetologia* **42**, 113 (Jan, 1999).
40. Y. Lee *et al.*, *Proc Natl Acad Sci U S A* **91**, 10878 (Nov 8, 1994).

41. A. Seppala-Lindroos *et al.*, *J Clin Endocrinol Metab* **87**, 3023 (Jul, 2002).
42. G. C. Yaney, B. E. Corkey, *Diabetologia* **46**, 1297 (Oct, 2003).
43. R. H. Eckel, S. M. Grundy, P. Z. Zimmet, *Lancet* **365**, 1415 (Apr 16-22, 2005).
44. N. B. Ruderman, A. K. Saha, D. Vavvas, L. A. Witters, *Am J Physiol* **276**, E1 (Jan, 1999).
45. R. Belfort *et al.*, *Diabetes* **54**, 1640 (Jun, 2005).
46. P. J. Voshol *et al.*, *Endocrinology* **144**, 3456 (Aug, 2003).
47. M. Syvanne, M. R. Taskinen, *Lancet* **350 Suppl 1**, SI20 (Jul, 1997).
48. B. A. Neuschwander-Tetri, *Curr Opin Gastroenterol* **23**, 193 (Mar, 2007).
49. P. Bjorntorp, *Arteriosclerosis* **10**, 493 (1990).
50. J. M. Miles, M. D. Jensen, *Diabetes Care* **28**, 2326 (Sep, 2005).
51. S. R. Smith *et al.*, *Metabolism* **50**, 425 (Apr, 2001).
52. G. M. Reaven, *Diabetes* **37**, 1595 (Dec, 1988).
53. S. M. Grundy, H. B. Brewer, Jr., J. I. Cleeman, S. C. Smith, Jr., C. Lenfant, *Circulation* **109**, 433 (Jan 27, 2004).
54. M. L. Cruz *et al.*, *J Clin Endocrinol Metab* **89**, 108 (Jan, 2004).
55. J. F. Youngren, J. Paik, R. J. Barnard, *J Appl Physiol* **91**, 2240 (Nov, 2001).
56. R. H. Eckel, *N Engl J Med* **320**, 1060 (Apr 20, 1989).
57. I. Shimomura *et al.*, *Proc Natl Acad Sci U S A* **96**, 13656 (Nov 23, 1999).
58. F. Foufelle, P. Ferre, *Biochem J* **366**, 377 (Sep 1, 2002).
59. E. Bugianesi, A. J. McCullough, G. Marchesini, *Hepatology* **42**, 987 (Nov, 2005).
60. G. F. Lewis, K. D. Uffelman, L. W. Szeto, B. Weller, G. Steiner, *J Clin Invest* **95**, 158 (Jan, 1995).
61. T. Murakami *et al.*, *Arterioscler Thromb Vasc Biol* **15**, 1819 (Nov, 1995).
62. E. Manzato *et al.*, *Clin Chim Acta* **219**, 57 (Oct 15, 1993).
63. C. J. Packard, *Curr Med Res Opin* **13**, 379 (1996).
64. A. J. Hanley *et al.*, *Diabetes* **51**, 2642 (Aug, 2002).
65. J. E. Tooke, M. M. Hannemann, *J Intern Med* **247**, 425 (Apr, 2000).
66. S. Kuroda *et al.*, *J Hum Hypertens* **13**, 257 (Apr, 1999).
67. B. M. Egan, *Curr Hypertens Rep* **5**, 247 (Jun, 2003).
68. D. Tripathy *et al.*, *Diabetes* **52**, 2882 (Dec, 2003).
69. A. A. Zandbergen, S. W. Lamberts, J. A. Janssen, A. H. Bootsma, *Eur J Endocrinol* **155**, 293 (Aug, 2006).
70. F. Facchini, Y. D. Chen, C. B. Hollenbeck, G. M. Reaven, *Jama* **266**, 3008 (Dec 4, 1991).
71. J. Choudhury, A. J. Sanyal, *Clin Liver Dis* **8**, 575 (Aug, 2004).
72. D. E. Cummings, M. W. Schwartz, *Annu Rev Med* **54**, 453 (2003).
73. Y. Lee *et al.*, *J Biol Chem* **276**, 5629 (Feb 23, 2001).
74. H. Ruan, N. Hacohen, T. R. Golub, L. Van Parijs, H. F. Lodish, *Diabetes* **51**, 1319 (May, 2002).
75. H. Ruan *et al.*, *Diabetes* **51**, 3176 (Nov, 2002).
76. H. Ruan, H. F. Lodish, *Cytokine Growth Factor Rev* **14**, 447 (Oct, 2003).
77. M. H. Porter, A. Cutchins, J. B. Fine, Y. Bai, M. DiGirolamo, *J Lab Clin Med* **139**, 140 (Mar, 2002).
78. J. F. Lawler, Jr., M. Yin, A. M. Diehl, E. Roberts, S. Chatterjee, *J Biol Chem* **273**, 5053 (Feb 27, 1998).
79. H. Tilg, A. R. Moschen, *Nat Rev Immunol* **6**, 772 (Oct, 2006).

80. E. E. Kershaw, J. S. Flier, *J Clin Endocrinol Metab* **89**, 2548 (Jun, 2004).
81. J. I. Odegaard *et al.*, *Nature* **447**, 1116 (Jun 28, 2007).
82. C. Weyer *et al.*, *Atherosclerosis* **161**, 233 (Mar, 2002).
83. T. Collins, *Lab Invest* **68**, 499 (May, 1993).
84. J. L. Evans, I. D. Goldfine, B. A. Maddux, G. M. Grodsky, *Endocr Rev* **23**, 599 (Oct, 2002).
85. E. J. de Koning, T. J. Rabelink, *Atheroscler Suppl* **3**, 11 (May, 2002).
86. T. Matsunaga, S. Hokari, I. Koyama, T. Harada, T. Komoda, *Biochem Biophys Res Commun* **303**, 313 (Mar 28, 2003).
87. T. P. Zwaka, V. Hombach, J. Torzewski, *Circulation* **103**, 1194 (Mar 6, 2001).
88. V. Pasceri, J. T. Willerson, E. T. Yeh, *Circulation* **102**, 2165 (Oct 31, 2000).
89. J. L. Bolaffi, G. G. Rodd, J. Wang, G. M. Grodsky, *Endocrinology* **134**, 537 (Feb, 1994).
90. I. L. Campbell, L. Oxbrow, L. C. Harrison, *Mol Cell Endocrinol* **52**, 161 (Jul, 1987).
91. R. K. Semple, V. K. Chatterjee, S. O'Rahilly, *J Clin Invest* **116**, 581 (Mar, 2006).
92. G. S. Hotamisligil, *Nature* **444**, 860 (Dec 14, 2006).
93. I. A. Leclercq, A. Da Silva Morais, B. Schroyen, N. Van Hul, A. Geerts, *J Hepatol* **47**, 142 (Jul, 2007).
94. C. Ji, N. Kaplowitz, *J Hepatol* **45**, 321 (Aug, 2006).
95. E. D. Werner, J. L. Brodsky, A. A. McCracken, *Proc Natl Acad Sci U S A* **93**, 13797 (Nov 26, 1996).
96. K. Zhang, R. J. Kaufman, *Neurology* **66**, S102 (Jan 24, 2006).
97. K. Zhang *et al.*, *Cell* **124**, 587 (Feb 10, 2006).
98. M. S. Brown, J. L. Goldstein, *Cell* **89**, 331 (May 2, 1997).
99. D. Ron, S. Oyadomari, *Dev Cell* **7**, 287 (Sep, 2004).
100. G. K. Hansson, *N Engl J Med* **352**, 1685 (Apr 21, 2005).
101. D. Wang, Y. Wei, D. Schmoll, K. N. Maclean, M. J. Pagliassotti, *Endocrinology* **147**, 350 (Jan, 2006).
102. K. Ozawa *et al.*, *Diabetes* **54**, 657 (Mar, 2005).
103. U. Ozcan *et al.*, *Science* **313**, 1137 (Aug 25, 2006).
104. U. Ozcan *et al.*, *Science* **306**, 457 (Oct 15, 2004).
105. D. M. Muoio, C. B. Newgard, *Science* **306**, 425 (Oct 15, 2004).
106. I. Kharroubi *et al.*, *Endocrinology* **145**, 5087 (Nov, 2004).
107. H. F. Lodish, Berk, A., Zipursky, S.L., Matsudaira, P., Baltimore, D., Darnell, J., *Molecular Cell Biology* (W.H.Freeman and Company, ed. 4th, 2000), pp. 1084 (p897).
108. G. Sesti, M. Federici, D. Lauro, P. Sbraccia, R. Lauro, *Diabetes Metab Res Rev* **17**, 363 (Sep-Oct, 2001).
109. Y. Yamaguchi, J. S. Flier, H. Benecke, B. J. Ransil, D. E. Moller, *Endocrinology* **132**, 1132 (Mar, 1993).
110. G. Sesti, *Best Pract Res Clin Endocrinol Metab* **20**, 665 (Dec, 2006).
111. F. Frasca *et al.*, *Mol Cell Biol* **19**, 3278 (May, 1999).
112. M. Federici *et al.*, *Mol Cell Endocrinol* **129**, 121 (May 16, 1997).
113. M. A. Soos, C. E. Field, K. Siddle, *Biochem J* **290 (Pt 2)**, 419 (Mar 1, 1993).
114. B. L. Seely, D. R. Reichart, Y. Takata, C. Yip, J. M. Olefsky, *Endocrinology* **136**, 1635 (Apr, 1995).

115. D. Voet, Voet JG, *Biochemistry : Biomolecules, Mechanisms of Enzyme Action, and Metabolism* (John Wiley & Sons, Inc, ed. 3rd, 2004), pp. 1178 (p648 & 734).
116. R. A. DeFronzo, *Diabetes* **37**, 667 (Jun, 1988).
117. G. I. Shulman *et al.*, *N Engl J Med* **322**, 223 (Jan 25, 1990).
118. D. A. Lauffenburger, Linderman, J.J., *Receptors : Models for Binding, Trafficking, and Signaling.* (New York : Oxford University Press, 1993), pp. p365.
119. L. Benzi *et al.*, *Eur J Endocrinol* **148**, 365 (Mar, 2003).
120. J. L. Carpentier, *Diabetologia* **37 Suppl 2**, S117 (Sep, 1994).
121. J. L. Carpentier, *Horm Res* **38**, 13 (1992).
122. R. A. Heller-Harrison, M. Morin, M. P. Czech, *J Biol Chem* **270**, 24442 (Oct 13, 1995).
123. G. M. Di Guglielmo *et al.*, *Mol Cell Biochem* **182**, 59 (May, 1998).
124. A. Balbis, G. Baquiran, J. J. Bergeron, B. I. Posner, *Endocrinology* **141**, 4041 (Nov, 2000).
125. X. Su, I. J. Lodhi, A. R. Saltiel, P. D. Stahl, *J Biol Chem* **281**, 27982 (Sep 22, 2006).
126. B. P. Ceresa, A. W. Kao, S. R. Santeler, J. E. Pessin, *Mol Cell Biol* **18**, 3862 (Jul, 1998).
127. J. O. Contreres, R. Faure, G. Baquiran, J. J. Bergeron, B. I. Posner, *J Biol Chem* **273**, 22007 (Aug 21, 1998).
128. P. J. Seabright, G. D. Smith, *Biochem J* **320 (Pt 3)**, 947 (Dec 15, 1996).
129. R. Faure, G. Baquiran, J. J. Bergeron, B. I. Posner, *J Biol Chem* **267**, 11215 (Jun 5, 1992).
130. Z. Ahmed, B. J. Smith, T. S. Pillay, *FEBS Lett* **475**, 31 (Jun 9, 2000).
131. V. P. Knutson, *Faseb J* **5**, 2130 (May, 1991).
132. A. P. Bevan *et al.*, *Mol Cell Endocrinol* **164**, 145 (Jun, 2000).
133. G. Arsenis, G. R. Hayes, J. N. Livingston, *J Biol Chem* **260**, 2202 (Feb 25, 1985).
134. T. Sasaoka *et al.*, *Endocrinology* **140**, 3826 (Aug, 1999).
135. T. Tsakiridis *et al.*, *Microsc Res Tech* **47**, 79 (Oct 15, 1999).
136. E. Ferrannini, B. Balkau, *Diabet Med* **19**, 724 (Sep, 2002).
137. J. F. Youngren, *Cell Mol Life Sci* **64**, 873 (Apr, 2007).
138. A. R. Saltiel, C. R. Kahn, *Nature* **414**, 799 (Dec 13, 2001).
139. P. Gual, Y. Le Marchand-Brustel, J. F. Tanti, *Biochimie* **87**, 99 (Jan, 2005).
140. B. Mlinar, J. Marc, A. Janez, M. Pfeifer, *Clin Chim Acta* **375**, 20 (Jan, 2007).
141. V. T. Samuel *et al.*, *J Biol Chem* **279**, 32345 (Jul 30, 2004).
142. C. Schmitz-Peiffer, *Ann N Y Acad Sci* **967**, 146 (Jun, 2002).
143. K. Cusi *et al.*, *J Clin Invest* **105**, 311 (Feb, 2000).
144. L. J. Goodyear, B. B. Kahn, *Annu Rev Med* **49**, 235 (1998).
145. A. Vander, Sherman, J , Luciano, D, *Human Physiology : The Mechanisms of Body Function* (McGraw-Hill, ed. 8th, 2001), pp. 800 (p607).
146. Y. Okabayashi *et al.*, *Diabetes* **38**, 182 (Feb, 1989).
147. L. Wells, G. W. Hart, *FEBS Lett* **546**, 154 (Jul 3, 2003).
148. Y. H. Abdel-Wahab *et al.*, *Diabetes* **45**, 1489 (Nov, 1996).
149. L. Pirola, A. M. Johnston, E. Van Obberghen, *Diabetologia* **47**, 170 (Feb, 2004).
150. J. W. Baynes, *Diabetes* **40**, 405 (Apr, 1991).
151. G. Basta *et al.*, *J Clin Endocrinol Metab* **91**, 4628 (Nov, 2006).

152. I. R. Schlaepfer *et al.*, *J Lipid Res* **44**, 1174 (Jun, 2003).
153. K. E. Wellen, G. S. Hotamisligil, *J Clin Invest* **115**, 1111 (May, 2005).
154. C. Weigert *et al.*, *J Biol Chem* **281**, 7060 (Mar 17, 2006).
155. M. Yuan *et al.*, *Science* **293**, 1673 (Aug 31, 2001).
156. K. Ueki, T. Kondo, C. R. Kahn, *Mol Cell Biol* **24**, 5434 (Jun, 2004).
157. K. Ueki, T. Kadowaki, C. R. Kahn, *Hepatol Res* **33**, 185 (Oct, 2005).
158. R. A. Mooney *et al.*, *J Biol Chem* **276**, 25889 (Jul 13, 2001).
159. P. Sartipy, D. J. Loskutoff, *Proc Natl Acad Sci U S A* **100**, 7265 (Jun 10, 2003).
160. J. Kusari, K. A. Kenner, K. I. Suh, D. E. Hill, R. R. Henry, *J Clin Invest* **93**, 1156 (Mar, 1994).
161. M. Vinciguerra, M. Foti, *Arch Physiol Biochem* **112**, 89 (Apr, 2006).
162. F. Ahmad *et al.*, *Metabolism* **46**, 1140 (Oct, 1997).
163. E. Asante-Appiah, B. P. Kennedy, *Am J Physiol Endocrinol Metab* **284**, E663 (Apr, 2003).
164. M. J. Dubois *et al.*, *Nat Med* **12**, 549 (May, 2006).
165. M. A. Carvalho-Filho *et al.*, *Diabetes* **54**, 959 (Apr, 2005).
166. S. Kapur, S. Bedard, B. Marcotte, C. H. Cote, A. Marette, *Diabetes* **46**, 1691 (Nov, 1997).
167. A. Balbis, G. Baquiran, V. Dumas, B. I. Posner, *J Biol Chem* **279**, 12777 (Mar 26, 2004).
168. S. S. Hori, I. J. Kurland, J. J. DiStefano, 3rd, *Ann Biomed Eng* **34**, 879 (May, 2006).
169. M. L. Hribal *et al.*, *Mol Pharmacol* **59**, 322 (Feb, 2001).
170. P. E. Scherer, S. Williams, M. Fogliano, G. Baldini, H. F. Lodish, *J. Biol. Chem.* **270**, 26746 (November 10, 1995, 1995).
171. E. Hu, P. Liang, B. M. Spiegelman, *J. Biol. Chem.* **271**, 10697 (May 3, 1996, 1996).
172. K. Maeda *et al.*, *Biochem Biophys Res Commun* **221**, 286 (Apr 16, 1996).
173. Y. Nakano, T. Tobe, N.-H. Choi-Miura, T. Mazda, M. Tomita, *J Biochem (Tokyo)* **120**, 803 (October 1, 1996, 1996).
174. Y. Arita *et al.*, *Biochem Biophys Res Commun* **257**, 79 (Apr 2, 1999).
175. T. Kadowaki *et al.*, *J Clin Invest* **116**, 1784 (Jul, 2006).
176. N. L. Brooks *et al.*, *Diabetes Obes Metab* **9**, 246 (May, 2007).
177. T. Kadowaki, T. Yamauchi, *Endocr Rev* **26**, 439 (May, 2005).
178. L. J. Martin, J. G. Woo, S. R. Daniels, E. Goodman, L. M. Dolan, *J Clin Endocrinol Metab* **90**, 4255 (Jul, 2005).
179. M. Takahashi *et al.*, *Int J Obes Relat Metab Disord* **24**, 861 (Jul, 2000).
180. I. B. Bauche *et al.*, *Endocrinology* **148**, 1539 (April 1, 2007, 2007).
181. A. V. Hertzel *et al.*, *Am J Physiol Endocrinol Metab* **290**, E814 (May, 2006).
182. Y. Zhang, M. Matheny, S. Zolotukhin, N. Tumer, P. J. Scarpace, *Biochim Biophys Acta* **1584**, 115 (Oct 10, 2002).
183. H. Motoshima *et al.*, *J Clin Endocrinol Metab* **87**, 5662 (Dec, 2002).
184. C. Lagathu *et al.*, *Diabetologia* **49**, 2162 (Sep, 2006).
185. X. Liang *et al.*, *Am J Physiol Endocrinol Metab* **290**, E103 (Jan, 2006).
186. D. Bedi *et al.*, *Biochem Biophys Res Commun* **345**, 332 (Jun 23, 2006).
187. K. Hotta *et al.*, *Arterioscler Thromb Vasc Biol* **20**, 1595 (Jun, 2000).
188. T. P. Combs *et al.*, *Diabetes* **52**, 268 (February 1, 2003, 2003).

189. M. Iwaki *et al.*, *Diabetes* **52**, 1655 (Jul, 2003).
190. S. Kaser *et al.*, *Gut* **54**, 117 (Jan, 2005).
191. M. Yoda-Murakami *et al.*, *Biochem Biophys Res Commun* **285**, 372 (Jul 13, 2001).
192. A. M. Delaigle, J. C. Jonas, I. B. Bauche, O. Cornu, S. M. Brichard, *Endocrinology* **145**, 5589 (Dec, 2004).
193. H. S. Berner *et al.*, *Bone* **35**, 842 (Oct, 2004).
194. M. Archanco, J. Gomez-Ambrosi, M. Tena-Sempere, G. Fruhbeck, M. A. Burrell, *J Histochem Cytochem* (Jun 12, 2007).
195. G. Ding *et al.*, *J Mol Cell Cardiol* **43**, 73 (Jul, 2007).
196. L. Shapiro, P. E. Scherer, *Current Biology* **8**, 335 (1998).
197. T.-S. Tsao *et al.*, *J. Biol. Chem.* **278**, 50810 (December 12, 2003, 2003).
198. J. Fruebis *et al.*, *PNAS* **98**, 2005 (February 13, 2001, 2001).
199. U. B. Pajvani *et al.*, *J. Biol. Chem.* **278**, 9073 (March 7, 2003, 2003).
200. H. Waki *et al.*, *Endocrinology* **146**, 790 (Feb, 2005).
201. Y. Wang *et al.*, *Proteomics* **4**, 3933 (Dec, 2004).
202. Y. Wang, A. Xu, C. Knight, L. Y. Xu, G. J. S. Cooper, *J. Biol. Chem.* **277**, 19521 (May 24, 2002, 2002).
203. P. W. Peake, J. T. Hughes, Y. Shen, J. A. Charlesworth, *J Mol Endocrinol* **39**, 45 (Jul, 2007).
204. Y. Wang *et al.*, *J Biol Chem* **281**, 16391 (Jun 16, 2006).
205. C. Lara-Castro, Y. Fu, B. H. Chung, W. T. Garvey, *Curr Opin Lipidol* **18**, 263 (Jun, 2007).
206. K. Hara *et al.*, *Diabetes Care* **29**, 1357 (Jun, 2006).
207. U. B. Pajvani *et al.*, *J Biol Chem* **279**, 12152 (Mar 26, 2004).
208. J. S. Bogan, H. F. Lodish, *J Cell Biol* **146**, 609 (Aug 9, 1999).
209. A. Gavrila *et al.*, *J Clin Endocrinol Metab* **88**, 2838 (Jun, 2003).
210. J. Koshimura *et al.*, *Biochem Biophys Res Commun* **316**, 165 (Mar 26, 2004).
211. T. Yamauchi *et al.*, *Nature* **423**, 762 (2003).
212. M. Fasshauer *et al.*, *FEBS Lett* **558**, 27 (Jan 30, 2004).
213. A. Tsuchida *et al.*, *J. Biol. Chem.* **279**, 30817 (July 16, 2004, 2004).
214. N. Kubota *et al.*, *Cell Metab* **6**, 55 (Jul 11, 2007).
215. M. S. Rasmussen *et al.*, *Obesity (Silver Spring)* **14**, 28 (Jan, 2006).
216. T. Yamauchi *et al.*, *Nat Med* **13**, 332 (Mar, 2007).
217. G. Chinetti, C. Zawadski, J. C. Fruchart, B. Staels, *Biochemical and Biophysical Research Communications* **314**, 151 (2004).
218. I. Kharroubi, J. Rasschaert, D. L. Eizirik, M. Cnop, *Biochem Biophys Res Commun* **312**, 1118 (Dec 26, 2003).
219. G. P. Rossi *et al.*, *Int J Mol Med* **17**, 975 (Jun, 2006).
220. L. Alberti *et al.*, *Diabetes, Obesity and Metabolism* **9**, 344 (2007).
221. X. Mao *et al.*, *Nat Cell Biol* **8**, 516 (May, 2006).
222. C. Hug *et al.*, *Proc Natl Acad Sci U S A* **101**, 10308 (Jul 13, 2004).
223. T. Yamauchi *et al.*, *Nat Med* 7, 941 (Aug, 2001).
224. Y. Okamoto, S. Kihara, T. Funahashi, Y. Matsuzawa, P. Libby, *Clin Sci (Lond)* **110**, 267 (Mar, 2006).
225. J. P. Whitehead, A. A. Richards, I. J. Hickman, G. A. Macdonald, J. B. Prins, *Diabetes Obes Metab* **8**, 264 (May, 2006).

226. X. Wu *et al.*, *Diabetes* **52**, 1355 (Jun, 2003).
227. T. Masaki *et al.*, *Diabetes* **52**, 2266 (Sep, 2003).
228. Y. Okamoto *et al.*, *Circulation* **106**, 2767 (November 26, 2002, 2002).
229. N. Kubota *et al.*, *J. Biol. Chem.* **277**, 25863 (July 12, 2002, 2002).
230. Y. Okamoto *et al.*, *Horm Metab Res* **32**, 47 (Feb, 2000).
231. N. Ouchi *et al.*, *Circulation* **100**, 2473 (December 21, 1999, 1999).
232. N. Ouchi *et al.*, *Circulation* **103**, 1057 (February 27, 2001, 2001).
233. M. Kumada *et al.*, *Circulation* **109**, 2046 (May 4, 2004, 2004).
234. T. P. Combs *et al.*, *Endocrinology* **145**, 367 (Jan, 2004).
235. N. Ouchi *et al.*, *J. Biol. Chem.* **279**, 1304 (January 9, 2004, 2004).
236. R. Shibata *et al.*, *J. Biol. Chem.* **279**, 28670 (July 2, 2004, 2004).
237. H. Chen, M. Montagnani, T. Funahashi, I. Shimomura, M. J. Quon, *J. Biol. Chem.* **278**, 45021 (November 7, 2003, 2003).
238. H. Kobayashi *et al.*, *Circ Res* **94**, e27 (Mar 5, 2004).
239. R. Shibata *et al.*, *Nat Med* **11**, 1096 (Oct, 2005).
240. H. Sell, D. Dietze-Schroeder, K. Eckardt, J. Eckel, *Biochem Biophys Res Commun* **343**, 700 (May 12, 2006).
241. A. M. Wolf, D. Wolf, H. Rumpold, B. Enrich, H. Tilg, *Biochem Biophys Res Commun* **323**, 630 (Oct 15, 2004).
242. N. Yamaguchi *et al.*, *FEBS Lett* **579**, 6821 (Dec 19, 2005).
243. N. Ouchi *et al.*, *Circulation* **107**, 671 (Feb 11, 2003).
244. P. H. Park, M. R. McMullen, H. Huang, V. Thakur, L. E. Nagy, *J Biol Chem* (May 30, 2007).
245. M. Neumeier *et al.*, *J Leukoc Biol* **79**, 803 (Apr, 2006).
246. H. Masaie *et al.*, *Exp Hematol* **35**, 947 (Jun, 2007).
247. A. Xu *et al.*, *J Clin Invest* **112**, 91 (Jul, 2003).
248. S. Shklyaev *et al.*, *Proc Natl Acad Sci U S A* **100**, 14217 (Nov 25, 2003).
249. Y. Fu, N. Luo, R. L. Klein, W. T. Garvey, *J. Lipid Res.* **46**, 1369 (July 1, 2005, 2005).
250. I. Kelesidis, T. Kelesidis, C. S. Mantzoros, *Br J Cancer* **94**, 1221 (May 8, 2006).
251. E. Brakenhielm *et al.*, *Proc Natl Acad Sci U S A* **101**, 2476 (Feb 24, 2004).
252. L. A. Colangelo, S. M. Gapstur, P. H. Gann, A. R. Dyer, K. Liu, *Cancer Epidemiol Biomarkers Prev* **11**, 385 (Apr, 2002).
253. M. Trevisan *et al.*, *Cancer Epidemiol Biomarkers Prev* **10**, 937 (Sep, 2001).
254. R. L. Ahmed, K. H. Schmitz, K. E. Anderson, W. D. Rosamond, A. R. Folsom, *Cancer* **107**, 28 (Jul 1, 2006).
255. T. Morita *et al.*, *Asian Pac J Cancer Prev* **6**, 485 (Oct-Dec, 2005).
256. S. Cowey, R. W. Hardy, *Am J Pathol* **169**, 1505 (Nov, 2006).
257. S. Watanabe, M. Hojo, A. Nagahara, *J Gastroenterol* **42**, 267 (Apr, 2007).
258. P. Pasanisi *et al.*, *Int J Cancer* **119**, 236 (Jul 1, 2006).
259. S. M. Najjar *et al.*, *Cell Metab* **2**, 43 (Jul, 2005).
260. N. Beauchemin *et al.*, *Exp Cell Res* **252**, 243 (Nov 1, 1999).
261. A. Olsen *et al.*, *Genomics* **23**, 659 (Oct, 1994).
262. G. S. Dveksler *et al.*, *J Virol* **67**, 1 (Jan, 1993).
263. G. S. Dveksler *et al.*, *J Virol* **65**, 6881 (Dec, 1991).
264. S. M. Najjar *et al.*, *J. Biol. Chem.* **268**, 1201 (January 15, 1993, 1993).
265. B. Obrink, *Curr Opin Cell Biol* **9**, 616 (Oct, 1997).

266. P. Nedellec, C. Turbide, N. Beauchemin, *Eur J Biochem* **231**, 104 (Jul 1, 1995).
267. K. Kuespert, S. Pils, C. R. Hauck, *Curr Opin Cell Biol* **18**, 565 (Oct, 2006).
268. C. Godfraind *et al.*, *Lab Invest* **73**, 615 (Nov, 1995).
269. P. Odin, M. Asplund, C. Busch, B. Obrink, *J Histochem Cytochem* **36**, 729 (Jul, 1988).
270. E. Daniels *et al.*, *Dev Dyn* **206**, 272 (Jul, 1996).
271. W. Hauck *et al.*, *Eur J Biochem* **223**, 529 (Jul 15, 1994).
272. C.-J. Chen, T.-T. Lin, J. E. Shively, *J. Biol. Chem.* **271**, 28181 (November 8, 1996, 1996).
273. R. C. Vassao *et al.*, *Virology* **274**, 278 (2000).
274. D. Phan *et al.*, *Molecular and Cellular Endocrinology* **184**, 115 (2001).
275. S. H. Lin, G. Guidotti, *J Biol Chem* **264**, 14408 (Aug 25, 1989).
276. S. D. Gray-Owen, R. S. Blumberg, *Nat Rev Immunol* **6**, 433 (Jun, 2006).
277. K. McCuaig, C. Turbide, N. Beauchemin, *Cell Growth Differ* **3**, 165 (March 1, 1992, 1992).
278. I. Hunter, K. Sigmundsson, N. Beauchemin, B. Obrink, *FEBS Letters* **425**, 141 (1998).
279. K. Tan *et al.*, *Embo J* **21**, 2076 (May 1, 2002).
280. G. Markel *et al.*, *Eur J Immunol* **34**, 2138 (Aug, 2004).
281. C. Kannicht, L. Lucka, R. Nuck, W. Reutter, M. Gohlke, *Glycobiology* **9**, 897 (Sep, 1999).
282. J. R. Bartles, L. T. Braiterman, A. L. Hubbard, *J Biol Chem* **260**, 12792 (Oct 15, 1985).
283. L. Lucka *et al.*, *Glycobiology* **15**, 87 (Jan, 2005).
284. C. Wagener, S. Ergun, *Exp Cell Res* **261**, 19 (Nov 25, 2000).
285. A. M. Mahrenholz, C. H. Yeh, J. E. Shively, S. A. Hefta, *J Biol Chem* **268**, 13015 (Jun 25, 1993).
286. S. M. Watt *et al.*, *Blood* **98**, 1469 (September 1, 2001, 2001).
287. C. V. Choice, M. N. Poy, P. Formisano, S. M. Najjar, *J Cell Biochem* **76**, 133 (Nov, 1999).
288. I. Hunter, H. Sawa, M. Edlund, B. Obrink, *Biochem J* **320 (Pt 3)**, 847 (Dec 15, 1996).
289. B. Obrink *et al.*, *Ann NY Acad Sci* **971**, 597 (October 1, 2002, 2002).
290. S. Oikawa, M. Kuroki, Y. Matsuoka, G. Kosaki, H. Nakazato, *Biochem Biophys Res Commun* **186**, 881 (Jul 31, 1992).
291. C. Turbide, T. Kunath, E. Daniels, N. Beauchemin, *Cancer Res* **57**, 2781 (Jul 1, 1997).
292. B. B. Singer, I. Scheffrahn, B. Obrink, *Cancer Res* **60**, 1236 (Mar 1, 2000).
293. B. Obrink *et al.*, *Ann N Y Acad Sci* **971**, 597 (Oct, 2002).
294. T. Chen *et al.*, *J Leukoc Biol* **70**, 335 (Aug, 2001).
295. N. Beauchemin *et al.*, *Oncogene* **14**, 783 (Feb 20, 1997).
296. M. Huber *et al.*, *J Biol Chem* **274**, 335 (Jan 1, 1999).
297. J. Brummer, M. Neumaier, C. Gopfert, C. Wagener, *Oncogene* **11**, 1649 (Oct 19, 1995).
298. K. M. Skubitz, K. D. Campbell, K. Ahmed, A. P. Skubitz, *J Immunol* **155**, 5382 (Dec 1, 1995).

299. D. Schumann, C. J. Chen, B. Kaplan, J. E. Shively, *J Biol Chem* **276**, 47421 (Dec 14, 2001).
300. J. Brummer *et al.*, *Am J Pathol* **159**, 537 (August 1, 2001, 2001).
301. A. Ebrahimnejad, R. Flayeh, G. Unteregger, C. Wagener, J. Brummer, *Experimental Cell Research* **260**, 365 (2000).
302. P. H. Cheung *et al.*, *J. Biol. Chem.* **268**, 24303 (November 15, 1993, 1993).
303. B. Fournes, J. Farrah, M. Olson, N. Lamarche-Vane, N. Beauchemin, *Mol Cell Biol* **23**, 7291 (Oct, 2003).
304. U. Sundberg, N. Beauchemin, B. Obrink, *J Cell Sci* **117**, 1091 (Mar 1, 2004).
305. U. Sundberg, B. Obrink, *J Cell Sci* **115**, 1273 (March 15, 2002, 2002).
306. N. Stern *et al.*, *J Immunol* **174**, 6692 (Jun 1, 2005).
307. S. H. Lin, W. Luo, K. Earley, P. Cheung, D. C. Hixson, *Biochem J* **311 (Pt 1)**, 239 (Oct 1, 1995).
308. C. Houde, S. Roy, N. Leung, D. W. Nicholson, N. Beauchemin, *J. Biol. Chem.* **278**, 16929 (May 2, 2003, 2003).
309. E. Klaile, M. M. Muller, C. Kannicht, B. B. Singer, L. Lucka, *J Cell Sci* **118**, 5513 (December 1, 2005, 2005).
310. P. Oh *et al.*, *Nature* **429**, 629 (Jun 10, 2004).
311. N. Kilic *et al.*, *J Biol Chem* **280**, 2361 (Jan 21, 2005).
312. W. J. Chen *et al.*, *Shock* **24**, 124 (Aug, 2005).
313. S. D. Gray-Owen, D. R. Lorenzen, A. Haude, T. F. Meyer, C. Dehio, *Mol Microbiol* **26**, 971 (Dec, 1997).
314. S. Ergun *et al.*, *Mol Cell* **5**, 311 (Feb, 2000).
315. M. M. Muller, B. B. Singer, E. Klaile, B. Obrink, L. Lucka, *Blood* **105**, 3925 (May 15, 2005).
316. E. Hemmila *et al.*, *J Virol* **78**, 10156 (Sep, 2004).
317. H. G. Leusch, Z. Drzeniek, Z. Markos-Pusztai, C. Wagener, *Infect Immun* **59**, 2051 (Jun, 1991).
318. S. L. Sauter, S. M. Rutherfurd, C. Wagener, J. E. Shively, S. A. Hefta, *J Biol Chem* **268**, 15510 (Jul 25, 1993).
319. M. Virji, S. M. Watt, S. Barker, K. Makepeace, R. Doyonnas, *Mol Microbiol* **22**, 929 (Dec, 1996).
320. C. R. Hauck, F. Agerer, P. Muenzner, T. Schmitter, *Eur J Cell Biol* **85**, 235 (Apr, 2006).
321. T. Nagaishi *et al.*, *Immunity* **25**, 769 (Nov, 2006).
322. C. J. Chen, J. E. Shively, *J Immunol* **172**, 3544 (Mar 15, 2004).
323. G. Greicius, E. Severinson, N. Beauchemin, B. Obrink, B. B. Singer, *J Leukoc Biol* **74**, 126 (Jul, 2003).
324. R. Mansson, A. Lagergren, F. Hansson, E. Smith, M. Sigvardsson, *Eur J Immunol* **37**, 1365 (May, 2007).
325. A. Ohwada, H. Takahashi, I. Nagaoka, S. Kira, *Am J Respir Cell Mol Biol* **11**, 214 (Aug, 1994).
326. T. J. Yeatman, W. Mao, R. C. Karl, *Journal of Gastrointestinal Surgery* **1**, 292 (1997).
327. A. Thies *et al.*, *J Clin Oncol* **20**, 2530 (May 15, 2002).
328. E. Laack *et al.*, *J Clin Oncol* **20**, 4279 (Nov 1, 2002).
329. W. Sienel *et al.*, *Clin Cancer Res* **9**, 2260 (Jun, 2003).

330. T. Kinugasa *et al.*, *Int J Cancer* **76**, 148 (Mar 30, 1998).
331. R. Kammerer, D. Stober, B. B. Singer, B. Obrink, J. Reimann, *J Immunol* **166**, 6537 (Jun 1, 2001).
332. B. B. Singer *et al.*, *J Immunol* **168**, 5139 (May 15, 2002).
333. L. Izzi, C. Turbide, C. Houde, T. Kunath, N. Beauchemin, *Oncogene* **18**, 5563 (Sep 30, 1999).
334. W. Luo, C. G. Wood, K. Earley, M. C. Hung, S. H. Lin, *Oncogene* **14**, 1697 (Apr 10, 1997).
335. B. Fournes, S. Sadekova, C. Turbide, S. Letourneau, N. Beauchemin, *Oncogene* **20**, 219 (Jan 11, 2001).
336. S. Nittka, J. Gunther, C. Ebisch, A. Erbersdobler, M. Neumaier, *Oncogene* **23**, 9306 (Dec 16, 2004).
337. J. Kirshner, C. J. Chen, P. Liu, J. Huang, J. E. Shively, *Proc Natl Acad Sci U S A* **100**, 521 (Jan 21, 2003).
338. S. Yokoyama, C. J. Chen, T. Nguyen, J. E. Shively, *Oncogene* (Jun 4, 2007).
339. I. Scheffrahn, B. B. Singer, K. Sigmundsson, L. Lucka, B. Obrink, *Exp Cell Res* **307**, 427 (Jul 15, 2005).
340. M. Hokari *et al.*, *Life Sci* **81**, 336 (Jul 4, 2007).
341. M. Neumaier, S. Paululat, A. Chan, P. Matthaes, C. Wagener, *Proc Natl Acad Sci U S A* **90**, 10744 (Nov 15, 1993).
342. M. Rosenberg *et al.*, *Cancer Res* **53**, 4938 (Oct 15, 1993).
343. A. M. Bamberger *et al.*, *Am J Pathol* **152**, 1401 (Jun, 1998).
344. L. Riethdorf *et al.*, *J Histochem Cytochem* **45**, 957 (Jul, 1997).
345. L. Oliveira-Ferrer *et al.*, *Cancer Res* **64**, 8932 (December 15, 2004, 2004).
346. T. W. Y. S. N. Y. K. H. Pauldion V. Cruz, *Cancer* **104**, 354 (2005).
347. J. T. Hsieh *et al.*, *Cancer Res* **55**, 190 (Jan 1, 1995).
348. P. Nollau *et al.*, *Cancer Res* **57**, 2354 (Jun 15, 1997).
349. D. Phan *et al.*, *Cancer Res* **64**, 3072 (May 1, 2004, 2004).
350. C. Busch, T. A. Hanssen, C. Wagener, B. brink, *Human Pathology* **33**, 290 (2002).
351. D. Tilki *et al.*, *Urologe A* (Jul 1, 2007).
352. N. Leung *et al.*, *Oncogene* **25**, 5527 (Sep 7, 2006).
353. R. W. Rees-Jones, S. I. Taylor, *J. Biol. Chem.* **260**, 4461 (April 10, 1985, 1985).
354. N. Perrotti, D. Accili, B. Marcus-Samuels, R. W. Rees-Jones, S. I. Taylor, *Proc Natl Acad Sci U S A* **84**, 3137 (May, 1987).
355. S. M. Najjar *et al.*, *Biochemistry* **34**, 9341 (Jul 25, 1995).
356. S. M. Najjar, *Biochemical and Biophysical Research Communications* **247**, 457 (1998).
357. P. Soni, K. A. Al-Hosaini, M. A. Fernstrom, S. M. Najjar, *Mol Cell Biol Res Commun* **1**, 102 (May, 1999).
358. P. Soni, M. Lakkis, M. N. Poy, M. A. Fernstrom, S. M. Najjar, *Mol Cell Biol* **20**, 3896 (Jun, 2000).
359. S. M. Najjar *et al.*, *Biochemistry* **36**, 6827 (Jun 3, 1997).
360. S. M. Najjar, C. V. Choice, P. Soni, C. M. Whitman, M. N. Poy, *J. Biol. Chem.* **273**, 12923 (May 22, 1998, 1998).
361. S. A. Phillips, N. Perrotti, S. I. Taylor, *FEBS Letters* **212**, 141 (1987).

362. M. Okamoto, A. Karasik, M. F. White, C. R. Kahn, *Biochemistry* **29**, 9489 (Oct 9, 1990).
363. P. Formisano *et al.*, *J Biol Chem* **270**, 24073 (Oct 13, 1995).
364. C. V. Choice, M. J. Howard, M. N. Poy, M. H. Hankin, S. M. Najjar, *J. Biol. Chem.* **273**, 22194 (August 28, 1998, 1998).
365. S. L. Calzi, C. V. Choice, S. M. Najjar, *Am J Physiol Endocrinol Metab* **273**, E801 (October 1, 1997, 1997).
366. G. Sesti *et al.*, *Biochem Biophys Res Commun* **181**, 1419 (Dec 31, 1991).
367. S. M. Najjar, *Trends Endocrinol Metab* **13**, 240 (Aug, 2002).
368. H. Barnes, E. J. Ackermann, P. van der Geer, *Oncogene* **22**, 3589 (Jun 5, 2003).
369. P. van der Geer, *Trends Cardiovasc Med* **12**, 160 (May, 2002).
370. P. A. Staubs *et al.*, *J Biol Chem* **269**, 27186 (Nov 4, 1994).
371. D. J. Van Horn, M. G. Myers, Jr., J. M. Backer, *J Biol Chem* **269**, 29 (Jan 7, 1994).
372. M. N. Poy, R. J. Ruch, M. A. Fernstrom, Y. Okabayashi, S. M. Najjar, *J Biol Chem* **277**, 1076 (Jan 11, 2002).
373. R. Malmstrom *et al.*, *Diabetes* **47**, 779 (May, 1998).
374. G. F. Lewis, G. Steiner, *Diabetes Care* **19**, 390 (Apr, 1996).
375. S.-Y. Park *et al.*, *Am J Physiol Endocrinol Metab* **291**, E517 (September 1, 2006, 2006).
376. T. Dai *et al.*, *J. Biol. Chem.* **279**, 45155 (October 22, 2004, 2004).
377. M. N. Poy *et al.*, *Nat Genet* **30**, 270 (Mar, 2002).
378. D. Komninou, A. Ayonote, J. P. Richie, Jr., B. Rigas, *Exp Biol Med (Maywood)* **228**, 396 (Apr, 2003).
379. E. Giovannucci, *J Nutr* **131**, 3109S (Nov, 2001).
380. D. B. West, C. N. Boozer, D. L. Moody, R. L. Atkinson, *Am J Physiol* **262**, R1025 (Jun, 1992).
381. R. S. Surwit, C. M. Kuhn, C. Cochrane, J. A. McCubbin, M. N. Feinglos, *Diabetes* **37**, 1163 (Sep, 1988).
382. M. Rebuffe-Scrive, R. Surwit, M. Feinglos, C. Kuhn, J. Rodin, *Metabolism* **42**, 1405 (Nov, 1993).
383. M. Rossmeisl, J. S. Rim, R. A. Koza, L. P. Kozak, *Diabetes* **52**, 1958 (Aug, 2003).
384. M. Laclaustra, D. Corella, J. M. Ordovas, *Nutrition, Metabolism and Cardiovascular Diseases* **17**, 125 (2007).
385. D. S. Ludwig *et al.*, *J Clin Invest* **107**, 379 (Feb, 2001).
386. R. P. Donahue, R. J. Prineas, R. DeCarlo Donahue, J. A. Bean, J. S. Skyler, *Int J Obes Relat Metab Disord* **20**, 76 (Jan, 1996).
387. F. Conus, R. Rabasa-Lhoret, F. Peronnet, *Appl Physiol Nutr Metab* **32**, 4 (Feb, 2007).
388. A. Katsuki *et al.*, *Diabetes Care* **26**, 2964 (Oct, 2003).
389. M. D. Michael *et al.*, *Mol Cell* **6**, 87 (Jul, 2000).
390. H. Ebinuma *et al.*, *Clin Chim Acta* **372**, 47 (Oct, 2006).
391. S. P. Singh *et al.*, *Trop Gastroenterol* **25**, 76 (Apr-Jun, 2004).
392. C. H. Chen *et al.*, *J Clin Gastroenterol* **40**, 745 (Sep, 2006).
393. S. Zelber-Sagi, D. Nitzan-Kaluski, Z. Halpern, R. Oren, *Liver Int* **26**, 856 (Sep, 2006).

394. D. A. McClain, *Am J Med Sci* **304**, 192 (Sep, 1992).
395. C. A. Dinarello, *Semin Nephrol* **27**, 98 (Jan, 2007).
396. I. Zavaroni *et al.*, *J Clin Endocrinol Metab* **65**, 494 (Sep, 1987).
397. Y. Shi, S. I. Taylor, S. L. Tan, N. Sonenberg, *Endocr Rev* **24**, 91 (Feb, 2003).
398. G. A. Kiunga *et al.*, *Cancer Lett* **211**, 145 (Aug 10, 2004).
399. M. Barnea, A. Shamay, A. H. Stark, Z. Madar, *Obesity (Silver Spring)* **14**, 2145 (Dec, 2006).
400. M. Bahceci *et al.*, *J Endocrinol Invest* **30**, 210 (Mar, 2007).
401. T. McLaughlin *et al.*, *Diabetologia* **50**, 1707 (Aug, 2007).

Appendix 1

Glucose homeostasis (results from Nelly Leung and Dr. André Marette's laboratory)
A) Blood glucose was measured after mice were fasted O/N. No significant differences were found between the +/+ and -/- mice. **B)** Plasma insulin levels were also measured. No significant differences were found between the +/+ and -/- fasted mice. **Insulin levels post-prandial are represented in the two rightmost panels. Significant differences are found in the females +/+ vs -/-, but no differences were found in the males.**
C) Glucose tolerance curves. Mice were fasted for 4h and given a dose of glucose either by IP injection or gavage. Left panel: glucose tolerance curve. Middle panel: insulin levels of the same mice used in the glucose tolerance test. Right panel: glucose tolerance test on mice fasted for 16 h and sampled by retro-orbital bleed. D) For the insulin tolerance test, male mice were fasted 5 h and injected with 1U/kg of insulin right after time 0, blood sampling was from the tail vein.

A: Fasting Blood Glucose

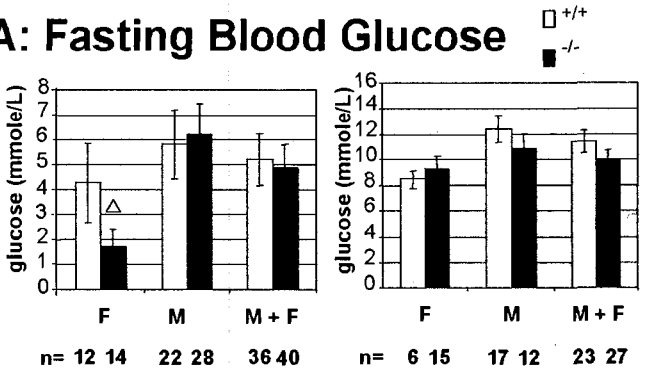

B: Plasma Insulin

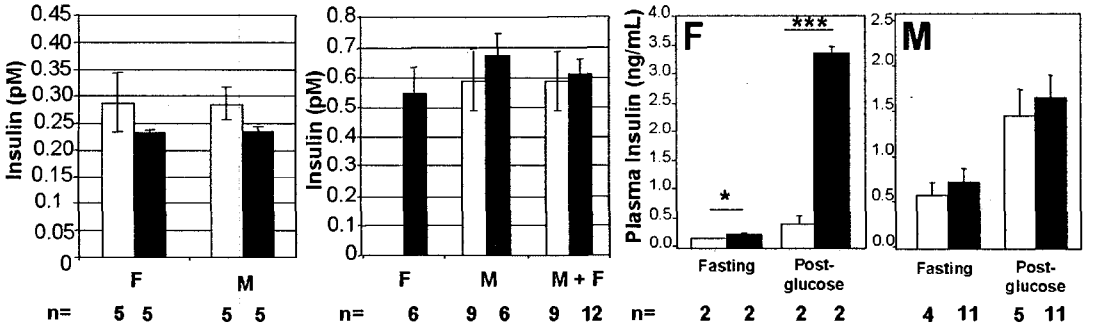

C: Glucose Tolerance Tests

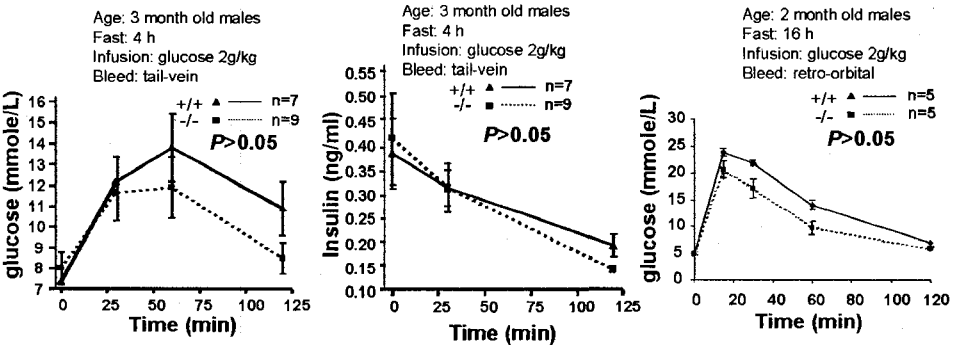

D: Insulin Tolerance Tests

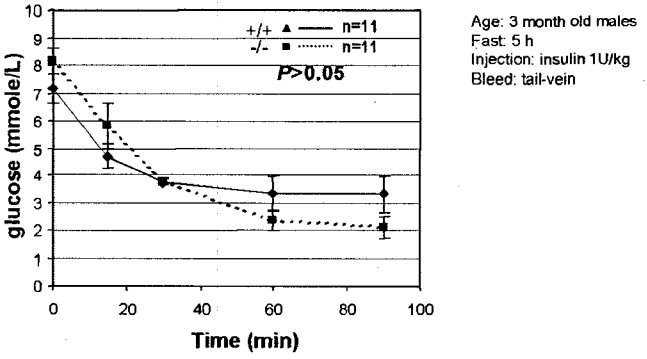

Appendix 2

Euglycemic clamp measurements (results from Dr. Alexandre Charbonneau in Dr. André Marette's laboratory)

A) Clamp measurements were done on mice fed a standard diet (ST) of a high fat diet (HF). Mice are injected with a low dose of insulin and continuously infused with glucose to maintain euglycemia. -/- mice require less glucose infusion than +/+ mice both on ST or HF diet. B) Hepatic glucose production at basal state is not different in -/- and +/+ mice. During the clamp measurement when low dose insulin is injected, -/- mice have an elevated hepatic glucose production. C) Glucose uptake by muscle tissue. Under clamp conditions, animals on HF diet have lower glucose uptake.

A. Whole body euglycemic clamp measurements

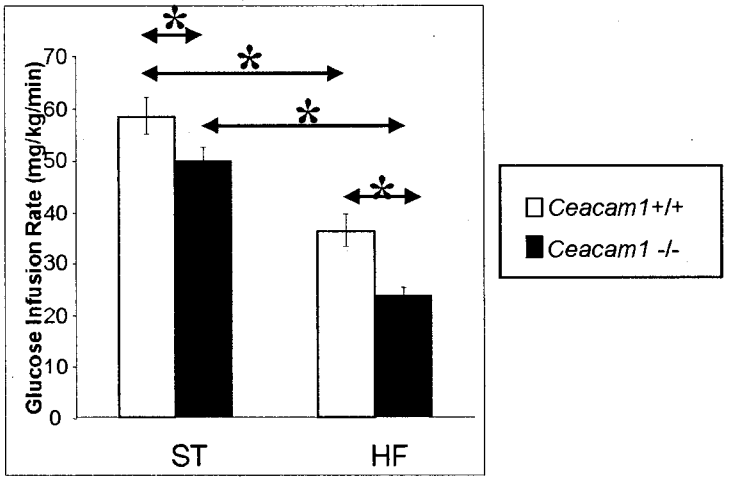

B. Hepatic glucose production

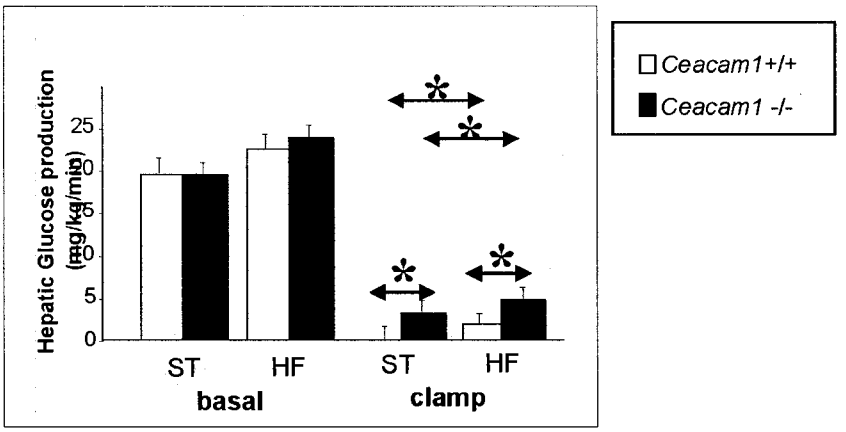

C. Glucose Uptake

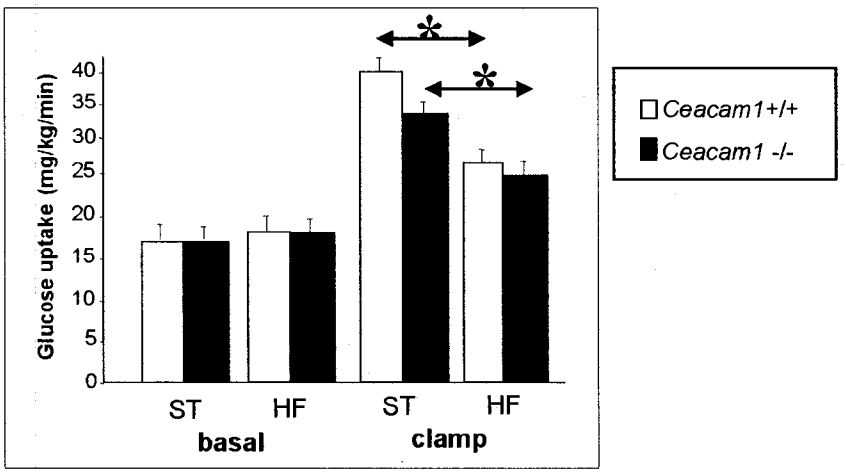

Appendix 3. Ethic certificates for research involving animal subjects, radioactivity and biohazardous materials

Appendix 4. Copyright waivers for figures

ELSEVIER LIMITED LICENSE
TERMS AND CONDITIONS

Jul 18, 2007

This is a License Agreement between Anne-Marie Charbonneau Allard ("You") and Elsevier Limited ("Elsevier Limited"). The license consists of your order details, the terms and conditions provided by Elsevier Limited, and the payment terms and conditions.

License Number	1751940763289
License date	Jul 18, 2007
Licensed content publisher	Elsevier Limited
Licensed content publication	The Lancet
Licensed content title	The metabolic syndrome
Licensed content author	Robert H Eckel, Scott M Grundy and Paul Z Zimmet
Licensed content date	16 April 2005-22 April 2005
Volume number	365
Issue number	9468
Pages	14
Type of Use	Thesis / Dissertation
Requestor type	STM signatory publisher
Portion	Figures/table/illustration/abstracts
Quantity	1
Format	Both print and electronic
You are an author of the Elsevier article	No
Are you translating?	No
Purchase order number	
Title of your article	
Publisher of your article	
Expected publication date	
Estimated size of your article (pages)	
Total	0.00 USD
Terms and Conditions	

INTRODUCTION

The publisher for this copyrighted material is Elsevier. By clicking "accept" in connection with completing this licensing transaction, you agree that the following terms and conditions apply to this transaction (along with the Billing and Payment terms and conditions established by Copyright Clearance Center, Inc. ("CCC"), at the time that you opened your Rightslink account and that are available at any time at http://myaccount.copyright.com).

NATURE PUBLISHING GROUP LICENSE TERMS AND CONDITIONS

Jul 16, 2007

This is a License Agreement between Anne-Marie Charbonneau Allard ("You") and Nature Publishing Group ("Nature Publishing Group"). The license consists of your order details, the terms and conditions provided by Nature Publishing Group, and the payment terms and conditions.

License Number	1750860094063
License date	Jul 16, 2007
Licensed content publisher	Nature Publishing Group
Licensed content publication	Nature
Licensed content title	Insulin signalling and the regulation of glucose and lipid metabolism
Licensed content author	Alan R. Saltiel and C. Ronald Kahn
Volume number	
Issue number	
Pages	
Year of publication	2001
Portion used	Figures
Number of figures	1
Requestor type	Student
Type of Use	Thesis / Dissertation
PO Number	
Total	$0.00
Terms and Conditions	

Terms and Conditions for Permissions

Nature Publishing Group hereby grants you a non-exclusive license to reproduce this material for this purpose, and for no other use, subject to the conditions below:

1. NPG warrants that it has, to the best of its knowledge, the rights to license reuse of this material. However, you should ensure that the material you are requesting is original to Nature Publishing Group and does not carry the copyright of another entity (as credited in the published version). If the credit line on any part of the material you have requested indicates that it was reprinted or adapted by NPG with permission from another source, then you should also seek permission from that source to reuse the material.

2. Permission granted free of charge for material in print is also usually granted for any electronic version of that work, provided that the material is incidental to the work as a whole and that the electronic version is essentially equivalent to, or substitutes for, the print version. Where print permission has been granted for a fee, separate

The Endocrine Society

Confirmation

The Endocrine Society
8401 Connecticut Avenue, Suite 900
Chevy Chase, MD 20815-5817
Telephone: 301-941-0200
Fax: 301-941-0259
www.endo-society.org
TIN Number: 73-0531256

This printable page is your letter granting copyright permission. A copy of this page will be sent to you via email for your records.

Form was submitted by: amca_06@hotmail.com

Not original author to publish

Date: August 12, 2007
Reference Number:

Name: Anne-Marie Charbonneau Allard
Organization: Student (McGill University)
Department:
Address: 4838 Cazelais
City, State and Postal Code: Montreal, Quebec H4C 1E7
Country: Canada
Phone: 514-680-2836
Fax:
Email: amca_06@hotmail.com

Journal: Endocrine Reviews
Author Name: T Kadowaki
Title: Adiponectin and Adiponectin Receptors
Year: 2005
Volume: 26
Page Range: 439-451
Figure Reproduction:
Figure Number(s): 9
Where will the figures appear:

Additional Comments:

Master thesis McGill University

The Endocrine Society grants permission to reproduce table/figure 9 from the selected article stated above contingent upon the following conditions: 1) That you give proper credit to the author(s) and to include in your citation, the title of journal, title of article, volume, issue number, date, and page numbers. 2) That you include the statement *Copyright 2005, The Endocrine Society.* Please understand that permission is granted for one-time use only. Permission must be requested separately for future editions, revisions,

NATURE PUBLISHING GROUP LICENSE
TERMS AND CONDITIONS

Aug 12, 2007

This is a License Agreement between Anne-Marie Charbonneau Allard ("You") and Nature Publishing Group ("Nature Publishing Group"). The license consists of your order details, the terms and conditions provided by Nature Publishing Group, and the payment terms and conditions.

License Number	1766720839712
License date	Aug 12, 2007
Licensed content publisher	Nature Publishing Group
Licensed content publication	Nature Reviews Immunology
Licensed content title	CEACAM1: contact-dependent control of immunity
Licensed content author	Scott D. Gray-Owen and Richard S. Blumberg
Volume number	
Issue number	
Pages	
Year of publication	2006
Portion used	Figures / tables
Requestor type	Student
Type of Use	Thesis / Dissertation
High-res requested	No
PO Number	
Total	$0.00
Terms and Conditions	

Terms and Conditions for Permissions

Nature Publishing Group hereby grants you a non-exclusive license to reproduce this material for this purpose, and for no other use, subject to the conditions below:

1. NPG warrants that it has, to the best of its knowledge, the rights to license reuse of this material. However, you should ensure that the material you are requesting is original to Nature Publishing Group and does not carry the copyright of another entity (as credited in the published version). If the credit line on any part of the material you have requested indicates that it was reprinted or adapted by NPG with permission from another source, then you should also seek permission from that source to reuse the material.

2. Permission granted free of charge for material in print is also usually granted for any electronic version of that work, provided that the material is incidental to the work as a whole and that the electronic version is essentially equivalent to, or substitutes for, the print version. Where print permission has been granted for a fee, separate